STRATIGRAPHY OF THE GOLDENVILLE GROUP-HALIFAX GROUP TRANSITION (GHT) OF THE MEGUMA SUPERGROUP AT CARIBOU GOLD DISTRICT (DRILLCORE LL81-5A), NOVA SCOTIA

Submitted by
Craig Gordon Burns
March, 1997

in partial fulfillment of a Bachelor of Science Honours Degree,
Department of Earth Sciences, Dalhousie University, Halifax, Nova Scotia

Distribution License

DalSpace requires agreement to this non-exclusive distribution license before your item can appear on DalSpace.

NON-EXCLUSIVE DISTRIBUTION LICENSE

You (the author(s) or copyright owner) grant to Dalhousie University the non-exclusive right to reproduce and distribute your submission worldwide in any medium.

You agree that Dalhousie University may, without changing the content, reformat the submission for the purpose of preservation.

You also agree that Dalhousie University may keep more than one copy of this submission for purposes of security, back-up and preservation.

You agree that the submission is your original work, and that you have the right to grant the rights contained in this license. You also agree that your submission does not, to the best of your knowledge, infringe upon anyone's copyright.

If the submission contains material for which you do not hold copyright, you agree that you have obtained the unrestricted permission of the copyright owner to grant Dalhousie University the rights required by this license, and that such third-party owned material is clearly identified and acknowledged within the text or content of the submission.

If the submission is based upon work that has been sponsored or supported by an agency or organization other than Dalhousie University, you assert that you have fulfilled any right of review or other obligations required by such contract or agreement.

Dalhousie University will clearly identify your name(s) as the author(s) or owner(s) of the submission, and will not make any alteration to the content of the files that you have submitted.

If you have questions regarding this license please contact the repository manager at dalspace@dal.ca.

Grant the distribution license by signing and dating below.

_____ _____

Name of signatory Date

Dalhousie University

Department of Earth Sciences
Halifax, Nova Scotia
Canada B3H 3J5
(902) 494-2358
FAX (902) 494-6889

DATE April 15, 1997

AUTHOR Craig Gordon Burns

TITLE STRATIGRAPHY OF THE GOLDENVILLE GROUP-HALIFAX GROUP TRANSITION (GHT) OF THE MEGUMA SUPERGROUP AT CARIBOU GOLD DISTRICT (DRILLCORE LL81-5A), NOVA SCOTIA

Degree BSc Convocation May Year 1997

Permission is herewith granted to Dalhousie University to circulate and to have copied for non-commercial purposes, at its discretion, the above title upon the request of individuals or institutions.

Abstract

Drillcore LL81-5A, recovered from Caribou gold district, Halifax County, Nova Scotia, by Sherritt Gordon Mines Ltd. in 1980, is a 625.40 m-long continuous section of the Cambro-Ordovician Meguma Supergroup, representing 500 stratigraphic metres of the transition between the sandy Goldenville Group and the overlying younger, shaly, Halifax Group (GHT). This core presents an unusually long and continuous section of the upper part of the GHT, which appears to exert significant control over trace metal concentration in the Meguma Supergroup. The purpose of this study is to characterize the geology of drillcore LL81-5A, which should promote a better local and regional understanding of the GHT.

Three conformable stratigraphic units are noted in LL81-5A. In order of decreasing age and depth, these are: Unit A (36 stratigraphic metres)- fining upward sequences of massive, carbonate-rich metawackes and silty slates; Unit B (113 m stratigraphic metres)- interbedded manganiferous, chloritic, pyrrhotitic meta-argillites and metawackes and Unit C (351 stratigraphic metres)- fining upward sequences of parallel- and ripple cross-laminated, pyrrhotitic, locally carbonate-rich metasiltstones and carbonaceous slates similar to base-cut-out Bouma sequences, with locally abundant soft-sediment deformation structures. These units are equivalent to undivided Goldenville Group lithologies and Moshers Island and Cunard formations of the lower Halifax Group, respectively.

Unit B meta-argillites host a trace element and trace metal assemblage that includes Ba, Pb, Zn, Ni, As and Mo, and are significantly enriched in MnO relative to other lithologies studied in LL81-5A. Unit C slates contain a trace element and metal assemblage of Ba, Rb, Sr, V, Cr, Sc, Cs, La, Ce and U and are interpreted as metalliferous black slates. Unit A metawackes are depleted in most trace elements and metals relative to the other main lithologies studied, whereas Unit C metasiltstones contain average relative concentrations of most trace elements and metals.

Decreasing grain size, fining-upward, generally sharply-bounded sedimentary sequences, many with an upward succession of sedimentary structures indicative of decreasing water energy, along with an increasing carbonaceous material and trace element and trace metal influence through the GHT in LL81-5A, implies deposition of these sediments from turbidity currents within a progressively anoxic, coarse sediment-starved basin.

Acknowledgements

Many people have been instrumental in the development and production of this thesis. First and foremost, I thank Dr. Marcos Zentilli for presenting me with the topic and encouraging me to pursue it. Milton Graves must be thanked for all of his efforts. He provided instrumental help through his critiques of my work and willingness to help with every problem. Don Fox provided me with materials and plenty of suggestions that I am thankful for. The staff of the Department of Natural Resources Drillcore Library in Stellarton: John McMullin, Donald Weir, Bill Palmer, John Horton and Jim Hayes, was extremely helpful during the developmental stages of this thesis, especially John McMullin. Dr. Paul Schenk provided valuable assistance through his advice on drillcore logging. Don Keith, my recently deceased high school geology teacher, encouraged me to pursue geology through his wit and enthusiasm and for this, I am truly grateful. Dr. Martin Gibling must be thanked for his guidance in capacity of professor of my thesis class. I am thankful to Gordon Brown for the exceptional thin sections that he provided me with and Bob MacKay for his help with microprobing. I must also extend my thanks to Robert Zimmerman, who played his part well. Above all, my family must be thanked. My parents, Gordon and Suzanne Burns and grandmother Allison Shipton provided me with tremendous support.

Table of Contents

List of Figures

List of Tables

Chapter 1
Introduction

1.1 General Statement

The Meguma Supergroup (Schenk, 1995b) is a thick metamorphosed sequence of deep-water Cambrian-Ordovician clastic sedimentary rocks, intruded by peraluminous Devonian-Carboniferous granitoids, that dominates the bedrock geology of southern Nova Scotia (Sangster, 1990). Abundant metal enrichment, including gold (Faribault, 1899; Malcolm, 1926, 1976; Graves and Zentilli, 1982; Haynes, 1986), tungsten and antimony (Graves and Zentilli, 1988b), lead and zinc (Binney *et al.*, 1986; MacInnes, 1986), manganese (Hingston, 1985; Graves and Zentilli, 1988b) and barium, molybdenum and tin (Graves and Zentilli, 1988b) has been recognized in these rocks. However, a significant proportion of this enrichment is noted to occur within less than 10% of the stratigraphic thickness of the Meguma Supergroup, specifically within the transition between the sandy Goldenville Group and the overlying slaty Halifax Group (Goldenville-Halifax transition (GHT)) (Graves and Zentilli, 1988b). It has been suggested that the GHT exerts significant metallogenic control within the Meguma Supergroup (Graves and Zentilli, 1988b). Graves and Zentilli (1976) proposed that characterization of the GHT should provide a guide to potential mineral occurrences in southern Nova Scotia.

In late 1980, Sherritt Gordon Mines Ltd. recovered drillcore LL81-5A from the Lake Mine property of the Caribou gold district, Halifax County, Nova Scotia (see Figure 1.1 for location map). This drillcore presents a 625.40 m (~500 stratigraphic metres) transect through the upper part of the GHT; specifically the basal portion of the Halifax Group. Exposed extended sections of the upper GHT are not common, thus, drillcore LL81-5A provides an excellent opportunity for its study.

1.2 Purpose and Scope

The purpose of this thesis is to characterize the geology of drillcore LL81-5A, through visual and petrographic observations, mineral chemistry and geochemical properties, in order to define its stratigraphy. Stratigraphic characterization of LL81-5A should help promote a better understanding of the GHT at Caribou gold district, as well as a better regional understanding through correlations with other described sections, such as in the Mahone Bay area (O'Brien, 1986), Lake Charlotte (Hingston, 1985; Mwenifumbo *et al.*, 1990), central Nova Scotia (Ryan *et al.*, 1995) and Eastville (Binney *et al.*, 1986, MacInnis, 1986). The long-term goal of studies such as these is regional characterization of the GHT.

1.3 Location

Caribou gold district is located in northeastern Halifax County, Nova Scotia, approximately 82 km northeast of Halifax and 14 km south of the village of Upper Musquodoboit (see Figure 1.1). Several properties constitute the district, including the Lake Mine property situated 3 km east of the village of Caribou Gold Mines, in the eastern part of the district, where drillcore LL81-5A was recovered.

The district is low-lying and relatively flat, with elevations averaging 170 m above sea level with rounded hills rising locally to about 190 m above sea level. Dense overgrowth, three lakes, several streams and numerous swamps and bogs are present. Glacial till averaging 1-4 m in thickness covers most of the district, limiting bedrock exposure to ~15% (James E. Tilsley and Associates Ltd., 1983).

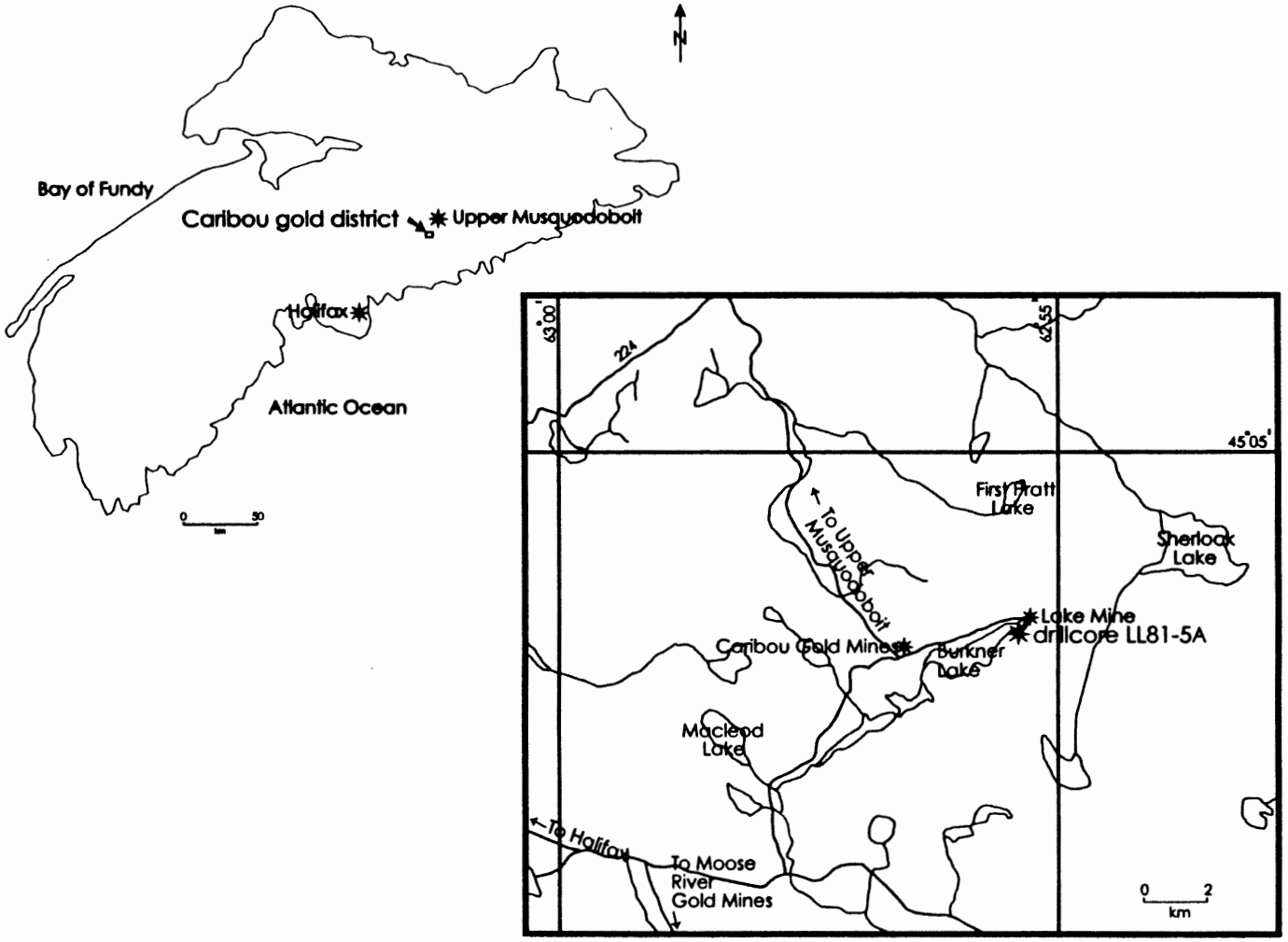

Figure 1.1. Location of Caribou gold district. Local base map after James E. Tilsley and Associates Ltd. (1983).

1.4 Previous Work

Investigation into the rocks of the Meguma Terrane began in the early 1800s, with the work of Jackson and Alger (1828-1829) and continues to present. Economic interest in these rocks has been extensive and can be traced back to 1858, with the discovery of placer gold at Mooseland, eastern Halifax County (Sangster, 1990). Gold was first discovered in the area of the present day Caribou gold district in the mid-1860s (James E. Tilsley and Associates Ltd., 1983). The first gold production in the area took place in 1869 (Bell, 1948) and the area was declared a gold district in 1870 (James E. Tilsley and Associates Ltd., 1983). Between 1869 and 1945, the district yielded 91 181 ounces of gold, second only to the Goldenville gold district to the east (Sangster, 1990).

The Lake Mine property hosts the highly productive Lake Lode auriferous vein. Production records are incomplete, but indicate that at least 10 160 ounces of gold were produced from 35 000 tons of processed mill rock obtained from this vein between 1885 and 1910 (James E. Tilsley and Associates Ltd., 1983). No record of gold production after 1910 in the Lake Mine area is noted, as interest and activity became redirected to central and western areas of the district.

The property remained idle until late 1980, when Sherritt Gordon Mines Ltd. of Lynn Lake, Manitoba, optioned claims covering most of the district, including the Lake Mine property (James E. Tilsley and Associates Ltd., 1983). An extensive exploration program that included magnetic and VLF-EM surveying and diamond drilling was undertaken at this time on the Lake Mine property, in an attempt to intersect the down-plunge extension of the Lake Lode vein (Sherritt Gordon Mines Ltd., 1981). Drilling resulted in 2 680 m of core from 16 drillholes (Sherritt Gordon Mines Ltd., 1981). All of the drillholes missed their target and Sherritt Gordon relinquished its claims options

in the district in late 1982 (Seabright Explorations Inc., 1988). At this time, drillcore LL81-5A, which is the focus of this study, was recovered. Upon recovery, this core was logged by Sherritt Gordon and analyzed for Au, Cu, Zn, Mn and Pb. These data are not examined in this thesis.

Significant scientific investigation of direct interest to this thesis has been directed at rocks of the Meguma Supergroup at Caribou gold district. Haynes (1986) studied Meguma rocks exposed in the Holman shaft, west of the Lake Mine property, when it was briefly de-watered in late 1983 and subsequently proposed a syngenetic hydrothermal model for the genesis of auriferous veins and sulphides in the district based on this underground study. Sangster (1987)used 16 arsenopyrite samples and 1 pyrrhotite sample obtained from LL81-5A as part of a Meguma sulphur isotope study, concluding that sulphide zones associated with gold occurrences in the Meguma Supergroup probably resulted from bacterially reduced sulphide formed in an anoxic sea floor environment. Unfortunately, the data obtained from LL81-5A have not been published and are unavailable for use in this study. Graves and Zentilli (1988a) conducted whole-rock major element, trace element and trace metal analyses on 42 samples obtained from drillcore LL81-5A. Several geochemical relationships were assessed based on the data acquired, but a full analysis was not undertaken, in part, due to an absence of a stratigraphic log of this drillcore to reference samples to. These data are presented in Appendix E and are used in Chapter 6 to assess some of the major geochemical properties and relationships of the main lithologies present in this drillcore.

1.5 Methods

Drillcore LL81-5A was studied between July and September, 1996, at the Nova Scotia Department of Natural Resources (N.S.D.N.R.) Drill Core Library in Stellarton, Pictou County, Nova

Scotia (shown in Figure 1.2), where it has been stored since being acquired by the Department of Mines and Energy from Sherritt Gordon Mines Ltd. in 1984. The author was employed at this location during this period, but core analysis was conducted outside of working hours. Measured sections of the NQ diameter core were visually analyzed bed-by-bed, at a rate of approximately 10 m per day throughout the study period. Based on observations of sedimentology, lithology, mineralization, metamorphism and deformation, a descriptive, and in parts graphic, log of the drillcore was produced at this time.

Sixty-five samples averaging ~15 cm in length and representative of typical features in the core were collected during logging. Unique, non-representative features were sampled as well. Samples were obtained by cutting the core lengthwise into two equal-sized pieces using a rock saw.

Samples were then photographed at Dalhousie University. Nineteen polished thin sections representing various lithologies and structures were produced from 19 of these samples and visually analysed and described using both transmitted and reflected light microscopy in December, 1996 and January, 1997. Hand samples from which thin sections were obtained were also described at this time. Sixty microprobe analyses were conducted on six thin sections from LL81-5A, using the electron beam microprobe facility at Dalhousie University in February, 1997. In addition, one trip to Caribou gold district was undertaken in late August, 1996, to view the location of the drill site.

Figure 1.2. Nova Scotia Department of Natural Resources Drill Core Library, Stellarton, Nova Scotia. Arrow is directed at the building in which drillcore LL81-5A was studied (courtesy of N.S.D.N.R.).

1.6 Organization

Chapter 2 presents a thorough overview of the Meguma Supergroup, with an emphasis on stratigraphy. Geology of Caribou gold district and the geology of drillcore LL81-5A are profiled in chapters 3 and 4, respectively. Mineral chemistry is presented in Chapter 5 whereas geochemistry is profiled in Chapter 6. Conclusions and recommendations are presented in Chapter 7. Additionally, five appendices covering samples used in this study, petrographic descriptions of many of these samples, a stratigraphic log of LL81-5A, mineral chemistry data and geochemical data, are presented in appendices A through E, respectively.

Chapter 2
Regional Geology

Introduction

Caribou gold district, shown in Figure 2.1, is hosted by rocks of the Meguma Supergroup, which together with the overlying Annapolis Supergroup and granitoid intrusions, defines the Meguma Terrane (Schenk, 1995b). It is more appropriate to discuss regional geology from the context of the Meguma Terrane, rather than from the context of the individual supergroups, because: both units are present in the same geographic area; both are considered to be fundamental components of the same stratigraphic section, interpreted in the same model of an evolving continental margin and both units have been affected by the Devonian Acadian Orogeny, exhibiting similar structural, metamorphic and plutonic effects (Schenk, 1995b).

2.1 The Meguma Terrane

The Meguma Terrane includes the Meguma Supergroup, composed of thick metamorphosed sequences of Late Cambrian or older to Early Ordovician siliciclastic sediments, divided into the older, sandy Goldenville Group and the overlying, younger, shaly Halifax Group; the overlying Annapolis Supergroup, consisting of Early Ordovician to Early Devonian siliciclastic and volcaniclastic sequences (Schenk, 1995b) and Devonian to Carboniferous granitoid intrusions (Clarke *et al.*, 1985) (see Figure 2.1 for a map showing the distribution of the Meguma Supergroup and these intrusions). The contact between the supergroups is assumed to be a paraconformity, but locally it is a disconformity or an angular unconformity (Schenk, 1995b). The composite thickness of the Meguma Terrane exceeds 23 km (Schenk, in prep.).

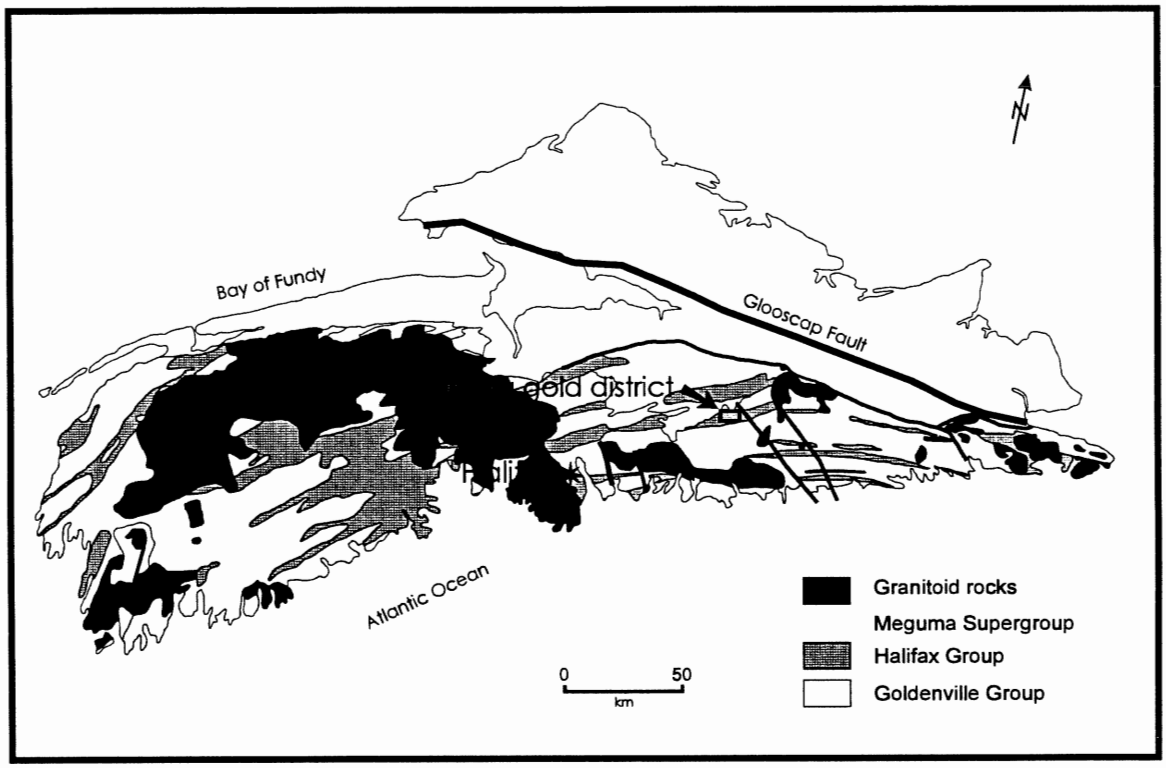

Figure 2.1. Distribution of the Meguma Supergroup and granitoid intrusions in southern Nova Scotia. Stratigraphy of the Meguma is discussed within section 2.3 (base map courtesy of Don Fox).

The Meguma Terrane is the youngest and largest terrane of the Canadian Appalachian region, with a total area of approximately 200 000 km^2 (Schenk, 1995b). The terrane underlies all of the southern mainland of Nova Scotia (Schenk, 1995b) and geophysical evidence suggests that it underlies a large part of the continental shelf off Nova Scotia (Pe-Piper and Loncarevic, 1989). To the north, the Glooscap Fault separates the Meguma Terrane from the Avalon Terrane (Schenk, 1995b), while Lefort and Haworth (1981) proposed that the Maine-Rhard fracture zone may be the southern limit of the Meguma Terrane. To the northwest, the Meguma Terrane is bounded by the Avalon Terrane, with the contact located under the Bay of Fundy, while to the east and south, the Meguma Terrane disappears under Mesozoic sediments of the Scotian Shelf. Similar rocks are present in southern Spain and northern Morocco (Lefort and Haworth, 1981). Contact relationships between the Meguma Terrane and underlying rocks are unclear due to lack of exposure, but geochemical evidence presented by Eberz *et al.* (1991, in Schenk, 1995b) suggests that the Meguma Terrane is at least in part, an allochthon situated on a thrust surface above the Avalon lower crustal block.

Post-Middle Devonian rocks overlie both the Meguma Terrane and the adjacent Avalon Terrane (Sangster, 1990). In northern areas of the Meguma Terrane, Upper Devonian to Mississippian Horton Group siliciclastic rocks overlie the Meguma Terrane, as do: Windsor Group marine limestones, dolomites, evaporites and siliciclastic rocks; mudstones, shales and evaporites of the transitional Pennsylvanian-Mississippian Watering Brook Formation of the Canso Group and feldspathic sandstones of the Late Carboniferous Scotch Village Formation of the Pictou Group (Keppie, 1979). In western parts of the Meguma Terrane, Triassic to Jurassic redbeds and basalts

of the Fundy Group are found (Keppie, 1979). In the Musquodoboit Valley, in the central Meguma Terrane, Early Cretaceous sands, clays, lignite and kaolin are present (Keppie, 1979). Pleistocene glacial till deposits overlie many of these units and much of the Meguma Terrane (Keppie, 1979).

2.2 Geological History

2.2.1 Source and Deposition

The sedimentary source of the Meguma Terrane is interpreted as lying to the southeast, in close proximity to the pre-Atlantic location of northern Africa (Schenk, 1995a,b). Schenk (1995a,b, in prep.) proposed that these sediments were glacially derived from Precambrian gneiss, granodiorite and metasedimentary and metavolcanic rocks and stored in extensive till sheets on the Saharan Platform, which were periodically tapped by northward moving streams, ice and wind from the Cambrian to the Devonian. Sediments that reached the northwestern margin of Gondwana, formed thick, expansive, deep-water submarine fan complexes of the Meguma Supergroup, while subsequent shallow water sedimentation on the Gondwanan shelf and periodic extensional volcanism resulted in deposition of the Annapolis Supergroup (Schenk, 1991, 1995a,b). The Meguma Supergroup represents a first order sequence of submergence and emergence (Schenk, in prep.).

2.2.2 Tectonics and Structure

The first major geological event to affect sediments of the Meguma Terrane after deposition and burial, was the Middle Devonian Acadian Orogeny (Schenk, 1995b). This was a major mountain-building phase of the Appalachian orogeny, which resulted from final closing of the

northern part of the Iapetus Ocean (Williams, 1995). In eastern Canada, this event resulted from a collision of North America with parts of Africa, a major consequence of which was docking of the Meguma Terrane with the eastern side of the Avalon Platform, along the Glooscap Fault (Keppie, 1985). As a result of this, the pre-Middle Devonian geological history of the Meguma Terrane is distinct from that of adjacent areas, while its post-Middle Devonian history is shared with the region in which it now occurs.

The main structural consequence of the Acadian Orogeny was the development of extensive folding over most of the Meguma Terrane (Schenk, 1995b). The main folds are large-scale, upright and low plunging, with very regular wavelengths of approximately 15 km and axes traceable over at least 55 km (Schenk, 1995b). Fold axes generally trend northeast-southwest, subparallel to the present-day Atlantic coast, but southwest of Shelburne, axes trend more southwards (Hicks, 1996). Domes and basins are present along fold axes where local variations in fold plunge have developed (O'Brien, 1986). Pervasive axial planar cleavage parallels near vertical axial surfaces on these folds (Schenk, 1995b). A second generation of north to northeast trending folds, with steeply plunging axial surfaces, is noted within upper parts of the Meguma Supergroup (Schenk, 1995b).

2.2.3 Regional Metamorphism

Regional metamorphism of the Meguma Terrane is associated with the Acadian Orogeny. Regional metamorphic grade is mainly greenschist facies within central and eastern parts of the terrane and amphibolite facies in southern and easternmost areas (Schenk, 1995b). $^{40}Ar/^{39}Ar$ studies by Muecke *et al.* (1988) suggest that the main regional metamorphic event occurred at 405-390 Ma.

2.2.4 Plutonism and Associated Contact Metamorphism

Peraluminous granitoids intruded the Meguma Terrane between 372 and 360 Ma (Late Devonian), post-dating the Acadian Orogeny (Clarke *et al.*, 1980; Clarke and Halliday, 1980; Reynolds *et al.*, 1981) and again at approximately 316 Ma (middle Carboniferous) (Schenk, 1995b). Hornblende-hornfels facies contact metamorphism overprints regional metamorphic assemblages in areas affected by these intrusions (Taylor and Schiller, 1966).

2.3 The Meguma Supergroup

The depositional model of the sedimentary protolith of the Meguma Supergroup records a shoaling upward system towards the overlying Annapolis Supergroup, from submarine fans through a channel-levee complex, to a prograding wedge and finally to shelf and nearshore environments (Schenk, 1995b). It is proposed by Schenk (1970) that sediments of the Meguma Supergroup were deposited from turbidity currents that were extensively reworked by contour-following bottom currents.

2.3.1 Stratigraphy

Rocks defining the Meguma have been known as part of the Transitional Clay-Slate Formation (Jackson and Alger, 1828, in Schenk, 1995b), the Meguma Series (Woodman, 1904, in Schenk, 1995b), the Meguma Group (Stevenson, 1959) and most recently, the Meguma Supergroup (Schenk, 1995b). As shown in Figure 2.2, the Meguma Supergroup in the southwestern half of the Meguma Terrane, is divided by Schenk (1995b) into the older Goldenville Group and the younger conformably overlying Halifax Group, and these in turn are subdivided into formations. In the

Mahone Bay area of southeastern Nova Scotia, O'Brien (1986) subdivided the Meguma Group into the conformable Goldenville, Green Bay and Halifax formations (see Figure 2.2), with the Green Bay Formation informally defined to include units in the transition zone between the Goldenville and Halifax formations. The stratigraphy adopted for this thesis is that of Schenk (1995b) and units reported herein are equivalents of this.

Meguma Supergroup Southwestern Meguma Terrane (Schenk, 1995b)			Meguma Group Mahone Bay area, Southwestern Meguma Terrane (O'Brien, 1986)			Meguma Group Central Meguma Terrane (Ryan *et al.*, 1995)		
Units		Maximum Thickness (m)	Units		Maximum Thickness (m)	Units		Maximum Thickness (m)
Halifax Group	Rockville Notch Formation	32						
	Delanceys Formation	1 850						
	Feltzen Formation	2 000	Halifax Formation	Feltzen Member	1 000-2 000	Halifax Formation	Glen Brook Unit	1 900
	Cunard Formation	8 000		Cunard Member	5 000-8 000		Rawdon Unit	1 100
	Moshers Island Formation	500	Green Bay Formation	Moshers Island Member	150-300		Beaverbank Unit	300
Goldenville Group	West Dublin (Green Bay area)/ and Tancook (Mahone Bay area) formations	1 000		West Dublin (Green Bay area) and Tancook (Mahone Bay area) members	200-300 to 600-800	Goldenville Formation	Steve's Road Unit	700
	Tancook (Mahone Bay area)/ Rissers Beach (Green Bay area) formations	1 000		Rissers Beach Member (Green Bay area)				
	New Harbour Formation	+7 000	Goldenville Formation	New Harbour Member	1 000		Lewis Lake Unit	1 700
							Long Lake Unit	1 100
							Mt. Uniacke Unit	1 200

Figure 2.2. Stratigraphic units and respective nomenclature for the Meguma Supergroup (Group) from several recent studies. Units are not scaled.

2.3.1.1 Goldenville Group

The Goldenville Group is interpreted as an abyssal-plain fan deposit (Schenk, 1970). Its sedimentary protolith is a massive, thick-bedded wacke, with thin interbeds of silty shale and siltstone (Sangster, 1990), corresponding to Bouma-type fining-upward sequences. Wacke beds typically range from a few metres to tens of metres in thickness, whereas shale beds are generally 0.1-2.0 m thick (Sangster, 1990).

The Goldenville Group has no known base (Sangster, 1990; Schenk, 1995b). Its maximum measured thickness is 6.7 km near Liverpool, Queens County (Faribault, 1914, in Schenk, 1995b), while 4-7 km of this unit is present below the Goldenville-Halifax group contact across southern Nova Scotia (Schenk, 1970). The overall minimum thickness of the Goldenville Group is approximately 7 km (Schenk, 1970).

The maximum age of deposition of the Meguma Supergroup is constrained by the presence of 650-560 Ma (Early Cambrian) detrital zircons in lower areas of the Goldenville Group (Krogh and Keppie, 1986). Trilobite fragments 235 m below the top of the uppermost Tancook Formation (Waldron and Graves, 1987) on Big Tancook Island, in Mahone Bay, have been dated by Pratt and Waldron (1991) as Middle Cambrian. The fragments are well sorted and mixed with sand (Pratt and Waldron, 1991), indicating transport and thus, provide only a maximum biostratigraphic age (Schenk, 1991). The presence of the trace fossil *Paleodictyon (Glenodictyum) cf. imperfectum* Seilacher, in the upper portion of the group, suggests an Ordovician age (Pickerill and Keppie, 1981). Muscovite K-Ar dates of 476 ± 19 and 498 ± 20 Ma (Late Cambrian to Late Ordovician), were interpreted by Poole (1971) as indicating the age of deposition or diagenesis of the lower

Goldenville Group.

The Goldenville Group has been stratigraphically subdivided in the southwestern part of the Meguma Terrane (O'Brien, 1986; Schenk and Adams, 1986; Schenk, 1995b; Hicks, 1996) and in the central part by Ryan *et al.* (1995). In the Green Bay area of Lunenburg County, the stratigraphic order defined by O'Brien (1986) and adjusted by Schenk (1995b), is: the New Harbour, Rissers Beach and West Dublin formations (see Figure 2.2). In the Mahone Bay area, southwestern Nova Scotia, the Tancook Island Formation is correlative to the Rissers Beach and West Dublin formations, based on the stratigraphy of O'Brien (1986). All formations are conformable (O'Brien, 1986). Preliminary stratigraphy in the central Meguma Terrane is similar to this (Ryan *et al.*, 1995).

2.3.1.1a New Harbour Formation

The New Harbour Formation is composed of thick beds of very mature, fine-grained, buff-weathered, quartzose to feldspathic metawacke and minor volcanic debris, interbedded with thin beds of green to grey slate (Schenk, 1995b), which decrease in abundance upwards in the Mahone Bay area (O'Brien, 1986). Mudstone-siltstone rip-up clasts are common and angular to rounded pebbles of phosphate are locally abundant (Schenk, 1995b). Individual sandy beds generally correspond to upward truncated Bouma sequences (Dzulynski and Walton, 1965). Sole marks are typical at the base of individual beds and slump structures, slide blocks and channels are common (Schenk, 1995b). Hicks (1996) noted varying styles of worm burrows and other escape structures in the New Harbour Formation in the Mahone Bay area. Strata tend to be laterally discontinuous and are either segregated into thinner beds or amalgamated into thicker strata (Harris and Schenk, 1975).

2.3.1.1b Rissers Beach Formation

The basal part of the Rissers Beach Formation consists of black slate that coarsens stratigraphically upwards through the addition of silt laminae (Schenk, 1995b). Thinly stratified, very fine-grained metasandstone beds stratigraphically succeed this and are followed by very thickly stratified amalgamated metasandstones that pinch out to the west, which are in turn overlain by thinly stratified metasiltstones (Schenk, 1995b).

2.3.1.1c West Dublin and Tancook formations

The West Dublin Formation consists mainly of thick, fine-grained metasandstone beds (Schenk, 1995b), that alternate with green metasiltstone beds and grey-green, finer-grained, laminated and cross-bedded metasandstone beds in the Mahone Bay area (Hicks, 1996). Soft sediment deformation structures in this unit in the Mahone Bay area, are similar to those noted for the previous formations (Hicks, 1996). In the Mahone Bay area, the West Dublin Formation is called the Tancook Formation (O'Brien, 1986) and may include equivalents of the Rissers Beach Formation (Waldron, 1987). The Tancook Formation consists mainly of metasandstone beds (Schenk, 1995b). The upper part of the formation consists of packages of amalgamated metasandstones between more typical Bouma sequences (Schenk, 1995b).

2.3.1.2 Halifax Group

The Halifax Group is interpreted as a deposit from a mid- or upper-area of a muddy deep-sea fan which passes upwards into a prograding continental slope and shelf (Schenk, 1981). The protolith of the Halifax Group is grey to black shale with thin silty interbeds (Sangster, 1990). Shale beds are commonly carbonaceous and contain several percent pyrrhotite, while minor pyrite is

common in coarser-grained, less carbonaceous beds (Sangster, 1990).

The contact between the Halifax Group and overlying units has been eroded over most of the group's exposure and its contact with the underlying Goldenville Group is obscure in many areas, so accurate thickness measurements are difficult to obtain (Schenk, 1995b). Additionally, there are few continuous sections of the Halifax Group to measure and there is a lack of structural continuity in upper areas of the group. At its stratotype in the Halifax area, the Halifax Group is 11.8 km thick (Clint Milligan, pers. comm., 1990, in Schenk, 1995b). As with the Goldenville Group, the overall minimum thickness of the Halifax Group is probably 7 km, as thicknesses of 4-7 km are known to occur above the GHT across southern Nova Scotia (Schenk, 1970).

Tremadoc (Lower Ordovician) acritarchs have been recovered from the Moshers Island and Cunard formations (W.A.M. Jenkins, pers. comm., in Schenk, 1995b). Poorly preserved graptolites within the lower Halifax Group at Tangier, Halifax County, noted by Poole (1971), indicate an Arenig (Early Ordovician) age of deposition for the Halifax Group. Crosby (1962) also noted the presence of Early Ordovician graptolites within the Halifax Group in the Wolfville area, Kings County.

The Halifax Group has been stratigraphically subdivided in the southwestern half of the Meguma Terrane by Schenk (1995b), in the Mahone Bay area by O'Brien (1986) and in the central Meguma Terrane by Ryan *et al.* (1995) as shown in Figure 2.2. In the southwestern part of the terrane, Schenk (1995b) divided the Halifax Group into five conformable formations, several of which can be traced into the eastern half. In stratigraphic order, these are: the Moshers Island, Cunard, Feltzen, Delanceys and Rockville Notch formations.

2.3.1.2a Moshers Island Formation

The Moshers Island Formation is a highly distinctive, relatively thin, calcareous and trace metal enriched unit, consisting of rhythmic millimetre- to centimetre-thick interlaminations of metasiltstone and fine-grained, parallel-laminated, dark green and grey-green slates (O'Brien, 1986; Schenk, 1995b). Rare small-scale current ripple cross-laminations, both starved and faded, mark some of the coarser laminated metasiltstone units (Waldron, 1987). Both normal and reverse grading are common (Schenk, 1995b). In the lowest 160 m of this unit in the Mahone Bay area, occasional packages of thin-to medium-bedded metasandstone, marked by well developed parallel-laminations and current ripple cross-laminations are present (Waldron and Graves, 1987). Also in this locality, scouring, loading, dewatering, starved ripples, worm burrows and cone-in-cone-type structures are present (Hicks, 1996).

Coticules; bands consisting of spessartine garnets, manganese carbonate and quartz-rich laminations, are prominent in this unit, as are calcsilicate nodules (Graves and Zentilli, 1988b; Schenk, 1995b). Graves and Zentilli (1988b) proposed that these spessartine garnets formed at the expense of manganese-carbonate minerals during greenschist metamorphism. The unit contains anomalous concentrations of Mn and Ba, total C and is enriched in the trace metals As, Au, Pb, Mo, Sb, W, Cu, Zn and U (Graves and Zentilli, 1988b). The unit is very useful as a marker horizon (Graves and Zentilli, 1988b; Hicks, 1996).

2.3.1.2b Cunard Formation

The Cunard Formation consists of very thick, highly carbonaceous, pyritiferous, fissile black slate, interbedded with thin, fine-grained metasiltstones and very fine-grained, grey metasandstones

(O'Brien, 1986; Schenk, 1995b). Laminations, fine cross-laminations and normal grading are the main sedimentary structures present in these slates and metasiltstones (Schenk, 1995b). Some beds are grossly lenticular and contain cross-sets with amplitudes of 5-10 cm (Waldron, 1987). In the Mahone Bay area, Hicks (1996) noted the presence of starved ripples, load structures, escape structures, rip-up clasts and slumps within this unit. The upward succession of sedimentary structures in individual sandy layers corresponds to bottom cut-out Bouma sequences (Schenk, 1995b). Vertical successions thin upwards in some places and thicken upwards in others (Stow *et al.*, 1984).

2.3.1.2c Feltzen Formation

The Feltzen Formation consists of banded grey slate with even laminae of light grey silty slates, interbedded with black carbonaceous slate and thin-bedded metasiltstone (Schenk, 1995b). Sedimentary structures, including parallel-laminations and cross-stratification are abundant in this unit (Schenk, 1995b). In the Mahone Bay area, soft sediment structures such as slumping, loading and escape structures are present in metasiltstone layers (Hicks, 1996). In the Mahone Bay area and at Blue Rocks, near Lunenburg, this unit contains abundant worm burrows (Hicks, 1996). Individual beds correspond to silty turbidites of Piper (1978, in Schenk, 1995b). Regional stratigraphic trends of this unit are not well understood (Schenk, 1970).

2.3.1.2d Delanceys Formation

The Delanceys Formation is a grey, laminated, silty slate, with abundant fine-scaled lenses of quartz metasiltstone (Schenk, 1995b). In some places, very thin beds of quartz metawacke are interbedded with these slates (Schenk, 1995b). The Delanceys Formation appears to be limited in

extent to the northwestern boundary area of the Meguma Terrane (Schenk, 1995b).

2.3.1.2e Rockville Notch Formation

The Rockville Notch Formation is a dark grey to black, pelitic laminite (Schenk, 1995b), consisting of alternating layers of pure, micaceous metasiltstone and coarse-grained quartzose metasiltstone (Lane, 1981) with some metasiltstone microlenses (Schenk, 1995b). At five localities over a 240 km distance, lens-shaped pods of pebbly to bouldery mudstones (diamictite) are present (Schenk, 1995b). The upper boundary of the formation is conformable and sharp with the overlying Annapolis Supergroup, except at Cape Saint Mary, and near Fales River (Schenk, 1995b).

2.4 Goldenville Group-Halifax Group Transition (GHT)

The transition from the Goldenville Group to the Halifax Group (GHT) is marked by a package of highly distinctive lithologies, typified by interstratified slate and metasandstone, representing a change from sandy, noncarbonaceous, sulphide-poor rocks to shaly, carbonaceous, sulphide-rich rocks (Sangster, 1990). The upper part of the transition is marked by a finely-laminated calcareous argillite, pink and brown laminae rich in spessartine garnet, manganese oxides and quartz (referred to as coticules) and calcareous or calcsilicate nodules (Graves and Zentilli, 1988b). Overall, the GHT is locally anomalous in Mn and Ba, total C and the trace metals: As, Pb, Cu, Zn, Sb, Mo, W, Au and U (Graves and Zentilli, 1988b). By definition, the GHT represents the stratigraphic region between coarse-grained Goldenville Group lithologies and finer-grained Halifax Group lithologies (Graves and Zentilli, 1988b). This transition is generally considered to begin in the upper Tancook Formation and end within the Cunard Formation, where 'typical' Halifax Group lithologies are encountered (Waldron, 1992).

The GHT is of variable thickness and extends sinuously over approximately 1 700 km of the Meguma Terrane (Sangster, 1990). In the Mahone Bay area, the GHT (Green Bay Formation of O'Brien, 1986) is up to 2 km thick, while at Eastville, Halifax County, it is only 35-45 m thick (Binney *et al.*, 1986).

The conformable and alternating slate and metasandstone nature of the GHT has presented problems in precisely locating the contact between the Goldenville and Halifax groups (Graves and Zentilli, 1988b; Hicks, 1996). Faribault (1914) used the location of the highest exposed bed of greywacke to define the position of the contact, while Schenk (1970) and Waldron (1987) used sand/shale ratios. Overall, the contact is sharp in eastern areas of the Meguma Terrane and more gradational in central and western areas (Graves and Zentilli, 1988b).

Chapter 3
Local Geology

Introduction

Caribou gold district is hosted by rocks of the Meguma Supergroup, which crop-out discontinuously throughout the district. Geological knowledge of rocks present in the district is based mainly on underground observations, drillcore observations, geophysical studies and soil and till sampling. This chapter presents information on the geology of the district based on studies by Malcolm (1926, 1976), Bell (1948), James E. Tilsley and Associates Ltd. (1983) and Seabright Explorations Inc. (1988), unless otherwise noted.

3.1 Structure and Metamorphism

Caribou gold district is located on a 6 km long and up to 900 m wide, expression of the regional Caribou-Cochrane Hill Anticline, referred to as the Caribou dome (see figures 3.1 and 3.2). This anticline is a southwest-northeast trending, tight, asymmetric fold, that originated during the Acadian Orogeny (Haynes, 1986). The Caribou dome is mainly a subsurface structure exposed only in a small number of crop-outs. The strike of the dome ranges from 055° at its southwestern extreme, northeast of MacLeod Lake, to 065° at its northeastern extreme, northwest of Sherlock Lake. The dome plunges more steeply to the northeast. The dip of the strata along the dome ranges from near 0° along the fold axis, to 65° along the northern limb and 70° on the southern limb, with local dip increasing in areas proximal to faults or subordinate flexures.

The Caribou dome shows local dextral displacement along discrete northwest trending brittle fault zones. Additionally, several subordinate folds are present within the dome. The main one is

a z-shaped fold located within the southeast limb, as shown in Figure 3.2. This fold is interpreted by Haynes (1986) to have originated as a syn-sedimentary monocline over a graben or transcurrent fault system. Subsequent deformation during the Acadian Orogeny is proposed to have refolded this structure and formed the Caribou dome (Haynes, 1986). This fold hosts the Lake Lode auriferous vein.

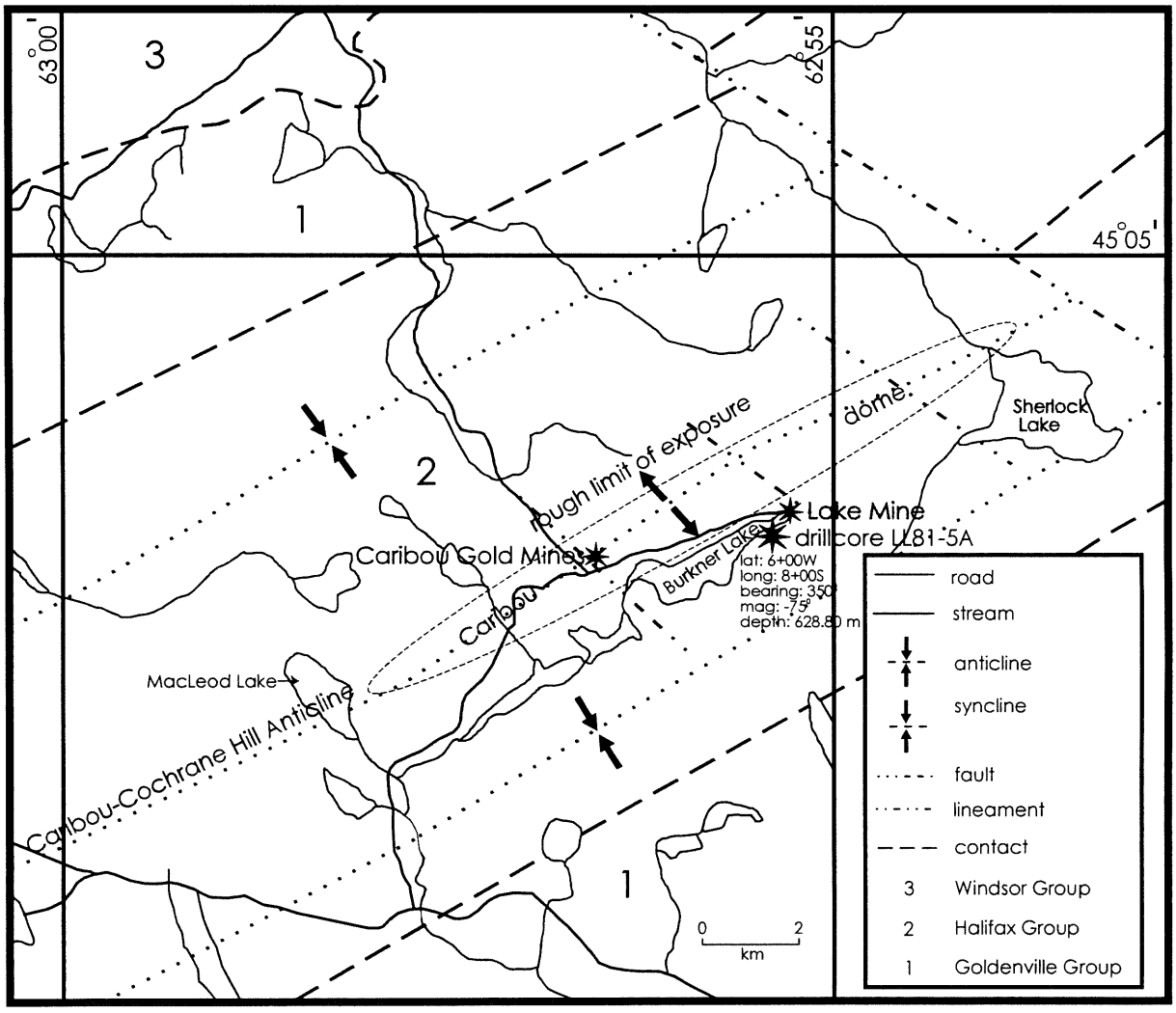

Figure 3.1. Geology of the Caribou gold district (after James E. Tilsley and Associates Ltd., 1983).

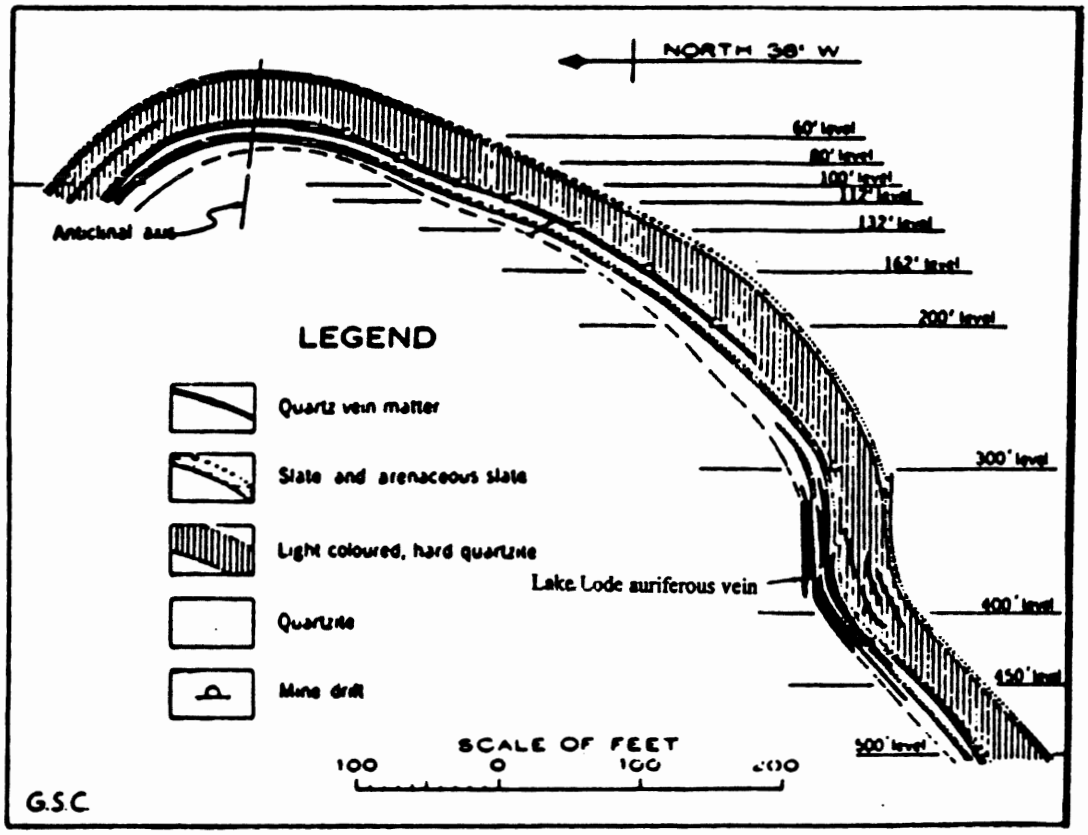

Figure 3.2. Cross-section of the Caribou dome. The location of the Lake Load auriferous vein is shown (after Bell, 1948).

Upper beds of the Goldenville Group are exposed along the center of the dome, while basal beds of the Halifax Group are exposed along the limbs. Where exposed, the contact between the groups is gradational over a few tens of metres.

Rocks throughout the Caribou gold district were regionally metamorphosed to chlorite zone, lower greenschist facies during the Acadian Orogeny (Smith, 1984).

Chapter 4
Geology of Drillcore LL81-5A

Introduction

This chapter profiles the geology of drillcore LL81-5A, recovered from the southern limb of the Caribou dome in the Caribou gold district by Sherritt Gordon Mines Ltd., in 1980. Logging of this drillcore revealed the presence of three conformable units, representing 500 stratigraphic metres of the Meguma Supergroup, mainly rocks of the basal Halifax Group within the upper part of the Goldenville Group-Halifax Group transition. These units are described below in order of decreasing age. Descriptions are based upon the personal observations of the author. Information contained in the drillcore log produced by Sherritt Gordon Mines Ltd. for this hole, is only used here in a few minor instances. A detailed stratigraphic log of this drillcore, along with relevant drillhole information, is presented in Appendix C.

Some petrographic information is included in the unit descriptions here, but petrography is examined in more detail in Chapter 5 and Appendix B. Most of the mineralogy noted below is not visible in the drillcore, mainly because of the fine-grained nature of the rocks. In these cases, only detailed petrographic and microprobe work has allowed mineralogical characterization. Hand sample and petrographic descriptions along with some photographs of most of the lithologies discussed below, can be found in appendices A and B which are intended to be a reference companion to this chapter.

Additionally, the terms metawacke and meta-argillite are used often throughout this chapter and the remainder of the thesis. Many contrasting and often confusing definitions of these terms exist, but in the present context, metawacke is used to refer to metamorphosed rocks with greater

than 50 % detrital sand-sized grains (mainly quartz) within in a silt and clay matrix, whereas the term meta-argillite is used to describe metamorphic rocks consisting of clay- to silt-sized grains, including mainly silty slates and metasiltstones.

Depths referred to in the following sections are drilling depths, not stratigraphic. However, thicknesses quoted are stratigraphic. Stratigraphic thicknesses were calculated using stratal dips measured during the logging process (stratal dip increases steadily from ~60° to ~30° from the horizontal, from the top of the core to the base, with minimal variation between units). The geology described below is summarized in Figure 4.14, located at the end of the unit descriptions.

4.1 Unit A

This unit is characterized by interstratified metawackes and silty slates over 36 stratigraphic metres. Fining-upward sequences typically consisting of a massive, generally thick, (~several decimetres-thick) basal interval of fine- to medium-grained, light grey-green, carbonate-rich metawacke (locally normally graded), overlain by a generally thin (~several centimetres-thick) interval of dark grey silty slate, can be differentiated throughout (see Figure 4.1). Metawacke is locally replaced by fine- to coarse-grained metasiltstone. Complete sequences are not always present and it is the silty slate interval that is most commonly absent. Many coarse intervals contain silty slate interbeds ranging from millimetre-thick partings to centimetre-thick beds. Sedimentary structures other than minor parallel-laminations in some coarse intervals are not noted. Contacts between intervals are both sharp and gradational, with both types occurring about equally frequently. Gradational contacts are characterized by thin interbedding over several millimetres to a few

centimetres. In many instances, gradational zones are truncated by overlying sequences and no intervening silty slate interval is present, just metawacke-silty slate interbedding. Contacts between individual sequences are generally sharp, although some are gradational over a few millimetres. Overall, the proportion of slate in this unit is approximately 15 %. Metawacke intervals appear to thicken upwards towards the contact with the overlying Unit B, however, this relationship is not well understood, due to the minimal presence of this unit in LL81-5A.

Figure 4.1. Metawacke overlain by silty slate, representing a typical fining-upward sequence from Unit A. Up-section is to the left.

Typical metawackes in this unit are quartz-rich (silt- to sand-sized), with abundant muscovite, carbonate and chlorite and lesser ilmenite and pyrrhotite (in some instances with minor chalcopyrite overgrowths). Quartz has a bimodal size distribution- large subhedral grains lend this lithology its coarseness, whereas smaller grains define much of the groundmass. Ilmenite is present as blebs

oriented parallel to cleavage planes and as disseminated blebs, typically < 0.05 mm in length and diameter, respectively. Pyrrhotite is present as both millimetre-long grains oriented parallel to cleavage planes and disseminated blebs generally < 0.05 mm in diameter. Chlorite is present as a groundmass phase and imparts a light green color to this lithology. Carbonate content generally increases with increasing grain size, often leading to variations in carbonate content within individual intervals, where grain size varies. Significant quantities of silt- and clay-sized grains are present locally in some intervals, resulting in moderate to strong cleavage development. Overall, though, metawackes lack significant cleavage development.

Typical silty slates in this unit are muscovite-rich, with lesser chlorite, quartz, ilmenite and minor pyrrhotite. Muscovite is present as small groundmass grains and as elongate and moderately aligned grains which define a weak to strong slaty cleavage. Ilmenite is present as both cleavage-parallel and disseminated blebs, typically < 0.05 mm in length and diameter, respectively. Pyrrhotite occurs as millimetre-long blebs oriented parallel to cleavage and as disseminated blebs generally < 0.05 mm in diameter, but overall, this phase is not abundant in this lithology.

Minor carbonate veins, generally a few millimetres-thick and discordant to both bedding and cleavage are noted in some areas of this unit. These are not restricted to any one lithology, but are more abundant in coarse intervals. Overall, this unit is sulphide-poor compared to the overlying units.

The contact between units A and B appears to be gradational, as suggested by the presence in Unit A of two thick and widely separated silty slate intervals lithologically equivalent to silty slate found in the lower area of Unit B. A more expansive representation of this unit in LL81-5A would

make location and definition of the contact more precise.

4.2 Unit B

Overall, Unit B is composed of thin-bedded, light-green, metamorphosed, manganiferous meta-argillites and very fine- to fine-grained metawacke over 113 stratigraphic metres. A combination of fine-grained lithologies and extensive post-recovery weathering make characterization of this unit difficult.

Approximately the bottom 25 stratigraphic metres of this unit are characterized by monotonous, thin-bedded (~several centimetres-thick), moderately cleaved, dark grey-green, chloritic, pyrrhotitic, extremely fine-grained silty slate (see Figure 4.2). Bedding contacts are not clearly visible in all parts of this lower section and additionally, no sedimentary structures are noted.

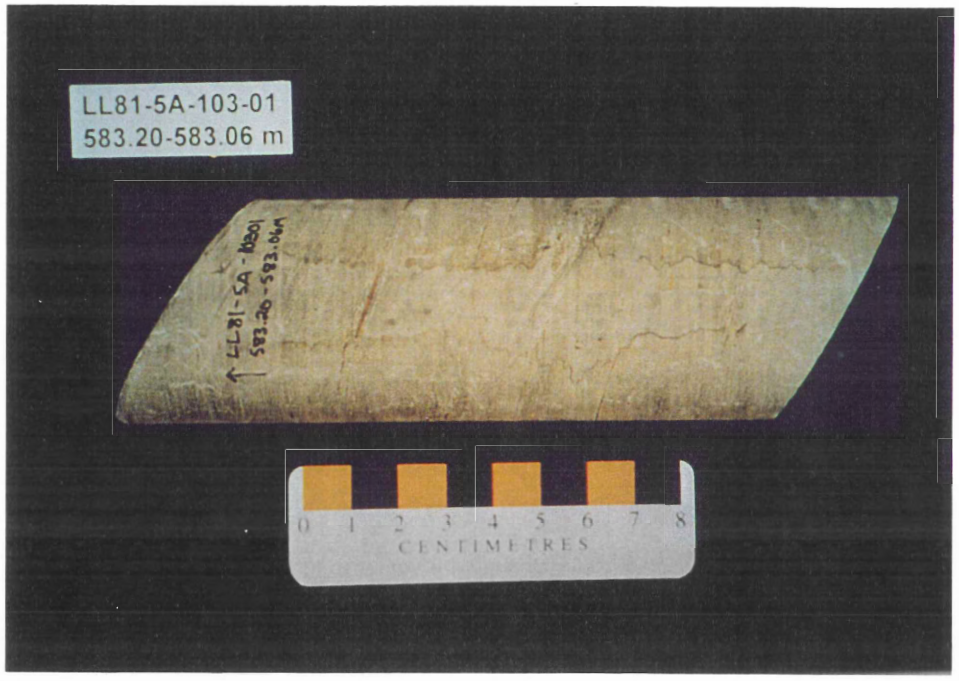

Figure 4.2. Typical chloritic silty slate from Unit B. Up-section is to the left.

Although difficult to define, even in thin section, this lithology is dominated by chlorite and muscovite, with lesser spessartine garnet, ilmenite and pyrrhotite. Garnet is generally idioblastic and disseminated. Chlorite-rich foliation is noted to wrap around many garnet grains in thin section. Garnet lends this lithology coarseness, where present. Ilmenite occurs mainly as cleavage-parallel blebs, but lesser disseminated and often poikiloblastic blebs are common as well. These are generally < 0.05 mm in length and diameter, respectively. Pyrrhotite is present as millimetre-long blebs oriented parallel to cleavage and as smaller disseminated blebs (generally < 0.1 mm in diameter), both locally intergrown with chalcopyrite and ilmenite. Fine-grained carbonate phases are locally abundant, especially where sulphides are present (known mainly due to effervescence in Hcl), but none have been mineralogically defined. Muscovite and chlorite grains large enough to observe, are generally strongly aligned, defining a moderate to strong cleavage.

A calcareous bed of fine- to medium-grained metawacke at ~569.00 m, marks the first appearance of a lithology coarser than silty slate. Above this point, lithologies become more variable and generally coarsen. Thin beds (generally several centimetres-thick) of light grey-green, chloritic, typically calcareous metasiltstone and light grey, often carbonate-rich, very fine- to fine-grained metawackes interbedded with chloritic silty slates similar to those noted above for the lower part of this unit, become common (see Figure 4.3). Normal grading and parallel- and poorly developed ripple cross-laminations are present in some coarser beds. Some coarser beds contain small (diameter of a few millimetres) carbonate-rich, ovoid-shaped inclusions, many with pyrrhotite mineralization. These inclusions are generally aligned with their long axis parallel to bedding planes. Metawacke clasts similar in size and orientation are noted in a few areas. Where observed,

bedding contacts are both sharp and gradational over a few millimetres to a few centimetres, but sharp contacts appear to dominate (both top and bottom of beds). Between 499.97-499.74 m and 497.79-497.46 m, intense tight folding of carbonate-rich silty slate is noted. Laminations are intact and only minimally distorted. Rocks on either side of these folded areas are not disturbed. These lithologies continue stratigraphically upwards to the contact with Unit C.

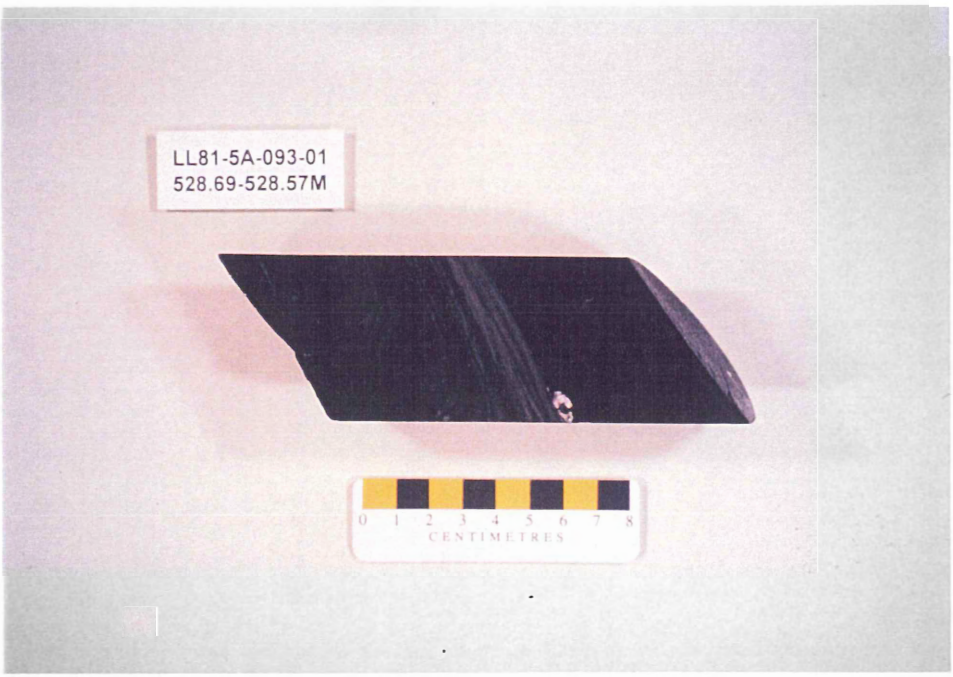

Figure 4.3. Chloritic silty slate overlain by carbonate-rich metasiltstone from Unit B. Convoluted parallel-laminations are present in the metasiltstone and are delineated by the rust color on the core surface. Up-section is to the left.

Mineralogically, metasiltstones and metawackes in this unit are composed of muscovite, chlorite, calcite, quartz and lesser ilmenite and pyrrhotite. Ilmenite and pyrrhotite are both present in the same styles described above for silty slates, but pyrrhotite is present in much smaller quantitites. Calcite-rich coarse lithologies have a rusty appearance when viewed on the core surface. Sulphides are preferentially concentrated in finer-grained lithologies.

Silty slates are mineralogically the same as that described above for the lower part of this unit, but spessartine garnet, pyrrhotite, and chalcopyrite are present in aggregates in some areas, generally with fine-grained, strongly-aligned pressure shadows of muscovite and chlorite. Within many of these aggregates, garnet has overgrown sulphides and in some instances, cleavage-parallel ilmenite blebs. In other instances, what resembles carbonaceous material is present within the cores of garnet grains.

Between approximately 549.70 and 547.00 m, closely-spaced, stratiform, carbonate-rich bands, generally 1-2 mm thick, are present. Host lithologies for these are the same as that noted above (silty slates, metasiltstones and metawackes). Minor pyrrhotite is present in some of these bands, mainly concentrated along contacts with host rock. Some of these bands have a pinch-and-swell appearance. These may represent a poorly-developed form of the structures noted below.

From 495.50 m to the contact with Unit C at 465.50 m, these bands become much more abundant, thicker, more structurally complex and mineralogically divergent from those described above. Thicknesses average ~1 mm, but some exceed 1 cm. Many have a pinch-and-swell or boudinage structure (often with an associated brecciated appearance) (see Figure 4.4), whereas some are folded and convoluted (see Figure 4.5). They appear to be strictly stratiform. Contacts with host rock are generally irregular in thick bands, but straighter and sharper in thin ones.

Mineralogically, these bands are rich in very fine- to coarse-grained quartz, carbonate and spessartine garnet, which imparts a pinkish-white color to the bands (see Figure 4.6). Garnet is idioblastic and generally present in granoblastic aggregates. Carbonate is present in many instances in clumps and is sometimes present within garnet aggregates. Quartz is typically separate from the

other phases, present within its own granoblastic clumps. Many garnet and carbonate aggregates are fractured and quartz is noted to have mineralized within many of these. In deformed bands, quartz grains are often stretched parallel to bedding. Many of these bands host pyrrhotite, generally along contacts with host rock. Minor chalcopyrite is noted in a few bands, but this may be related to cross-cutting calcite-pyrrhotite-rich veins which are present in these cases. Small (< ~0.5 cm in diameter) ovoid-shaped spessartine garnet-carbonate-rich nodules are present close to many of these bands (see Figure 4.7). Foliation, composed mainly of chlorite, is observed wrapping around many of these in thin section. Host rock for these bands and nodules is notably rich in spessartine garnet.

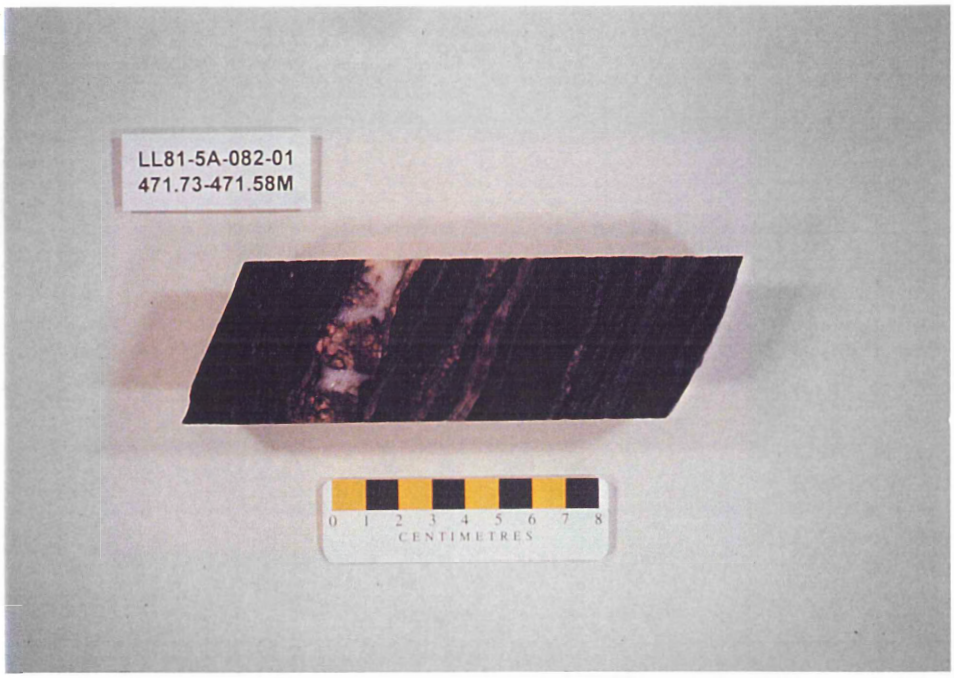

Figure 4.4. Coticule-rich silty slate from Unit B. Note the boudinage structure in the large coticule to the extreme left. Up-section is to the left.

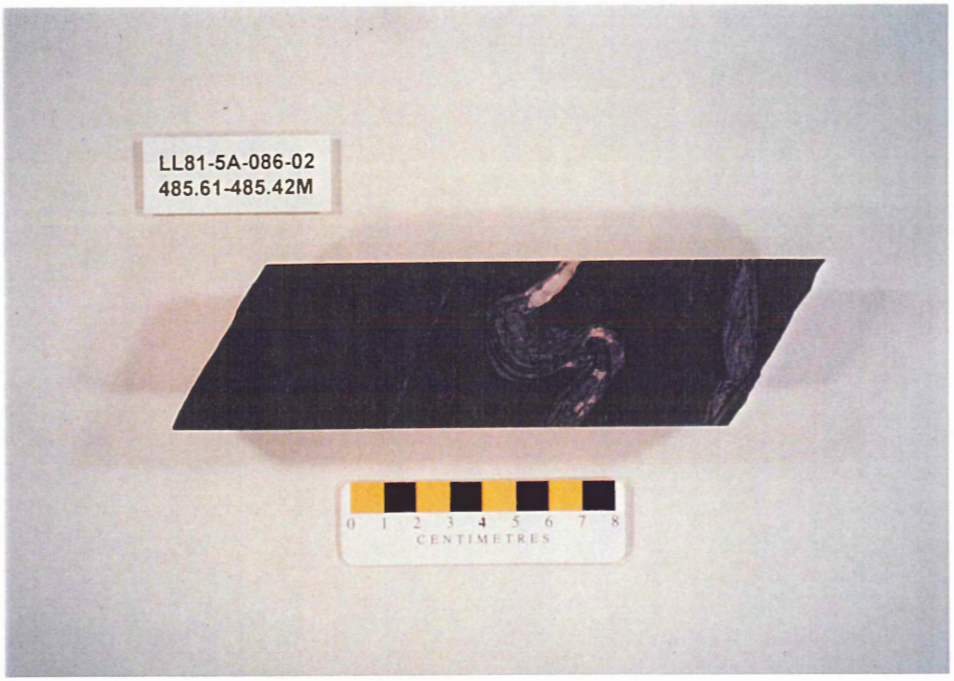

Figure 4.5. Folded coticule in silty slate from Unit B. Up-section is to the left.

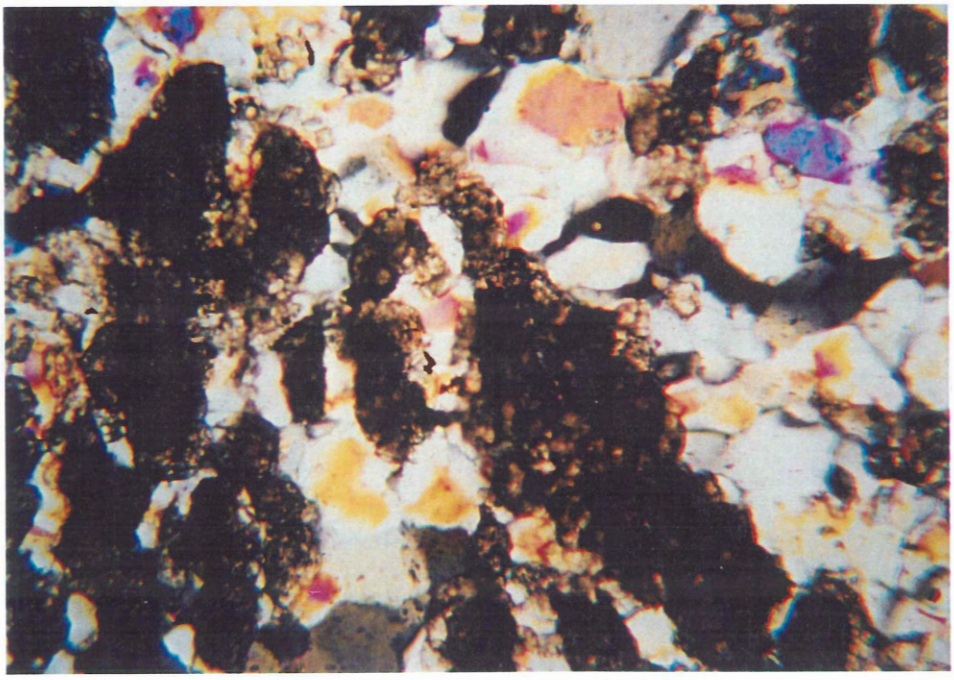

Figure 4.6. Photomicrograph of coticule from sample LL81-5A-082-02, Unit B. Dark clumps are composed of spessartine garnet and carbonate and these are separated by quartz. Photo taken in transmitted light under crossed polars. Field of view is 1.8 mm.

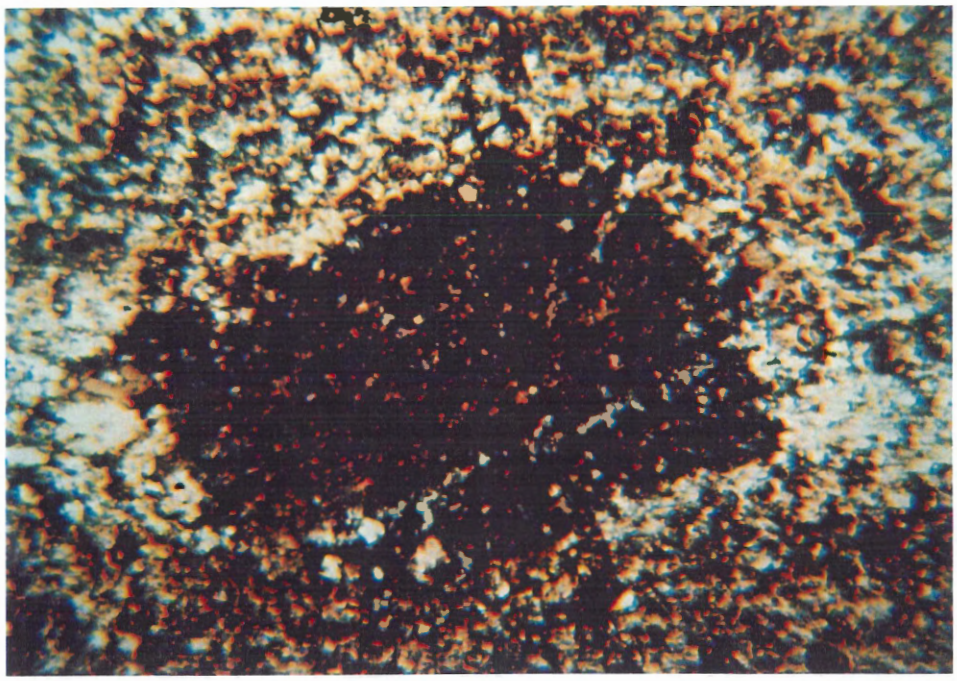

Figure 4.7. Typical spessartine garnet- and carbonate-rich nodule from Unit B (sample LL81-5A-084-01). Photo taken in transmitted light under uncrossed polars. Field of view is 1.8 mm.

Calcite, quartz, and calcite-quartz veins are abundant in the bottom half of Unit B. Veins are generally < 1 cm in width, have both sharp and irregular contacts with host rock and are discordant to both bedding and cleavage. Some of the carbonate veins host pyrite and pyrrhotite and more rarely, chalcopyrite are present, as well. The presence of these veins is not lithologically controlled.

The contact between units B and C is gradational over approximately 5 m. Through this area, the core darkens as the silt content in the slate decreases and carbonaceous material increases in abundance. Pyrrhotite content also increases through the contact zone and minor pyrite and chalcopyrite are present. Coticule and nodule quantity and style remain constant through the zone and only disappear when Unit C lithologies are attained.

4.3 Unit C

Overall, this unit is characterized by metasiltstone interstratified with carbonaceous slate, generally corresponding to base cut-out Bouma sequences of Bouma (1956), over approximately 351 stratigraphic metres. Complete sequences fine upwards and typically consist of a basal interval of parallel-laminated, weak- to moderately cleaved, light grey, locally carbonate-rich, pyrrhotitic, very fine- to coarse-grained metasiltstone, often variable to very fine- to fine-grained metawacke or slaty metasiltstone, succeeded by a ripple cross-laminated interval of the same lithology, followed by an interval of parallel-laminated, dark grey, muddy metasiltstone and capped by an interval of generally featureless, strongly cleaved, locally pyrrhotite-rich, carbonaceous, black slate (see figures 4.8 and 4.9).

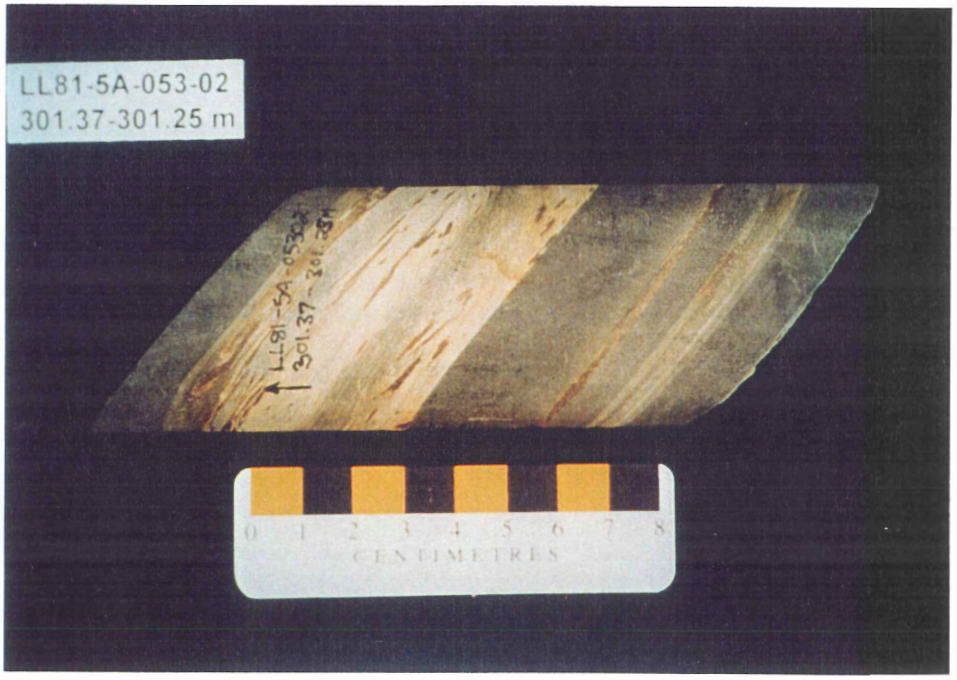

Figure 4.8. Typical base-cut-out Bouma sequence from Unit C. Dewatering has convoluted many laminations. Up-section is to the left.

Individual sequences rarely conform to this complete succession. Ripple cross-laminated metasiltstone and mudstone intervals are absent from many sequences and basal metasiltstone intervals are locally massive. Additionally, grey slate, which is commonly carbonate-rich, is present in many sequences, typically in the place of black slate.

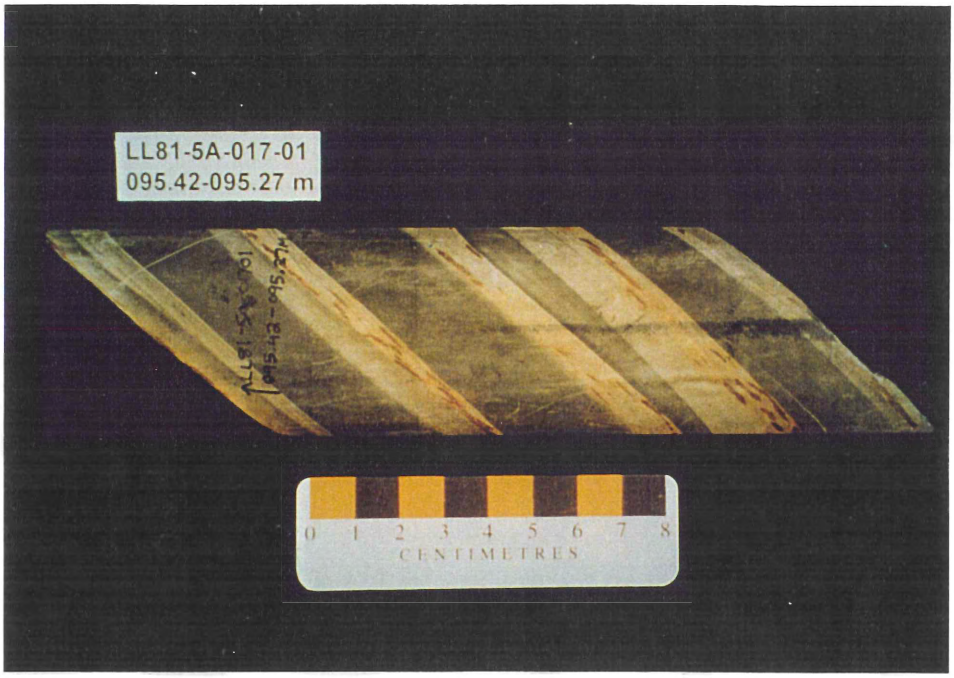

Figure 4.9. Thin-bedded base-cut-out Bouma sequences from Unit C. Note concentration of pyrrhotite in metasiltstone intervals (light colored). Up-section is to the left.

Carbonate content is variable in many metasiltstone intervals. Many intervals have a thin (a few millimetres up to ~5 centimetre-thick) carbonate-rich base (often rusty colored), sharply overlain by a carbonate-poor or carbonate-deficient upper section. Carbonaceous material is noted to vary in quantity between slate intervals, but slates in this unit are always carbonaceous.

Parallel-laminated metasiltstone and carbonaceous slate intervals range from several millimetres up to several decimetres in thickness, whereas ripple cross-laminated metasiltstone and

mudstone intervals rarely exceed 1 cm in thickness. Individual sequences range from a few millimetres in thickness, up to ~0.75 m, but most are less than ~8 cm in thickness. Contacts between metasiltstone intervals are generally gradational, whereas contacts with slate are both sharp and gradational over a few millimetres to a few centimetres, with both types being approximately equally common. Contacts between individual sequences are typically sharp. Metasiltstone and slate are approximately equally common in this unit.

Metasiltstone in this unit is typically dominated by muscovite, quartz and chlorite and contains lesser pyrrhotite, rutile and very minor carbonaceous material Calcite is locally present as well. Pyrrhotite is present as millimetre-long blebs oriented parallel to cleavage planes and as tiny disseminated blebs < 0.1 mm in diameter, locally with rutile overgrowths. Chalcopyrite is locally intergrown with pyrrhotite. Rutile is present as tiny (generally < 0.05 mm along their longest dimension) cleavage-parallel blebs and locally poikiloblastic, disseminated blebs, generally < 0.05 mm in length and diameter, respectively. Some of these blebs are intergrown with and rim disseminated pyrrhotite blebs. Muscovite and chlorite occur as individual groundmass phases that typically define a moderate to strong cleavage, but they are also present in ovoid-shaped porphyroblasts that range in size from << 0.5 mm to as large as ~0.5 mm in diameter (see Figure 4.10). These porphyroblasts are composed of chlorite, but muscovite is found within narrow fractures that have developed in many of them, subparallel to perpendicular to cleavage. Muscovite is also found within cleavage planes that cut across many of these structures. These porphyroblasts are generally strongly oriented parallel to cleavage planes and typically define a strong foliation. These structures have been referred to as chlorite-mica stacks by many authors, including Hicks (1996) who studied them in excellent detail in Meguma Supergroup rocks from the Mahone Bay

area. The origin and development of these is explored in Chapter 5.

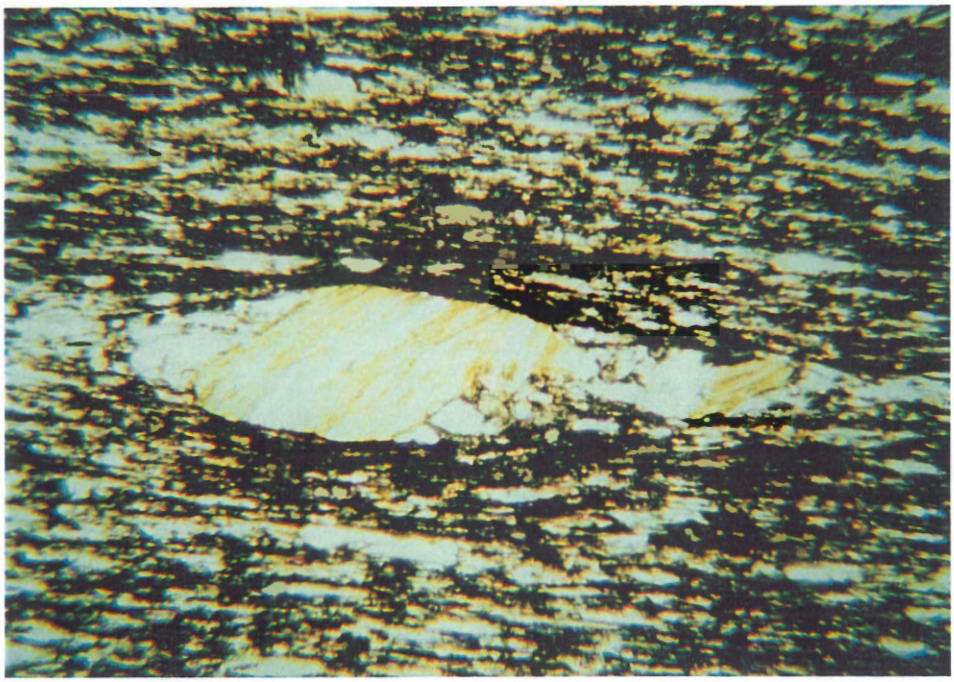

Figure 4.10. Photomicrograph of a typical chlorite-mica stack in black slate from Unit C (sample LL81-5A-081-02). Photo taken in transmitted light under uncrossed polars. Field of view is 1.8 mm.

Black slate in this unit is rich in carbonaceous material and muscovite and contains lesser chlorite, rutile, pyrrhotite and pyrite. Carbonaceous material is present in large enough quantities to render mineral identification difficult in thin section. As in metasiltstone in this unit, chlorite and muscovite are present as individual groundmass phases, but they are also found together in strongly oriented, ovoid-shaped porphyroblasts. These porphyroblasts are more highly concentrated in slate than metasiltstone in this unit. Rutile and pyrrhotitte styles are the same as noted for metasiltstone above, but rutile is additionally noted to fully rim large, cleavage-parallel pyrrhotite blebs in a weathering zone present in the upper region of this unit (discussed in more detail below). Sulphides are preferrentially concentrated in metasiltstone in this unit.

Mineralogically, grey slate in this unit is rich in carbonaceous material, chlorite, muscovite and

typically (an) unknown extremely fine-grained carbonate phase(s) and contains lesser pyrrhotite, rutile, arsenopyrite and pyrite. Strongly aligned muscovite and chlorite results in strong cleavage development in both grey and black slate.

An interesting occurrence in this unit is the presence of dark grey meta-argillites that locally contain very fine-grained cone-like structures, rimmed by (an) extremely fine-grained carbonate phase(s) (see Figure 4.11). Visual and microprobe study reveals little as to the mineralogy of this lithology, due to its small grain size, but microprobe work suggests that calcium and manganese oxides rim the cones, whereas the cones themselves are rich in Si and Al. These meta-argillites locally host pyrrhotite and arsenopyrite, as well. Where present, these cones are rarely well-developed, but where they are, they are found nestled together, with successive cones decreasing in size. When cones are absent, this lithology typically has a mottled appearance. This lithology decreases in abundance upwards in this unit.

Carbonate bands, typically a few millimetres-thick, are present in several locations in this unit. Many have a pinch-and-swell structure and some are extensively convoluted. Pyrrhotite and more rarely pyrite are present in many of these, often lining the contact with host rock. These are very similar to the carbonate bands discussed above for Unit B.

Probable shear zones within carbonaceous slate intervals are common throughout this unit. These zones are generally < 1 cm in width and are marked by broken-up and often powdered slate within an otherwise undisturbed slate interval. Contacts with host rock are typically sharp.

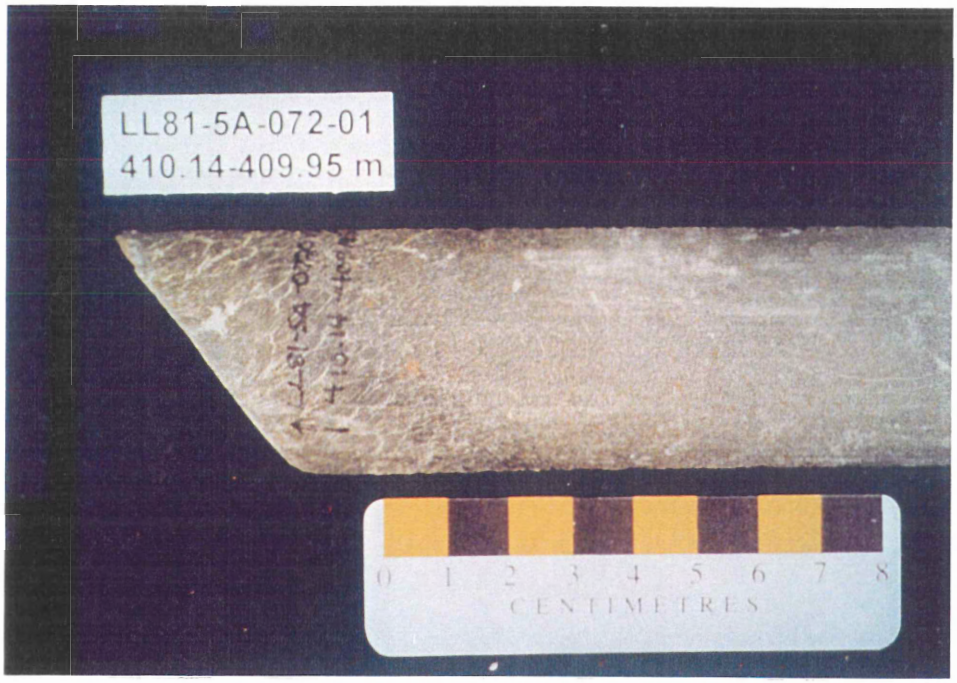

Figure 4.11. Cone-in-cone-type structures present within a carbonate-rich argillite from Unit C. Up-section is to the left.

Extensive soft-sediment deformation structures, including convoluted stratification (see Figure 4.12), load casts and ball-and-pillows (see Figure 4.13) are common in this unit. The first appearance of significant deformation is at ~417 m, but deformation does not become frequent until ~305 m, above which it is present sporadically until approximately the top 50 m of the unit, where it is absent. Soft-sediment deformation is almost exclusively restricted to coarse lithologies.

Veining is common throughout this unit. Most veins are dominated by calcite, but many are quartz-rich and several contain both calcite and quartz. Pyrrhotite is often present and in upper areas of this unit, pyrite is present in many calcite veins. Most calcite veins are < 1 mm thick and some have undergone differential movement, typically normal, on the order of 1-2 mm. In some instances, veins are oriented sub-parallel to each other within small stratigraphic intervals. Thin (1-2 mm wide) fractures lacking significant mineralization are present throughout this unit as well. Veining

is not lithologically controlled; being approximately equally common in both fine and coarse lithologies.

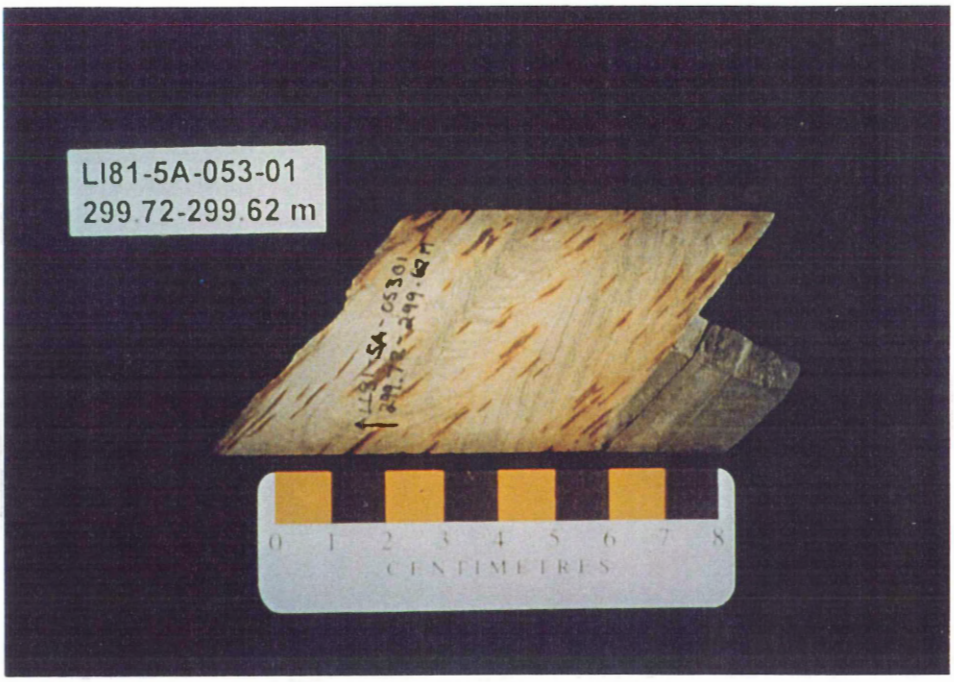

Figure 4.12. Typical convoluted laminations in metasiltstone from Unit C. Up-section is to the left.

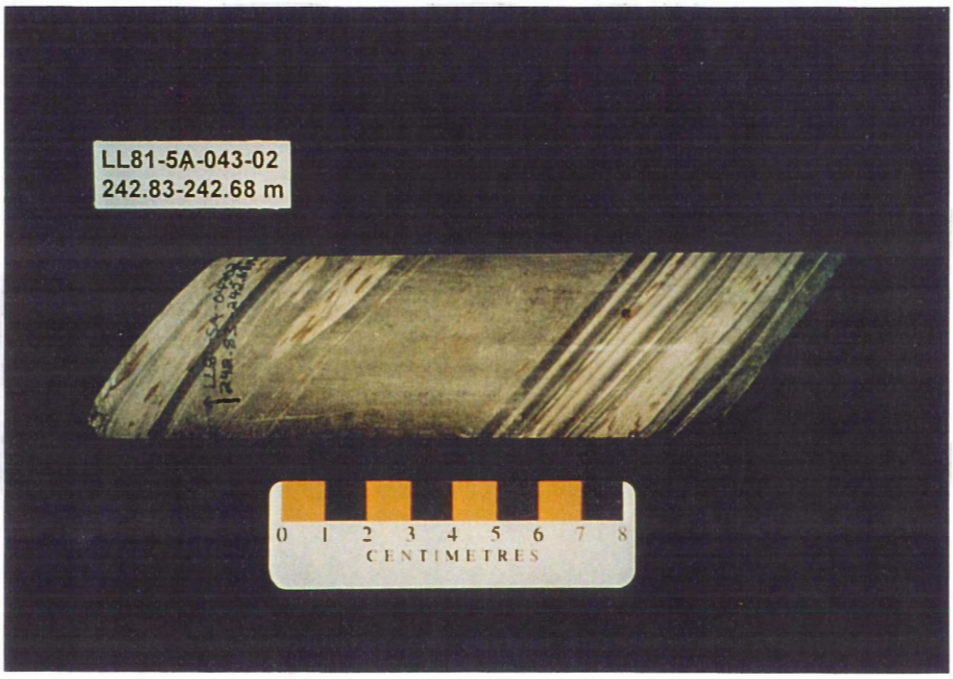

Figure 4.13. Metasiltstone ball structures in grey slate from Unit C. Up-section is to the left.

The upper 135 m of this unit exhibits evidence of extensive weathering, although weathering

was only noted to be present in the top 25.60 m when LL81-5A was recovered and first logged (Sherritt Gordon Mines Ltd., 1981). Within this weathering zone, the core is highly fractured, pyrrhotite has weathered out in many places, the core is stained red and vugs, often with associated pyrite and calcite (dog's tooth spar) mineralization are present. Pyrite blebs, often discordant to both bedding and cleavage are present in a few areas in this zone. Pyrrhotite is generally rimmed with unknown weathering products within this zone, as well.

The top of this unit is not represented in LL81-5A. Approximately 3.40 m of glacial till was unconformably overlying this core when it was recovered (Sherritt Gordon Mines Ltd., 1981) and the contact was angular and erosional.

Unit	Depth (m)	Stratigraphic Thickness (m)		Description
overburden	0.00-3.40			
Unit C	3.40-465.50	351		Fining-upward sequences similar to Bouma sequences of Bouma (1956); typically consisting of a basal interval of parallel-laminated, in part carbonate-rich, pyrrhotitic metasiltstone, overlain by an interval of ripple cross-laminated, metasiltstone, followed by an interval of parallel-laminated mudstone and capped by an interval of locally pyrrhotitic, carbonaceous slate.
Unit B	465.50-589.18	113	32	Similar lithologies as noted immediately below, but with abundant quartz-carbonate- and spessartine garnet-rich bands and nodules.
			56	Interbedded chloritic, manganiferous meta-argillites and very fine- to fine-grained metawacke.
			25	Interbedded pyrrhotitic, chloritic, manganiferous metasiltstones.
Unit A	589.18-628.80	36		Fining-upward sequences of massive, thick-bedded, carbonate-rich, fine- to medium-grained metawacke, overlain by generally thin-bedded silty slates.

Figure 4.14. Simplified scaled stratigraphic log of LL81-5A. See Appendix C for a more detailed version.

4.4 Stratigraphical Discussion

The units delineated and described in sections 4.1-4.3 are interpreted to be equivalent to Meguma Supergroup units in the southwestern Meguma Terrane, noted by Schenk (1995b) and can be correlated with Meguma Group units noted in the Mahone Bay area by O'Brien (1986) and in the central Meguma Terrane noted by Ryan *et al.* (1995) (these are discussed in Chapter 2 and summarized in Figure 4.15). Unit A is interpreted as being equivalent to lithologies found in the Goldenville Group, but has not been divided below this due to its minimal presence in LL81-5A. Units B and C are interpreted as equivalents of the Moshers Island Formation and the Cunard Formation of the Halifax Group, respectively. Assignment of this nomenclature to these units is based mainly on comparison with Meguma Supergroup units defined by Schenk (1995b), visual observations made by the author during a trip to Big Tancook Island, in Mahone Bay, in the fall of 1996, where the GHT is well exposed and easily studied and comparison with a preliminary stratigraphic analysis conducted on LL81-5A by Graves and Zentilli (1988a).

The Sherritt Gordon Mines Ltd. drillcore log for LL81-5A, produced by Vincent Scime, notes the presence of upper Goldenville Formation lithologies at the base of the drillcore, followed by lower Halifax Formation lithologies, divided into lower, middle and upper members. The Goldenville Formation unit conforms to Unit A noted in this study, whereas the basal Halifax member conforms to Unit B and the middle and upper Halifax members conform to Unit C (middle and upper Halifax members were not noted in the present study, only a continuous section of the lower Halifax Group). The units defined by the author in the present study were done so independently of the information presented by Sherritt Gordon Mines Ltd. (1981).

Comparisons between the units delineated in this study and those described in others are

necessary in order to understand regional changes in individual units and relationships between these units within the Meguma Supergroup. Even though units present in LL81-5A represent only approximately 2.3 % of the total stratigraphic thickness of the Meguma Supergroup (based on thickness estimates of Schenk, 1995b for the southwestern Meguma Terrane), this is a fruitful exercise. However, Unit A is only 36 stratigraphic metres-thick and represents a transition between the Goldenville and Halifax groups. The ability to correlate this unit is thus limited. Unit C is thick, but is not stratigraphically bounded and thus it is difficult to draw conclusions based on its thickness, but it *is* possible to correlate it. Unit B is stratigraphically bounded and can thus be relatively easily correlated.

As shown in Figure 4.2, at 113 m, Unit B is substantially thinner than its equivalents in other parts of the Meguma Terrane: 500 m for the Moshers Island Formation in southwestern parts of the terrane (Schenk 1995b); 150-300 m for the Moshers Island Member in the Mahone Bay area (O'Brien, 1986) and 300 m for the Beaverbank Unit in the central Meguma Terrane (Ryan *et al.*, 1995). It can be seen that the equivalents of Unit C seem to thin to the northeast.

Unit C is the thickest unit in LL81-5A, but at 351 m, it is much thinner than its regional equivalents. Because it is not stratigraphically bounded, thickness correlations with its equivalents cannot be undertaken, but its mere presence in LL81-5A in Caribou gold district is important for regional studies.

Comparisons between units noted in this study and those noted in other studies in northern areas of the Meguma Terrane, such as Eastville (MacInnis, 1986; Binney *et al.* 1986) and Lake Charlotte (Hingston, 1985), are extremely important, as this part of the terrane is not as stratigraphically well studied as southern and central areas. These studies were conducted before the

Meguma had been stratigraphically subdivided below formation level and thus, comparisons are difficult. It can be said with confidence, though, that units noted in this study are equivalent, at least in part, to some of those noted at Eastville and Lake Charlotte.

Meguma stratigraphy noted by MacInnis (1986) and Binney *et al.* (1986) for Eastville, includes: a + 30 m-thick basal unit of massive quartz metawacke, overlain by a 30-35 m-thick unit of interbedded massive quartz metawacke and black slate, succeeded by a 7-10 m-thick unit of thin, contorted interbeds of calcareous and manganiferous quartz metawacke and black slate, overlain by a 0-10 m-thick unit of black pyrrhotitic slate and capped by a + 150 m-thick unit of black slate and fine-laminated to cross-bedded quartz metawacke. MacInnis (1986) and Binney *et al.* (1986) interpret the first three units as Goldenville Formation lithologies and the latter two as Halifax Formation lithologies. This stratigraphy is significantly different than that noted for LL81-5A in this study. For example, no massive quartz metawacke unit is noted in LL81-5A and Unit A does not contain black slate, unlike the uppermost Goldenville lithology noted at Eastville. The manganiferous unit at Eastville can be correlated to Unit B in LL81-5A, but it is substantially thinner at Eastville (7-10 m at Eastville compared to 113 m in LL81-5A). Additionally, the manganiferous unit at Eastville is capped by a 0-10 m-thick interval of black slate, which is not noted above the manganiferous unit in LL81-5A. The transition between units B and C is marked by carbonaceous slates interbedded with other argillites and coticules, over approximately 5 m, but this is not as distinctive a zone as that noted at Eastville and is not viewed by this author as a zone of black slate. The uppermost unit at Eastville is equivalent to Unit C in LL81-5A. An additional stratigraphic difference is that MacInnis (1986) and Binney *et al.* (1986) place the manganiferous unit within the Goldenville Formation, whereas in this present study, it is placed within the Halifax Group.

At Lake Charlotte, Hingston (1985) noted the presence of a lower unit of massive quartzite, interpreted as belonging to the Goldenville Formation, followed by a unit of banded, calcareous quartzite, interpreted as occurring at the base of the Halifax Formation and an upper unit of blue slate with occasional interbeds of quartz metawacke, interpreted as typical Halifax Formation lithologies. Hingston (1985) also suggested that a unit of black slate similar to that noted at Eastville may be present between the calcareous unit and the top of the typical Halifax Formation unit. With the exception of the possible unit of black slate, this stratigraphy appears to be quite similar to that noted in LL81-5A in the present study.

Meguma Supergroup Southwestern Meguma Terrane (Schenk, 1995b)		Meguma Group Mahone Bay area (O'Brien, 1986)		Meguma Group Central Meguma Terrane (Ryan *et al.*, 1995)		Meguma Supergroup Caribou gold district (this study)	
Units		Units		Units		Units	
Halifax Group	Rockville Notch Formation 32 m						
	Delanceys Formation 1 850 m						
	Feltzen Formation 2 000 m	Halifax Formation	Feltzen Member 1 000-2 000 m	Halifax Formation	Glen Brook Unit 1 900 m		
	Cunard Formation 8 000 m		Cunard Member 5 000-8 000 m		Rawdon Unit 1 100 m	Halifax Group	Cunard Formation 351 m
	Moshers Island Formation 500 m		Moshers Island Member 150 -300 m		Beaverbank Unit 300 m		Moshers Island Formation 113 m
Goldenville Group	West Dublin (Green Bay area)/ Tancook (Mahone Bay area) formations 1 000 m	Green Bay Formation	West Dublin Member (Green Bay area) (200-300 m) Tancook Member (Mahone Bay area) 600-800 m	Goldenville Formation	Steve's Road Unit 700 m	Goldenville Group	undivided 36 m
	Tancook (Mahone Bay area)/ Rissers Beach (Green Bay area) formations 1 000 m		Rissers Beach Member (Green Bay area)				
	New Harbour Formation +7 000 m	Goldenville Formation	New Harbour Member 1 000 m		Lewis Lake Unit 1 700 m		
					Long Lake Unit 1 100 m		
					Mt. Uniacke Unit 1 200 m		

Figure 4.15. Units and respective stratigraphic nomenclature for the Meguma Supergroup (Group) from several recent studies, compared to units defined in this study. Units are not scaled.

4.5 General Discussion

A number of interpretations can be offered concerning the depositional and post-depositional history of rocks of the GHT at Caribou gold district, based on observations of drillcore Ll81-5A. However, these rocks represent sediments that have undergone extensive changes in mineralogy, texture, color and structure through diagenetic, metamorphic and tectonic processes since their deposition. But, nonetheless, several important deductions can still be offered.

The most obvious interpretation is that the stratigraphic succession of rocks present in LL81-5A represents a rapid and significant change in sedimentary environment, manifested mainly in a fining-upward trend, decreasing bed thicknesses from Unit A through Unit B and an increasing manganese and carbonaceous influence. These changes can only be understood with reference to regional trends in deposition of the GHT.

Waldron (1992) suggested that units of the GHT were deposited in a relatively deep ocean rift-basin, between Gondwanaland (likely the west African margin (Schenk, 1970)) and a continental fragment, possibly Avalonia, that grew progressively anoxic as it became increasingly isolated from general oceanic circulation during relative sea-level rise (see Figure 4.16). Deposition of sands of the upper Goldenville Group in this basin occurred during a lowstand of relative sea-level (Waldron, 1992). It is unclear as to whether relative sea-level rise was eustatic or controlled tectonically. This lowstand allowed large volumes of coarse sediments to be eroded from a source region and delivered to a wide shelf region (Waldron, 1992). These sediments were subsequently redeposited in the basin through turbidity currents (Waldron, 1992). According to Waldron (1992), this lowstand was part of a large series of rapid transgression-regression cycles, superimposed on an overall sea-level transgression in the Meguma basin. These cycles may have been controlled by variations in the rate

of basin subsidence, sea-level change or changes in the volume of sediment supplied from the source region (Waldron, 1992). As the overall sea-level transgression progressed, coarse sediments could not reach the basin and were instead trapped on the flooded shelf (Waldron, 1992). At this time, only fine-grained sediments could be transported and deposited within the basin (Waldron, 1992). The Moshers Island and Cunard formations were deposited in this basin, as turbidity current transported fine-grained sediments to the lower part of a continental rise prism or prodeltaic wedge that prograded over fan deposits of the lower Goldenville Group (Schenk, 1995b).

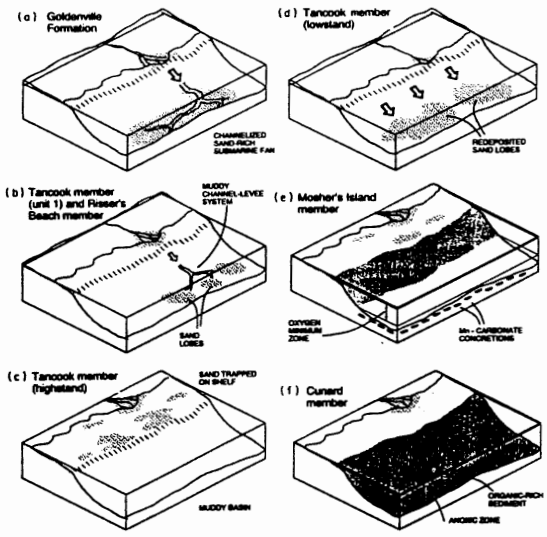

Figure 4.16. Cartoon summarizing the development of the Meguma sedimentary basin and adjacent source craton during deposition of sediments of the Goldenville Group-Halifax Group transition (GHT). a) deposition of large volumes of sandy turbidites during relative lowstand of sea-level. b) sea partially floods craton, resulting in the establishment of a muddy submarine fan, with sand deposited in lobes and channels. c) highstand of sea-level results in craton being flooded and sand supply is consequently cut-off. d) lowstand of sea-level occurs and sand and bioclasitic material is deposited in lobes. e) shelf is flooded, cutting off sediment supply. Laminated, manganese-rich argillites are deposited under progressively anoxic conditions, as the Moshers Island Formation. f) silt reaches shelf break and is redistributed as turbidites of the Cunard Formation. Basin is fully anoxic at this point and black, sulphide-rich shales and siltstones are deposited. Only stages e and f are discussed in text the (after Waldron, 1992).

Fining-upward, predominantly sharply-bounded sedimentary sequences, often hosting successions of sedimentary structures indicative of decreasing water energy, suggest deposition of the rocks present in LL81-5A from gravity flows, likely turbidity currents. These rocks represent sedimentation distal to the sediment sourceland, according to model proposed by Schenk (1970) and discussed in Schenk (1995b). According to Schenk (1995b), an increase in clay-sized sediments in the downstream direction is interpreted as representing deeper water sedimentation, as well.

Changes in basin circulation can account for high levels of manganese in the Moshers Island Formation (discussed more in chapter 6). A strong correlation exists between seawater manganese concentration and anoxic conditions (Brewer and Spencer, 1974; Waldron, 1992). Plankton proliferated at the time of deposition of the Cunard Formation. These organisms contributed significant quantities of carbon to bottom sediments after death, due to anoxic bottom water conditions which prevented oxidation of organic matter (Schenk, 1995b). This anoxia may also explain the deficiency of bioturbation in these units, although worm burrows are present in this unit in the Mahone Bay area (Hicks, 1996). Based on CaO isotope data, Graves and Zentilli (1988b) proposed that organic carbon may have been an abundant constituent of the Moshers Island Formation during deposition, but oxygenation events may have subsequently resulted in oxidation of this carbon during early diagenesis. A consequence of this oxidation was the production of carbonate minerals (Graves and Zentilli, 1988b), which are abundant in this unit. Schenk (1995b) suggested that black slates of the Cunard Formation are similar to black shale deposits in several world-wide localities of Tremadoc through Arenig age, that record a eustatic oceanic anoxic event related to a high-stand of sea-level.

Carbonate-spessartine garnet (Mn-rich)- and quartz-rich bands and nodules noted in Unit B

are equivalent to the coticules and nodules of Schiller and Taylor (1965), who were among the first workers to address the presence of these in Meguma rocks. Spessartine garnet quartzites in the Ardenennes region of Belgium were first termed coticules by Renard (1878, in Schiller and Taylor, 1965). These structures are generally found as thin beds in black, often sulphide-bearing, pelitic rocks and less often, in coarse-grained clastic rocks within Lower Ordvician sections of the Caledonian-Appalachian Orogen in New England, Massachusetts, Newfoundland, Nova Scotia, Ireland, Wales, Norway (Kennan and Kennedy, 1983) and Belgium (Lamens *et al.*, 1986). Coticules are found throughout the Moshers Island Formation of the Halifax Group, as well as sporadically within surrounding units (Graves and Zentilli, 1988b), such as Unit C within LL81-5A. The origin of these structures is elusive, but it has been suggested that they are metamorphosed sedimentary phenomena (Schiller and Taylor, 1965). Fransolet and Kramm (1983, in Graves and Zentilli, 1988b) suggested that coticules may have a protolith that includes: manganiferous sedimentary ironstone, mangnese-rich sand, chert or siliceous sediment rich in montmorillonite. The structural complexity of coticules present in LL81-5A has been previously mentioned. Boudinaged and convoluted and folded coticules are indicative of extensional and compressional forces operating during ductile deformation.

The presence of coticules and mineralogically similar nodules in the Meguma Supergroup can be related to anoxia in the Meguma sedimentary basin. In the Meguma basin, Waldron (1992) proposed that manganese became highly concentrated as anoxic conditions developed. Organic matter produced in sunlit, oxic, surface waters, was oxidized near the sediment-water interface during early diagenesis, generating reducing conditions that stimulated the precipitation of manganese carbonate minerals from pore fluids (Zentilli and Graves, 1988b). Spessartine garnet

in these coticules and nodules subsequently developed during regional metamorphism (MacInnis, 1986). In Unit B, the presence of foliation wrapping around spessartine garnets and garnet-rich nodules suggests that garnet is a pre- and/or syn-tectonic phase.

Anoxia in the Meguma basin is also responsible for the presence of sulphides in rocks of the GHT . δ^{34} S values in the Meguma Supergroup are consistent with closed system sulphate reduction in the anoxic portion of a stratified water column (Sangster, 1992). Pyrite formation during early diagenesis was the initial result of this reduction (Jenner, 1982). Sangster (1992) proposed that seawater sulphate acted as a sulphur source for this process. Pyrrhotite developed from pyrite during early metamorphism (Haysom, 1994). Stratiform pyrrhotite was redistributed along cleavage planes and remobilized within veins and fractures during deformation related to the Acadian Orogeny. The presence of pyrrhotite within cores of spessartine garnets confirms that transformation to pyrrhotite occurred early in the history of these rocks.

Chapter 5
Mineral Chemistry and Petrography

Introduction

Petrographical analyses were conducted on 19 polished thin sections obtained from drillcore LL81-5A, in an attempt to characterize the mineralogy of the main lithologies present. From these 19 thin sections, 6 were selected for mineral chemistry study. Mineral chemistry data were obtained using the JEOL 733 electron beam microprobe at Dalhousie University in February, 1997. This system is equipped with four wavelength dispersive spectrometers and an Oxford Link eXL energy dispersive system. Sixty microprobe analyses were conducted on six samples from LL81-5A, with the following breakdown: 27 sulphide, 18 garnet, 13 oxide and 2 arsenide analyses. A probe spot of approximately 1 μm was used and the microprobe was calibrated using mineralogical standards (garnet, jadeite and kaersutite for silicates and oxides and pyrrhotite and chalcopyrite for sulphides). An energy dispersive spectra, which provided a resolution of 137 eV at 5.9 keV, was employed and analysis of this spectra was conducted with an accelerating voltage of 15 kV and a beam current of 15.47 nA for a period of 40 seconds. Efforts were made to analyse the most common and geochemically significant phases and to acquire results which accurately represent variations in composition both within individual grains, within individual samples and between samples obtained from LL81-5A. Many of the grains analysed are extremely small and were thus difficult to probe. Petrographical and mineral chemistry data discussed in the following sections are presented in appendices B and E, respectively.

This chapter opens with an overview of petrological and petrographical relationships in LL81-5A. This information is already contained in Chapter 4 and in Appendix B and this section is meant

to be a summary companion to these.

5.1 Petrological and Petrographical Overview

Five main lithologies are noted in the three units in LL81-5A (see Table 5.1 below). A cursory glance at the composition of these lithologies presented in Table 5.1 and Appendix B, demonstrates that these lithologies are overall, compositionally similar to one another. In fact, rock texture and absolute percentages of individual phases are the only main differences.

Lithology	Minerals										
	chlorite	muscovite	chlorite-muscovite porphyroblasts	quartz	spessartine garnet	feldspar	rutile	ilmenite	carbonate	carbonaceous material	pyrrhotite
Unit C slates	3	4	2	–	–	–	5	–	–	1	6
Unit C metasiltstones	2	1	4	3	–	–	6	–	7	8	5
Unit B silty slates	1	2	–	7	3	–	–	5	4	–	6
Unit A silty slates	2	1	–	3	–	–	4	–	–	–	5
Unit A metawackes	3	2	–	1	–	5	6	–	4	–	7

Table 5.1. Average scaled relative mineralogical abundances of the main lithologies present in LL81-5A. Number 1 corresponds to the most abundant phase present and increasing numbers denote decreasing average abundance Note that these lithologies are mineralogically quite similar to one another and seem to contrast mainly in relative abundance of individual phases. Only the most common minerals are noted. – = not detected.

As shown above, all lithologies contain large volumes of muscovite and chlorite and an oxide phase. Carbonaceous material and quartz are also common constituents

5.2 Garnet

Garnet is observed only in Unit B, where it is a minor constituent, never present in quantities greater than approximately 10 % by volume. Three distinct styles of garnet are present: 1) small (< ~0.01-0.05 mm in diameter), disseminated, idioblastic grains within chloritic silty slate (see Figure 5.1); 2) small (< ~0.01-0.075 mm in diameter), idioblastic garnets present both individually and within aggregates, in silty slate, with coarse-grained (coarse-grained relative to the fine-grained nature of the lithology) pressure shadows of muscovite and chlorite. Many garnets of this style are noted to overgrow sulphides, generally pyrrhotite and oxide blebs oriented parallel to cleavage planes (see figures 5.1 and 5.2) and some contain what appears to be carbonaceous material within their cores and 3) small (< ~0.01-0.05 mm in diameter) idioblastic grains, present both individually and within granoblastic aggregates (containing up to several dozen grains), within quartz- and carbonate-rich bands (coticules) and nodules (these are discussed more in Chapter 4). In several areas proximal to coticules, strong foliation, composed mainly of chlorite, is noted to wrap around disseminated garnets (see Figure 5.3) and garnet-rich nodules. Of these three styles of garnet present, only examples of 1) and 3) were microprobed.

Overall, these garnets contain between 25 and 33 Wt. % MnO and between 8.8 and 15 Wt. % FeO, along with lesser CaO (1.7-4.8 Wt. %) and minor MgO (see Table 5.2). In general, garnet composition can be expressed by the standard structural formula $A_3B_2(SiO_4)_3$, where site A may host Ca, Mg, Fe^{2+} and Mn^{2+} and site B may incorporate Al, Fe^{3+} and Cr^{3+} (Klein and Hurlbut, 1993). Differentiation of element valences is not possible through microprobing, thus, it is not possible to determine what site(s) Fe in garnet analysed in this study occupies in this formula. Thus,

determining a precise mineralogical formula for these garnets is not possible. However, a general formula of $(Mn, Fe, Ca)_3(Al, Fe)_2(SiO_4)_3$, can be defined. Thus, mineralogically, these garnets are spessartine, with a limited almandine and in some cases grossular, component. However, these are referred to as spessartine garnets throughout this thesis, due to the spessartine dominance.

All garnets analysed are zoned, with MnO decreasing on average 3.43 Wt. % and FeO increasing on average 3.57 Wt. %, from core to rim, as shown in Table 5.2. The majority of grains show a decrease in CaO from core to rim, on the order of < 1 %, as well. No significant compositional differences are noted between disseminated and coticule-hosted garnets.

Sample LL81-5A-	Grain	Analysis	SiO_2	Al_2O_3	FeO (t)	MnO	MgO	CaO	Description of Grain Probed
082-02	1	1	36.20	20.56	9.23	31.83	—	2.09	core of grain outside coticule
082-02	1	2	36.31	20.24	15.04	26.03	0.29	2.18	rim of grain outside coticule
082-02	2	3	37.39	20.63	8.84	32.59	—	2.12	core of grain outside coticule
082-02	2	4	36.53	20.64	14.28	26.30	0.25	2.40	rim of grain outside coticule
082-02	3	5	36.70	20.52	14.37	26.91	—	2.30	core of grain outside coticule
082-02	3	7	36.42	20.38	14.79	25.75	—	2.36	rim of grain outside coticule
082-02	4	8	35.95	20.07	10.50	30.43	—	2.37	core of grain outside coticule
082-02	4	10	36.38	20.48	9.60	30.85	—	2.56	rim of grain outside coticule
082-02	5	9	36.62	20.53	13.08	27.81	0.22	2.25	core of grain within coticule
082-02	5	11	35.99	20.62	12.41	27.47	—	2.26	rim of grain within coticule
082-02	6	12	36.36	20.74	11.27	29.98	0.26	2.39	core of grain within coticule
082-02	6	13	36.83	20.82	14.26	27.50	0.29	1.73	rim of grain within coticule
082-02	7	14	36.57	20.51	12.28	28.95	—	2.63	core of grain within coticule
082-02	7	15	36.58	20.81	15.01	26.61	0.25	1.96	rim of grain within coticule
095-01	8	16	36.53	20.47	9.02	29.05	0.23	3.80	core of grain in silty slate
095-01	8	17	36.71	20.66	13.78	25.60	0.32	3.42	rim of grain in silty slate
095-01	9	18	36.71	20.32	9.59	28.44	—	4.81	core of grain in silty slate
095-01	9	19	36.56	20.62	14.17	25.13	0.28	3.48	rim of grain in silty slate

Table 5.2. Microprobe analyses for garnets in Unit B. Only most abundant oxides are shown. Data are presented as obtained and are not recalculated. See Appendix D for remainder of data and analytical techniques used and see Appendix B for petrographical information concerning these samples. Values are in Wt. %. — = not detected.

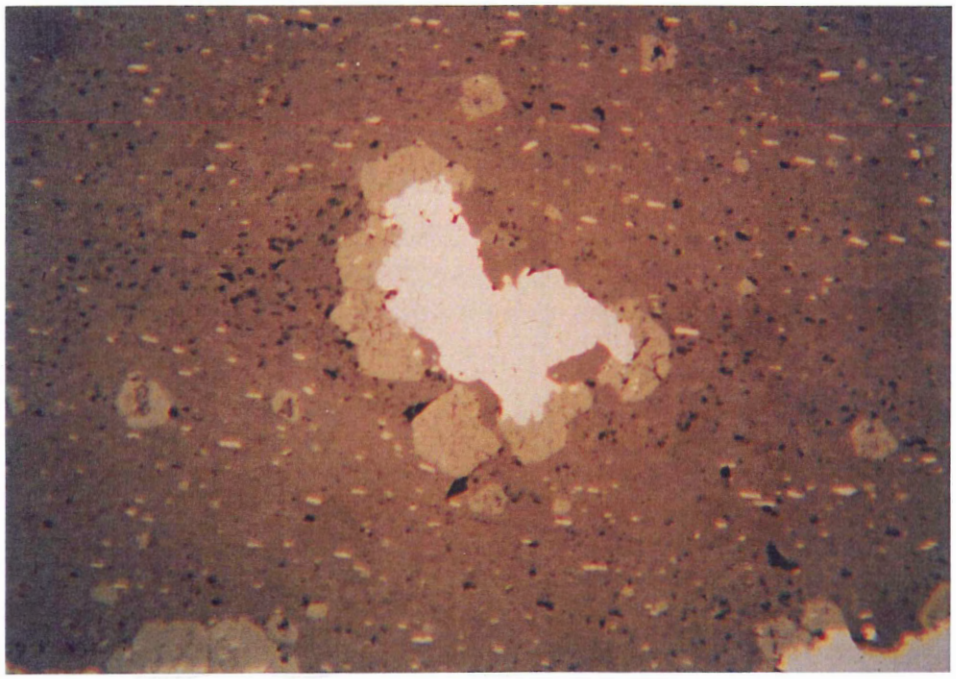

Figure 5.1. Photomicrograph showing an aggregate of spessartine garnet and pyrrhotite within silty slate from Unit B (sample LL81-5A-101-01). Note that garnet has partially overgrown pyrrhotite. Large grains in the surrounding groundmass are spessartine garnet, while the oriented, light-colored grains are ilmenite. Photo taken in reflected light. Field of view is 1.8 mm.

Figure 5.2. Photomicrograph showing aggregate of spessartine garnet and pyrrhotite within a poorly-developed coticule lens from Unit B (sample LL81-5A-081-02). Large grains in the groundmass are spessartine garnet. Light colored grains are ilmenite. Some ilmenite grains are present within garnet. Photo taken in reflected light. Field of view is 1.8 mm.

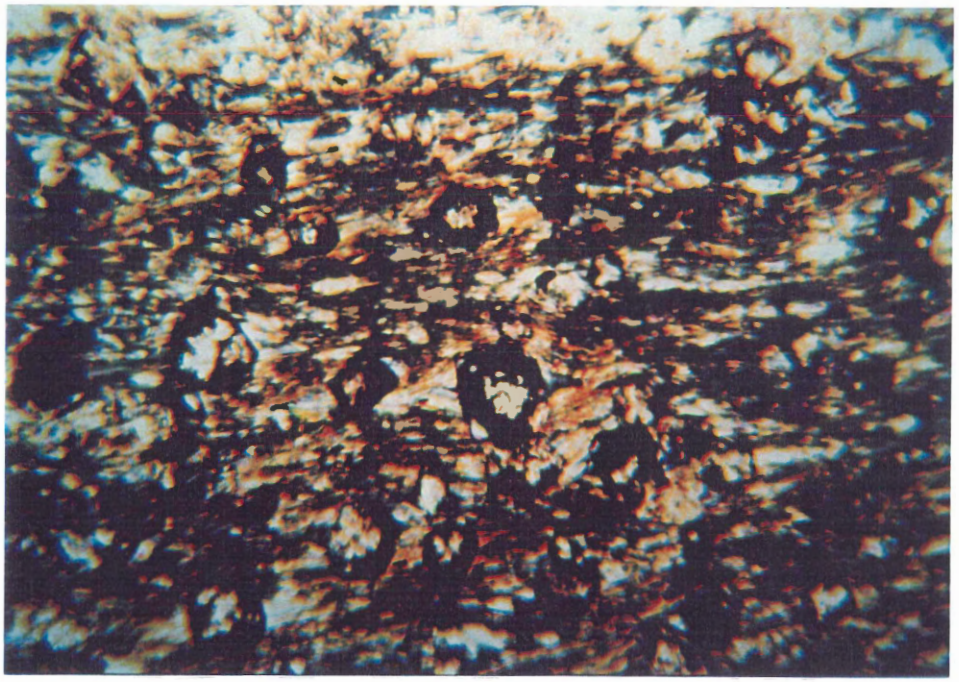

Figure 5.3. Photomicrograph showing relationship between idioblastic spessartine garnet and foliation in Unit B (sample LL81-5A-082-02). Foliation composed mainly of chlorite clearly wraps around garnet grains. Photo taken in transmitted light. Field of view is 1.8 mm.

5.3 Muscovite and Chlorite

Muscovite and chlorite are ubiquitous phases in LL81-5A, present in all lithologies in all three units. In Unit A, muscovite is a major primary and secondary phase. Primary muscovite is present as small anhedral groundmass grains showing few metamorphic effects. Secondary muscovite is present as elongate (generally < 1 mm-long) idioblastic laths, locally defining a slaty cleavage in silty slates and a weak foliation in coarser lithologies. Two cleavages at ~30° to one another, defined by weak- to strongly-oriented muscovite laths, are noted in silty slates in this unit. In sample LL81-5A-107-01, muscovite laths are observed wrapping around large quartz grains. Chlorite appears to be solely a secondary phase in Unit A, present as a minor, fine-grained groundmass phase.

In Unit B, muscovite and chlorite are the major phases present. Both of these are found as extremely fine-grained groundmass phases and they are also the main constituents of pressure shadows associated with garnets and sulphides, noted in section 5.1, above.

Muscovite and chlorite are also the main phases present in Unit C, abundant in both slates and metasiltstones, but moreso in slates. These are present as: groundmass constituents, typically defining a moderate to strong cleavage in both slates and metasiltstones; as coarse-grained pressure shadows on sulphides and garnet and as the defining phases in chlorite-muscovite porphyroblasts, which are extremely common in Unit C slates and less common in metasiltstones in this unit. These porphyroblasts range in size from << 0.5 mm up to ~0.5 mm, along their longest axis. In most samples studied, these structures define a moderate to strong foliation. These porphyroblasts are referred to as chlorite-mica stacks in the literature and are discussed further below. Chlorite and muscovite were not microprobed for this study.

5.4 Quartz

Quartz is present as a major phase in metawackes and metasiltstones in Unit A. In Unit B, it is minor component of pressure shadows on sulphides and garnets and a major constituent in coticules, whereas in Unit C, quartz is present as a major phase in metasiltstones and metawackes. Quartz in Unit A has a bimodal size distribution. In metawackes, small, subround, subhedral to anhedral quartz grains are a major groundmass constituent, along with muscovite and chlorite. Larger (~0.2 mm in diameter), subround, subhedral to anhedral grains, imbedded within this groundmass, are abundant. In silty slates in this unit, quartz is present as abundant, small, anhedral groundmass grains. Quartz in both of these lithologies is noted to bear no major visible effects of

metamorphism and/or deformation. Only the presence of minor undulose extinction suggests that deformation affected this mineral, but whether this is the result of deformation associated with the Acadian Orogeny or whether this is related to pre-Meguma deformation, is unclear.

Quartz present in pressure shadows associated with sulphide and garnet grains in Unit B, is generally elongate, recrystallized and coarse-grained. Within coticules in this unit, quartz is generally present as granoblastic grains in tightly-packed, granoblastic aggregates, separated by carbonate and aggregates of spessartine garnet. In some of these cases, quartz appears to be fracture-filling in garnet-carbonate aggregates. In some instances, quartz is present as elongate grains that have a stretched appearance.

In metasiltstones in Unit C, quartz is present as small, anhedral groundmass grains aligned parallel to cleavage planes. In slates in this unit, quartz is a minor phase and is not generally observed, but when it is, it is present as small, anhedral, foliation-aligned grains, within a strongly oriented muscovite- and chlorite-rich groundmass. No microprobe analyses were conducted on quartz for this study.

5.5 Oxides

Oxides are ubiquitous minor phases throughout LL81-5A. Rutile and ilmenite are the main oxide phases present and rarely exceed 1 % by volume. They occur as extremely small grains, generally < 0.05 mm along their longest axis and, thus are only observed in thin section. Two distinct styles of these phases are noted in LL81-5A: 1) blebs oriented parallel to cleavage which look like prismatic laths in thin section (sections are cut perpendicular to cleavage) (see figures 5.1 and 5.2) and 2) typically idioblastic and commonly poikiloblastic, disseminated blebs.

Unfortunately, it is difficult to discern whether or not overgrown blebs are oriented with cleavage in the groundmass, due to the small-scale and the fact that only small number are noted. Additionally, rutile rims are present on pyrrhotite grains in the upper area of Unit C and many disseminated pyrrhotite blebs throughout this drillcore are overgrown and intergrown with rutile and ilmenite. Cleavage-parallel oxide blebs of unknown composition are locally overgrown with spessartine garnets (see Figure 5.2).

Overall, ilmenite is composed of 48-53 Wt. % TiO_2, 31-43 Wt. % FeO and 3-14 Wt. % MnO and contains lesser amounts of SiO_2, NaO, K_2O and Al_2O_3 (see Table 5.3). Ilmenites analysed can be compositionally defined as (Fe, Mn)TiO_3, where Mn^{2+} has substituted for Fe^{2+}.

Rutile analysed contains 92-99 Wt. % TiO_2, along with lesser SiO_2, Al_2O_3, FeO, CaO and K_2O (see Table 5.3). Rutile analysed in this study is compositionally defined as TiO_2. Extremely limited substitution of Fe^{2+} for Ti^{4+} has occurred (0-0.7 Wt. %) in most samples studied.

The presence of SiO_2, Al_2O_3, K_2O, NaO and CaO in these analyses can be attributed to the presence of inclusions within oxide grains or the occurrence of X-ray diffusion into surrounding groundmass during microprobing (a likely possibility due to the extremely fine-grained nature of these grains). Hingston (1985) noted the presence of small quartz and muscovite inclusions in ilmenite present in GHT rocks from Lake Charlotte, which may account for the presence of these minor components.

Two separate rutile rims on pyrrhotite grains from the upper area of Unit C were analysed. One of these was analysed twice; once in its inward area and once along its outward region. These two analyses show a compositional variation outwards in the rim, with ~5 % decrease in TiO, a

slight decrease in FeO and the appearance of a minor amount of Al_2O_3.

Ilmenite is the only oxide phase noted through units A and B, whereas rutile is the only oxide phase observed in Unit C. This, however, may be misleading because of the limited number of samples analysed. An additionally interesting observation is that Mn content in ilmenite increases through units A and B, but again, this relationship cannot be elaborated upon, again due to the small number of analyses carried out.

Compositional differences are noted between cleavage-parallel ilmenite blebs and disseminated blebs. Disseminated blebs contain up to 12 Wt. % more FeO and up to 11 Wt. % less MnO. Rutile blebs are present in this drillcore, but none were analysed, due to difficulty in locating an appropriate grain to microprobe. It is interesting to note that rutile rims on pyrrhotite grains in Unit C are compositionally quite similar to cleavage-parallel rutile blebs, although, the latter generally contain less TiO_2.

Sample LL81-5A-	Grain	Analysis	SiO_2	TiO_2	Al_2O_3	FeO (t)	CaO	K_2O	Na_2O	Description of Grain Probed
020-01	19	29	0.21	99.21	—	0.69	—	—	—	rutile rim on large pyrrhotite bleb
020-01	20	30	0.20	99.59	—	0.43	—	—	—	inward rim of rutile on large pyrrhotite bleb
020-01	2o	31	2.15	94.76	1.41	0.36	—	0.3	—	outward rim of rutile on large pyrrhotite bleb
020-01	22	32	2.18	91.94	0.96	0.48	—	0.35	—	cleavage-parallel rutile bleb
047-01	17	27	2.40	92.77	1.34	0.36	0.53	0.29	—	cleavage-parallel rutile bleb
047-01	18	28	2.96	96.76	0.37	—	0.35	0.20	—	cleavage-parallel rutile bleb
082-02	13	23	0.19	52.17	—	32.28	—	—	14.44	cleavage-parallel ilmenite bleb
082-02	14	24	0.21	52.30	—	32.89	—	—	14.44	cleavage-parallel ilmenite bleb
095-01	10	220	0.20	52.53	—	36.02	—	—	10.78	cleavage-parallel ilmenite bleb
095-01	11	21	0.20	51.84	—	35.29	—	0.15	11.26	cleavage-parallel ilmenite bleb
095-01	12	22	4.64	48.08	2	31.36	—	0.60	12.12	cleavage-parallel ilmenite bleb
107-01	15	225	—	52.87	—	43.19	—	—	3.26	disseminated ilmenite bleb
107-01	16	26	0.20	53.32	—	42.99	—	—	3.24	disseminated ilmenite bleb

Table 5.3. Microprobe analyses for ilmenite and rutile from all units in LL81-5A. Only the most abundant oxides are shown. Data are presented as obtained and are not recalculated. See Appendix D for remainder of data and analytical techniques used and see Appendix B for petrographical information on these samples. Values are in Wt. %. — = not detected.

5.6 Sulphides

Sulphides are extremely common throughout all three units in LL81-5A. Pyrrhotite is the most common, followed by chalcopyrite. Minor amounts of pyrite are also noted, generally within calcite and calcite-quartz veins in Unit C. Single grains of sphalerite and galena were found through

microprobing, as was minor pentlandite on the side of a grain of pyrrhotite. Only enough data were obtained to accurately assess pyrrhotite, due to a paucity of the others.

Pyrrhotite is noted in all lithologies in LL81-5A. Two main styles are noted: 1) elongate (millimetre-long) blebs oriented parallel to cleavage, resembling laths in thin section (sections are cut perpendicular to cleavage) and 2) tiny, disseminated blebs, generally < 0.05 mm in diameter, locally intergrown with ilmenite and rutile see (Figure 5.4). No significant compositional differences are noted between these two types. Additionally, no substantial compositional differences are noted between cores and rims of individual pyrrhotite grains. Overall, pyrrhotite is close to FeS in composition, with only extremely minor substitution of As, Ni and W in some grains studied.

Cleavage-parallel pyrrhotite blebs in the upper area of Unit C are overgrown with rutile, as discussed in the previous section. Chalcopyrite and sphalerite of standard composition are noted intergrown on the rims of two separate cleavage-parallel pyrrhotite blebs, whereas pentlandite is noted in a vein along the rim of a large, cleavage-parallel pyrrhotite bleb.

An interesting feature of Unit B, is the presence of sulphides, mainly pyrrhotite and chalcopyrite, overgrown by both individual *and* aggregates of spessartine garnet. Garnets do not generally completely overgrow these grains.

Chalcopyrite is a common phase in silty slates in Unit B, where it is easily visible in hand sample, whereas it is a minor to rare phase in Unit A metawackes. Grains are typically elongate (millimetre-long), cleavage-parallel blebs. They are locally intergrown with pyrrhotite.

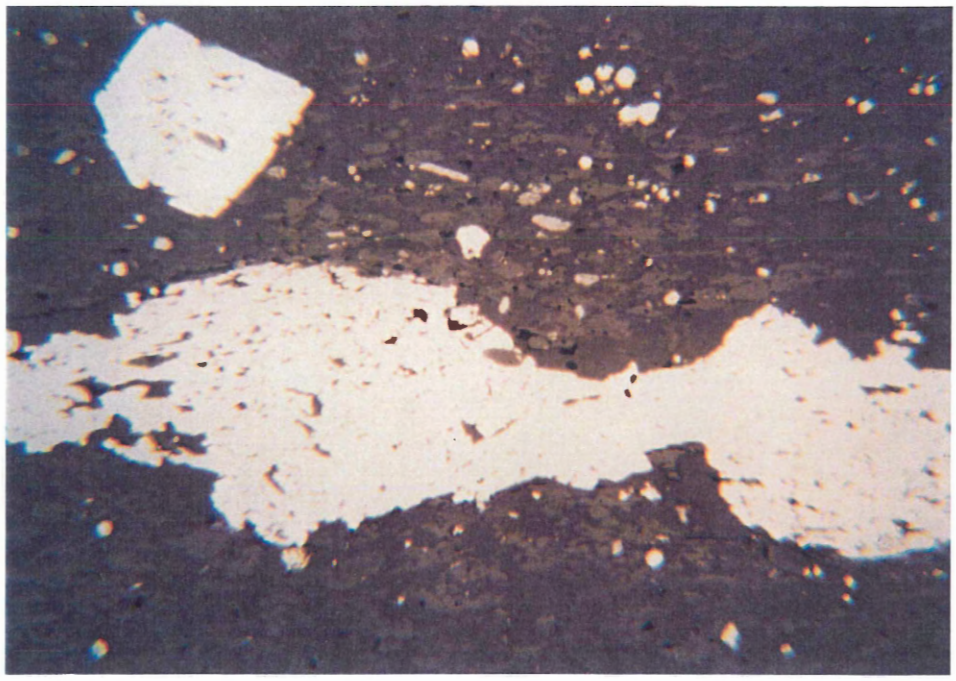

Figure 5.4. Photomicrograph of sulphides in carbonaceous, carbonate-rich slate from Unit C (sample LL81-5A-047-01). Large grain is pyrrhotite, idioblastic grain in the top left corner is arsenopyrite. Small blebs throughout the groundmass are mainly pyrrhotite, with lesser pyrite and rutile. Photo taken in reflected light. Field of view is 1.8 mm.

5.7 Arsenides

Arsenopyrite is noted only within grey slates present in Unit C and generally only within carbonate-rich grey slate. Grains are disseminated and are typically euhedral (see Figure 5.4) and visible in hand sample. Both pyrite and pyrrhotite are present in close association with arsenopyrite in at least one grey slate interval studied. One arsenopyrite grain was microprobed and this showed no compositional variation from core to rim.

5.8 General Discussion

Based upon petrographic observations and mineral chemistry data presented above, it is possible to develop a paragenetic sequence for development of the main phases present in drillcore

LL81-5A. Before this is presented, however, interpretations concerning many of the above observations need to be discussed.

Spessartine garnets are interpreted as metamorphic in origin, due to their idioblastic shape, within a matrix of extensively recrystallized muscovite and chlorite. A pre- and/or syn-tectonic origin is suggested by the presence of foliation wrapping around some of these. The fact that some garnets has overgrown sulphides and oxides, leads to the suggestion that these sulphides may have contributed Mn and/or Fe to garnets. MacInnis (1986) discussed the possibility that Mn-rich sulphides may have contributed Mn to spessartine garnets from Eastville, as may have an Mn-rich carbonate and possibly ilmenite (it is unlikely that sulphide contributed Mn (Milton Graves, pers. comm., 1997). As discussed below, an Mn-rich oxide phase may have contributed to the growth of spessartine garnet. The fact that garnets both within and outside coticules are compositionally equivalent, suggests that both groups developed under similar physical and chemical conditions.

Chlorite-mica stacks are an interesting feature of Unit C. These have been noted and studied in rocks in several areas of the world. Milodowski and Zalasiewicz (1991) studied samples of these stacks preserved at various stages of development in diagenetic concretions in central Wales and concluded that pyroxenes, amphiboles and volcanic rock particles were their precursors. Hicks (1996), studying these structures in rocks of the Meguma Supergroup in the Mahone Bay area of Nova Scotia, interpreted them as pre-tectonic, originally bedding-parallel structures, reoriented and recrystallized through later deformation and metamorphism, until they were perpendicular to cleavage. Deformation also resulted in splitting of these structures along 001 fracture planes parallel to the long axis of the grains (Hicks, 1996). Muscovite then proceeded to grow within dilatant

fracture zones (Hicks, 1996). Stacks noted in the present study are structurally and compositionally similar to those noted by Hicks (1996). Some are noted to have associated pressure shadows. This suggests that they were present in some stage of development before deformation affected these rocks. However, tails that may suggest syn-tectonic rotation are not present. No microprobe analyses were conducted on chlorite-mica stacks in this study.

The sequence of oxide development in rocks of LL81-5A is difficult to interpret. Texturally, cleavage-parallel oxide blebs are interpreted as pre- or syn-kinematic, as they are oriented parallel to foliation. If they were post-kinematic, they would not be expected to be aligned parallel to cleavage. The relative age of the disseminated blebs is less clear. The idioblastic grain shape sharply contrasts with the habits of most other phases present, suggesting that these are not detrital, but possibly diagenetic or metamorphic in origin. However, they may represent grains that have not been fully reoriented parallel to cleavage planes during deformation, possibly supported by the observation that not all cleavage-parallel grains are strongly aligned. Whether they are pre- or post-tectonic is unclear, as these oxides are generally much finer-grained than other phases present and thus their relationship with foliation is difficult to assess. However, compositional differences between cleavage-parallel and disseminated ilmenite blebs (no disseminated rutile blebs were analysed) is great enough to suggest that they were derived from two different mineralization events.

It has been mentioned previously that tiny pyrrhotite blebs are commonly intergrown with ilmenite and rutile. The small size of these intergrowths did not permit microprobe analyses to be conducted, so unfortunately, further elaboration on the relationship between these phases is difficult, as is assessing geochemical and paragenetic relationships between these oxides and other styles of

ilmenite and rutile present in this drillcore. It can be concluded, however, that since pyrrhotite and rutile and ilmenite are intergrown, growth of these phases must have been at least in part, simultaneous.

The presence of Mn-bearing ilmenite coincides with the presence of spessartine garnet in Unit B. This is intriguing, because it was proposed in Chapter 4 that an early Mn-rich carbonate phase contributed at least some Mn for garnet growth. Cleavage-parallel ilmenite (Mn-enriched compared to disseminated blebs) appears to have grown before and/or simultaneously with garnet, with Mn-rich carbonate acting as an Mn source (sulphides may have also contributed Mn). Haysom (1994) notes the presence of ilmenite within spessartine garnet cores and samples from LL81-5A show this feature as well, but none of these were microprobed. Disseminated blebs may have then formed later, possibly post-tectonically and in a Mn-reduced lithological environment (Mn would have already been used to produce garnet and ilmenite in this model). It was discussed in Chapter 4, that pyrite developed in Meguma rocks during early diagenesis and pyrrhotite formed later from this phase during early regional metamorphism (Jenner, 1982). Intergrowths of oxides and pyrrhotite, thus suggests the possibility that at least some of the oxides present in this core are early diagenetic in origin as well, so the possibility exists that an early-formed oxide phase may have been available to supply Mn to spessartine garnets, in conjunction with manganese-rich carbonate.

Another possible interpretation is that an Mn-rich oxide, such as pyrophanite ($MnTiO_3$) developed early in the history of these rocks, possibly during diagenesis, simultaneously with pyrite and an Mn-rich carbonate, then during regional metamorphism, Mn may have been derived from this phase and utilized in spessartine garnet production. Loss of Mn may have resulted in the formation

of ilmenite after pyrophanite. A detrital Mn-rich oxide phase may have instead *or* additionally have present early in the history of these rocks. The Mn-poor ilmenite (disseminated blebs) may have developed later, after garnet formation and possibly after deformation. If the relationship of foliation to these disseminated oxide blebs could be determined, much could be clarified in terms of the paragenesis of these phases. The presence of Mn-bearing phases in units A and B and their absence in Unit C may testify to the local nature of MnO in the sedimentary environment or at least a change in the processes influencing MnO concentration lithologically.

The presence of sulphides overgrown by spessartine garnet has already been discussed, but further elaboration of this relationship is necessary. Sulphides may have provided something that the garnets required during growth, possibly Mn. Based on the presence of Mn-bearing sulphides within cores of spessartine garnet in rocks from Eastville, MacInnis (1986) proposed that sulphides provided Mn that catalyzed the early growth of spessartine garnets. Considering the amount of Mn that seems to have been available during deposition of these rocks, the possibility that substantial quantities of Mn could have been incorporated into sulphides during their growth (discussed in Chapter 4) is a distinct possibility. Unfortunately, the absence of Mn in all but one chalcopyrite analyses (within a primitive coticule) in this study, restricts further elaboration of this possibility. The low-stability of Mn-bearing sulphides (Roy, 1981) may be the reason for their absence in LL81-5A.

A paragenetic sequence can be defined for rocks of LL81-5A. Unfortunately, as can be concluded from the above discussion, such an undertaking is fraught with uncertainty and speculation as not all phase relationships are well understood. Nevertheless, it is an important

exercise.

Pyrite was likely the first secondary mineral phase to develop within sediments of GHT as noted in LL81-5A. This phase developed during early diagenesis (Jenner, 1982) within a progressively anoxic basin (Waldron, 1992). Seawater sulphate acted as a sulphur source (Sangster, 1992), while detrital iron-bearing minerals supplied iron for this process (Haysom, 1994). Detrital oxide phases, such as pyrophanite and ilmenite may have been present at this time, but intergrowths of sulphides and oxides suggest some coincident oxide and sulphide growth. Additionally, the presence of cleavage-parallel oxide grains overgrown by spessartine garnet, demonstrates that at least some oxides were present early in the history of these rocks. Accompanying anoxia in the sediments was an increasing concentration of manganese through deposition of the upper Goldenville Group and Moshers Isand Formation, but Mn concentration declined through deposition of the Cunard Formation (Waldron, 1992). Some of this manganese was likely incorporated into early sulphide and oxide phases. Much of this manganese, however, was probably concentrated in manganese-rich carbonate (MacInnis, 1986) that developed during periodic diagenetic oxidation events. Oxidation of organic matter near the sediment-water interface generated reducing conditions that stimulated the precipitation of manganese carbonate minerals from pore fluids (MacInnis, 1986; Graves and Zentilli, 1988b). Lithification of these sediments occurred as sediments were buried progressively deeper in the basin.

Early metamorphism related to the Acadian Orogeny in the Middle Devonian, resulted in replacement of pyrite with pyrrhotite (Haysom, 1994) and the development of other sulphide minerals, such as chalcopyrite. Ilmenite and rutile and then spessartine garnet, probably formed next.

Ilmenite developed within the upper Goldenville Group and through the Moshers Island Formation, but within the Mn-poor Cunard Formation, rutile developed. Spessartine garnet growth was restricted to the Al- and Mn-rich Moshers Island Formation. Chlorite and secondary muscovite developed at this time, as well.

Deformation resulted in substantial development of foliation and pressure shadows on sulphides, oxides and garnets. Manganese-depleted, disseminated ilmenite blebs appear to have formed after deformation.

When samples of drillcore LL81-5A are observed in thin section (and also in hand sample to some degree), one of the more intriguing characteristics of these rocks is noted to be that metamorphism and deformation seem to have differentially affected each individual unit. Metamorphism and deformation seem to have only minimally affected mineralogies of Unit A, whereas units B and C contain a large volume of secondary phases and recrystallization and extensive reorientation has taken place (moreso in Unit B). Discontinuity in regional metamorphism and deformation would likely not account for variations on this scale. Instead, this contrast can be related to variations in original mineralogies and textures in each unit.

Regional metamorphic grade in the Caribou gold district is chlorite zone, greenschist facies, as it is throughout much of the Meguma Terrane. Two of the prevalent minerals of chlorite zone metamorphism are chlorite and muscovite (Yardley, 1989). Chlorite zone metamorphism of Unit A metawackes would result in chlorite and muscovite development from Al-rich clay present in the matrix. However, less than half of this lithology likely originally consisted of clays and clay-sized minerals from which to develop a secondary mineral assemblage, so secondary mineral development

would be expected to be less than that for the overlying units. A large quantity of fine- to medium-grained quartz is present in this lithology. Additionally, quartz is stable under greenschist facies conditions. This quartz would be expected to increase the structural competence of these metawackes, preventing appreciable flow and internal shear during deformation. Instead, metawackes would likely have just flexed and possibly fractured during deformation. As a result, anything but minor foliation development would not be expected to result.

On the other hand, Unit B meta-argillites were originally clay-rich sediments (Al-rich) (Waldron, 1992). Chlorite zone regional metamorphism of this lithology resulted in production of large quantities of chlorite and muscovite. Coarse-grained phases, such as quartz, were not common in this lithology and so nothing was present to impede deformation. The lower competence of this lithology likely permitted flow and internal shear during deformation. Hence, the large amount of deformation of this lithology.

Unit C is intermediate between units A and B in terms of deformational effects; strong foliation is present, but grains are not extensively recrystallized and grain boundaries are generally sharp. Substantial quantities of chlorite and muscovite developed during metamorphism of the original clay-rich shales and metasiltstones, but sufficient quartz was present to impede strong deformation.

A final comment needs to be made concerning the metamorphic grade of rocks of the GHT present in LL81-5A. The presence of large quantities of chlorite in all three units defines chlorite zone, greenschist facies, regional metamorphic grade for these rocks. The presence of spessartine

garnet in Unit B meta-argillites does not imply garnet zone regional metamorphism. Garnet zone in pelitic rocks is defined by the presence of almandine (Fe-rich) garnet (Yardley, 1989). The abundance of spessartine in pelitic rocks reflects the bulk chemistry of their protoliths and the relatively low temperature of metamorphism (Bennett, 1989). The lower temperature limit of stability of spessartine garnet is much lower than that of almandine (Miyashiro, 1973). Thus, spessartine garnet may form in low-grade pelitic rocks provided that sufficient manganese is available (Bennett, 1989).

Chapter 6
Geochemistry

Introduction

Drillcore LL81-5A was extensively sampled and geochemically analysed by Sherritt Gordon Mines Ltd. (1981) and by Graves and Zentilli (1988a). None of the Sherritt Gordon data are used in this study. Graves and Zentilli (1988a) conducted whole-rock analyses for major elements, trace elements and trace metals from 42 samples, incorporating all major lithologies. Five samples were studied from Unit A, 12 from Unit B and 25 from Unit C. Analytical methods used in this study are noted in Appendix E as are all data referred to in this chapter.

This chapter focuses on developing a general geochemical profile of the stratigraphy of LL81-5A using the geochemical data acquired by Graves and Zentilli (1988a). An absence of multiple silty slate analyses from Unit A (only one was conducted) presents a hindrance to this, since it is unclear how representative this analysis is of this lithology and so only limited amounts of this data are discussed.

Before any geochemical discussion can take place concerning this drillcore, it is necessary to determine or at least speculate, whether there have been any significant post-depositional changes in the bulk chemistry of the rocks in LL81-5A. This is necessary if the geochemical history of the protolith of these rocks in an evolving sedimentary basin is expected to be understood. MacInnis (1986) suggested that metamorphism was isochemical, while Graves and Zentilli (1988b) argued that some of the more mobile elements may have been lost during metamorphism (oxidation of organic carbon in Unit B is not thought to have affected the bulk chemistry of this unit). For the purpose of this study, it is assumed that geochemical properties of LL81-5A closely resemble those

present at the time of deposition of the protolith or shortly thereafter during diagenesis.

6.1 Geochemical Trends in LL81-5A

A number of major geochemical trends can be delineated in this drillcore. Unfortunately, no lithologies studied are continuous in this core ie. no equivalent lithologies are found in all three units in LL81-5A, making it difficult to assess whether or not these trends are lithologically or stratigraphically controlled. Discussion of these trends is undertaken in succeeding sections on major elements and trace elements and metals, respectively. In this section, all trends, enrichments and depletions discussed are relative to rocks present in LL81-5A and do not infer enrichments or depletions in relation to lithological standards or rocks considered more geochemically 'typical' of the Meguma Supergroup. Additionally, all values quoted are geochemical averages, based upon multiple analyses. Average concentrations for all elements discussed are compiled in tables 6.1 (major elements) and 6.2 (trace elements and trace metals).

6.1.1 Major Elements

One of the most noteworthy geochemical trends in this drillcore is the variation in manganese concentration with lithology (see Table 6.1) and stratigraphy (see Figure 6.1). On average, Unit B meta-argillites are enriched 34-fold in MnO over Unit A metawackes (0.15 Wt. % as opposed to 5.07 Wt. %) and are enriched 11- and 30-fold with respect to Unit C metasiltstones and slates. Within Unit B, Mn values increase steadily stratigraphically towards and through the coticule- and nodule-rich zone in the upper region of this unit. However, MnO concentration subsequently sharply decreases at the contact between units B and C and then tapers off upwards through the remainder

of the unit, with concentrations substantially higher lower in the unit, as opposed to the upper portion. This distribution is expected, due to the concentration of ilmenite in units A and B and spessartine garnet in Unit B and an absence of Mn-bearing phases in Unit C.

Sulphur distribution in LL81-5A is also interesting. Overall, average sulphur concentration increases in units A through C (see Table 6.1 and Figure 6.1). Unit A metawackes have an average S concentration of 0.16 Wt. %, which increases 3-fold in Unit B meta-argillites and 11-fold in Unit C metasiltstones and almost 7-fold on average in Unit C slates. Within Unit B, S values increase stratigraphically towards the contact with Unit C. However, S concentration in individual samples in units A and C is erratic, irrespective of lithologies. This S distribution pattern closely correlates with variations in sulphide mineral distribution in LL81-5A, with sulphide concentration reduced in Unit A, increased in Unit B and substantially elevated in Unit C.

The distribution of oragnic C, CO_2 and CaO with stratigraphy is additionally noteworthy. As shown in Figure 6.2, organic carbon concentration is depressed in units A and B, relative to Unit C, which hosts large quantities of carbonaceous slates. On average, the concentrations of CO_2 and CaO are depressed in Unit A metawackes, but are elevated in Unit B meta-argillites and Unit C metasiltstones (Unit C slates contain depressed average levels of these and therefore overall, Unit C is depleted in these relative to Unit B). The stratigraphic distribution of C, CO_2 and CaO can be related to oxidation events in the Meguma sedimentary basin, as explained in chapters 4 and 5. As organic matter originally present in Unit B was oxidized, carbonate was produced (present mainly as carbonate-rich coticules and nodules) accounting for the elevated levels of CO_2 and CaO and depressed levels of organic carbon. Oxidation events were not as important through deposition of

Unit C and thus, organic carbon was not oxidized and remains.

	Unit A metawackes			Unit B meta-argillites			Unit C metasiltstones			Unit C slates		
	mean	standard deviation	# samples	mean	standard deviation	# samples	mean	standard deviation	# samples	mean	standard deviation	# samples
SiO_2	81.28	6.91	4	56.02	6.20	9	70.26	5.22	12	60.56	4.95	12
Al_2O_3	10.05	3.77	4	19.12	2.05	9	14.76	3.36	12	24.47	2.50	12
Fe_20_3	0.49	0.40	4	0.77	0.42	9	2.80	1.20	12	1.90	0.98	12
FeO	2.05	1.27	4	9.18	2.56	9	3.58	0.57	12	3.84	1.24	12
MgO	0.81	0.47	4	2.63	0.50	9	1.63	0.44	12	1.74	0.69	12
CaO	1.03	0.38	4	1.81	1.74	9	2.20	4.42	12	0.13	0.08	12
Na_2O	1.40	0.21	4	0.47	0.26	9	1.24	0.57	12	1.71	0.56	12
K_2O	2.18	0.96	4	3.74	1.32	9	2.44	0.61	12	4.52	0.78	12
TiO_2	0.50	0.13	4	1.05	0.24	9	0.56	0.22	12	0.89	0.43	12
MnO	0.15	0.06	4	5.07	4.64	9	0.45	0.74	12	0.17	0.19	12
P_2O_5	0.06	0.02	4	0.15	0.07	9	0.07	0.02	12	0.07	0.02	12
Total	100			100			100			100		
S	0.16	0.22	4	0.48	0.41	9	1.83	0.68	12	1.39	0.90	12
CO_2	0.57	0.24	4	3.52	0.68	9	1.92	3.43	12	0.02	0.06	12
C	0.19	0.17	4	0.25	0.26	9	0.81	0.75	12	1.88	1.00	12

Table 6.1. Selected whole-rock major element averages for the main lithologies in LL81-5A. All elements are in weight percent (Wt. %). Oxides are recalculated volatile-free (data after Graves and Zentilli, 1988a). See Appendix E for information on samples analysed and analytical techniques used.

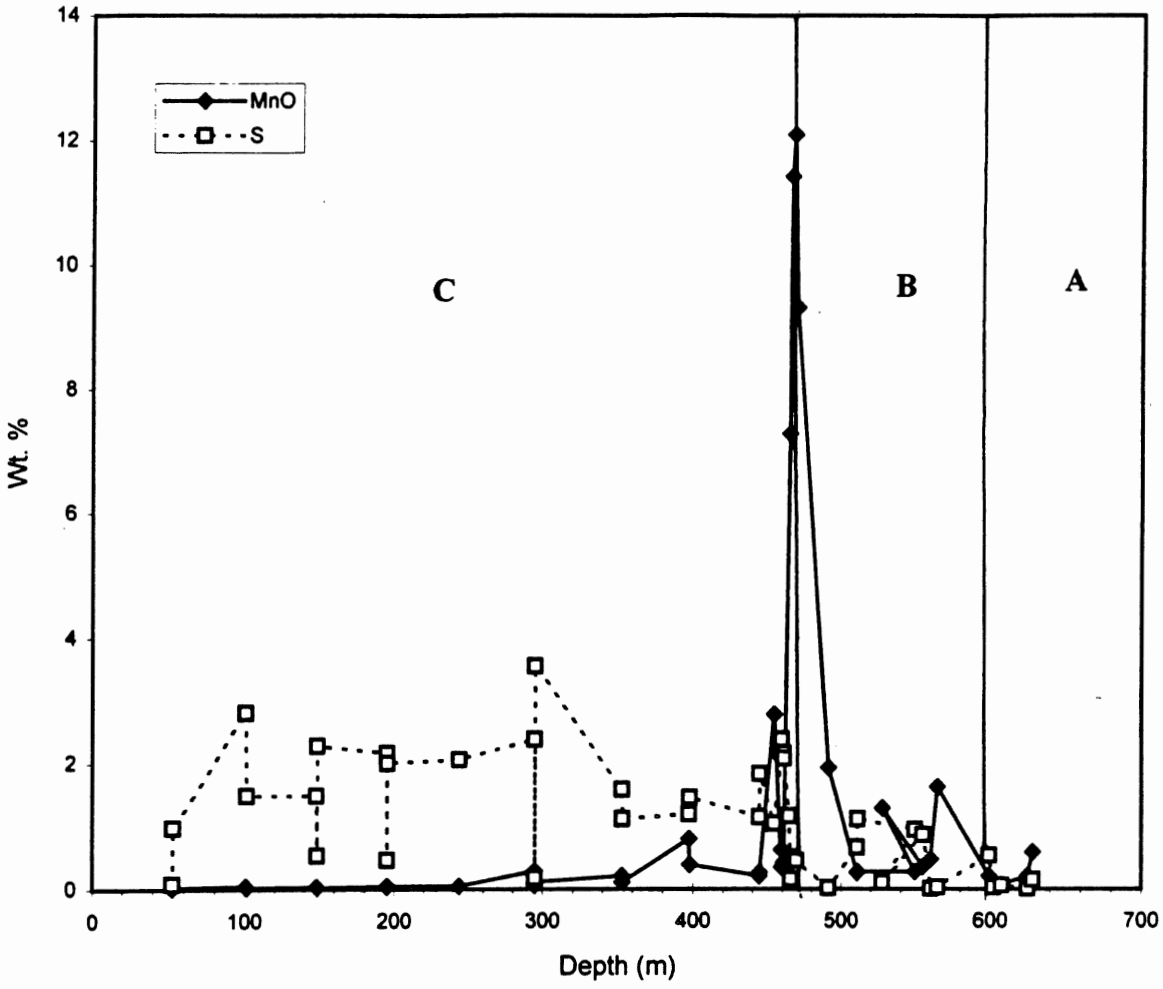

Figure 6.1. Variation in MnO and S with stratigraphy in LL81-5A. Letters A, B and C denote units in LL81-5A, discussed in Chapter 4.

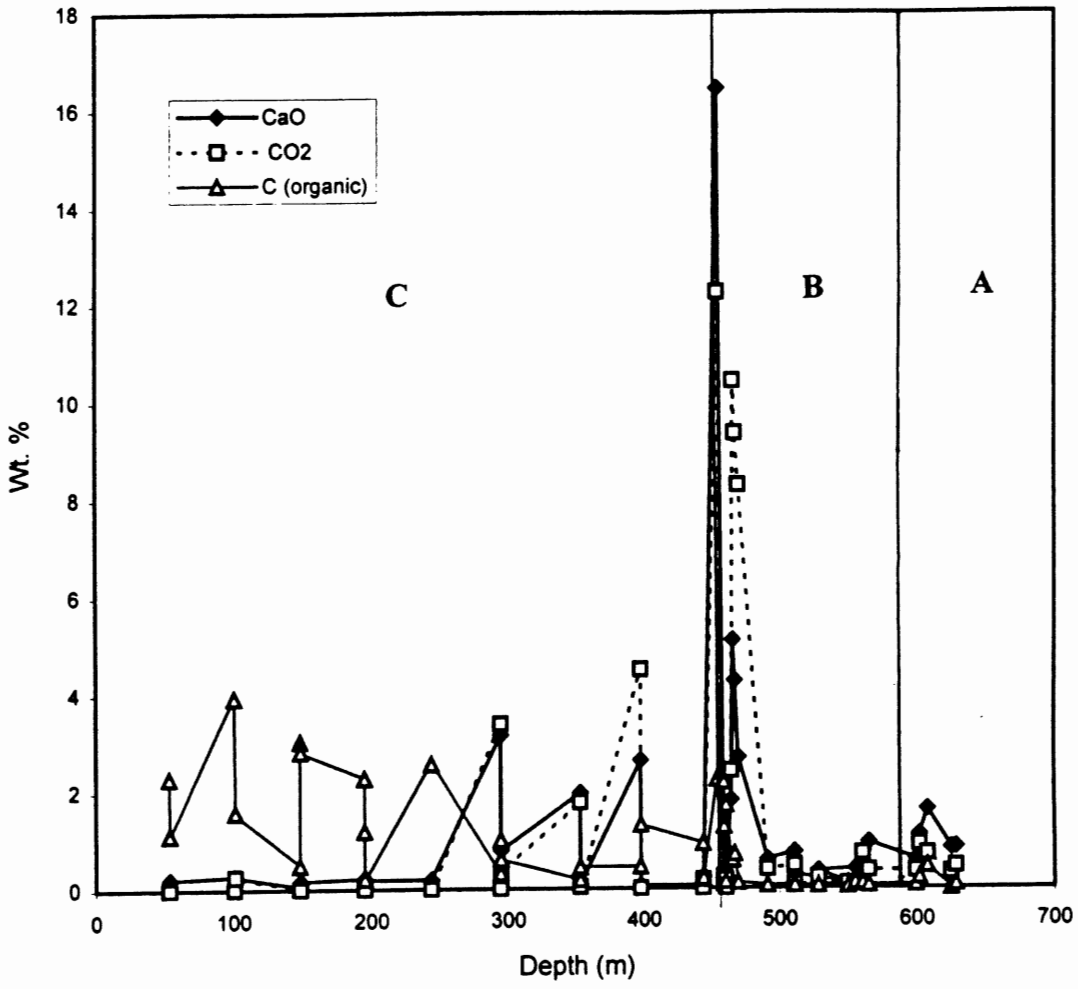

Figure 6.2. Variation in organic C, CO_2 and CaO with stratigraphy in LL81-5A. Letters A, B and C denote units in LL81-5A, discussed in Chapter 4.

6.1.2 Trace Elements and Trace Metals

Perhaps the most interesting geochemical trend in this core is the divergence in trace element and trace metal concentration between meta-argillites and slates in units B and C, respectively and metawacke in Unit A (see Table 6.2). These meta-argillites and slates show average relative enrichment in many trace elements and metals over these metawackes. Barium, Pb, Zn, Cu, Ni, Fe, Co, As and Mo are preferentially concentrated in meta-argillites, while slates are enriched, on average, in Ba, Rb, Sr, Y, V, Cr, Sc, Cs, La, Ce, Th and U. Interestingly, few of these are enriched in *both* Unit B meta-argillites and Unit C slates. Barium, however, is one of these elements, being enriched, on average, 3-fold in meta-argillites and slates over Unit A metawackes. Barium is also depleted in Unit C metasiltstones. In general, however, few relative geochemical anomalies are noted in these metasiltstones.

	Unit A metawackes			Unit B meta-argillites			Unit C metasiltstones			Unit C slates		
	mean	standard deviation	# samples	mean	standard deviation	# samples	mean	standard deviation	# samples	mean	standard deviation	# samples
Ba	463	239	2	1242	281	9	603	148	8	1205	432	7
Rb	92	43	2	128	45	9	80	15	8	160	28	7
Sr	220	18	2	113	22	9	171	80	8	385	126	7
Y	20	7	2	35	2	9	26	12	8	46	10	7
Zr	208	7	2	148	19	9	201	53	8	186	42	7
Nb	11	3	2	14	2	9	11	3	8	16	1	7
Pb	10	2	2	33	48	8	13	5	8	12	2	7
Ga	14	4	2	26	3	9	17	2	8	27	4	7
Zn	56	33	2	121	24	9	83	19	8	96	28	7
Cu	18	15	2	53	33	9	32	10	8	23	13	7
Ni	17	8	2	68	31	9	21	6	8	24	11	7
V	65	31	2	154	37	9	79	25	8	174	20	7
Cr	69	28	2	115	17	9	79	19	8	174	18	7
Sc	7.4	3.4	4	18.2	1.9	9	10.8	3.4	9	24.6	3.8	8
Fe	2.1	1.2	4	8.4	2.1	9	5.9	2.0	9	4.7	1.8	8
Co	8.7	3.1	3	39.2	11.9	5	27.0	21.9	3	24.5	8.4	4
As	10.8	2.5	4	87.2	68.9	9	52.2	86.5	9	5.3	4.6	4
Mo	2.5	1.5	2	27.8	38.4	4	3.0	1.1	9	10.0	4.8	8
Sb	1.0	0.3	4	1.4	0.4	9	0.9	0.4	9	1.9	1.2	8
Cs	4.4	1.6	4	6.4	2.4	9	5.3	1.2	9	11.6	1.6	8
La	3.4	9	4	49	16	9	22	8	9	70	16	8
Ce	65	21	4	103	28	9	47	20	9	129	25	8
Tb	0.8	0.2	3	1.5	0.4	9	4.1	0.3	9	8.9	0.5	8
Yb	0	0	1	3.3	0.5	3	2.7	0.7	6	5.5	0.8	6
Hf	9.0	3.5	4	4.7	1.3	9	8.1	2.9	9	6.0	1.6	8
Ta	0.9	0.1	3	1.0	0.0	4	1.2	0.1	2	1.6	0.5	5
Th	8.9	2.7	4	10.0	2.4	9	8.7	2.5	9	14.4	1.8	8
U	2.1	0.7	4	2.8	1.1	9	2.5	0.8	9	6.0	1.7	8

Table 6.2 Selected whole-rock trace element and trace metal averages for the main lithologies in LL81-5A. Trace elements are in parts per million (ppm). Trace metals are in ppm except gold which is in parts per billion (ppb) (data after Graves and Zentilli, 1988a). See Appendix E for information on samples analysed and analytical techniques used.

6.1.3 Geochemical Correlations

The above exercise is important in assessing geochemical trends in drillcore LL81-5A, but it is not as informative unless concentrations noted are compared with other rocks, especially lithologically similar rocks considered more geochemically typical. Rocks of the Meguma Supergroup stratigraphically distal to the GHT and considered more geochemically typical of the Meguma as a whole can be used, as can international rock standards. The New Harbour Formation is stratigraphically distal to the GHT and may be considered an appropriate Meguma standard for metawackes and slates (geochemically). Whole-rock analyses were conducted on samples obtained from this unit by Graves and Zentilli (1988b) and some of these are presented in Table 6.3. Unfortunately, there are no appropriate Meguma standards for Unit B meta-argillites and Unit C metasiltstones and slates (data on non-geochemically anomalous lithologies distal to the GHT is not available), so only limited intra-Meguma correlations can be undertaken.

Average sandstone and slate standards of Mason and Moore (1982), shown in Table 6.4 and Appendix E, can be used for further comparison with metawackes and slates in LL81-5A. Meta-argillites and slates from units B and C can be contrasted with black shale data of Huyck (1990), as explained below. For ease of discussion, Unit A is examined separately from units B and C, which are discussed together. This is reasonable, because as previously noted, units B and C are metal-rich, fine-grained rocks and as discussed below, the protoliths of these lithologies are considered to be similar.

6.1.3.1 Unit A

Only ~36 stratigraphic metres of Unit A are represented in LL81-5A and as previously mentioned, this unit seems to represent a transition between Goldenville Group lithologies below and Moshers Island lithologies above, so it is difficult to interpret its geochemical trends. Adding to this difficulty is the lack of multiple analyses for silty slates in this unit, as previously mentioned. However, an attempt can be made.

Metawackes in Unit A exhibit elevated average concentrations of MnO (2.5-fold), S (16-fold), CaO and CO_2 (almost 2-fold) and C (9.5-fold), over New Harbour Formation metawacke, as well as greater average amounts of several trace elements and metals, including: Sc, Co, Cs, Ce and W. Unit A metawackes are therefore geochemically much different than more typical Goldenville Group metawacke. The one silty slate analysis from Unit A shows elevated amounts of MnO, S, CaO and CO_2, increased levels of Pb, Cu, Co, Cs and Ce and decreased levels of Sr and Zr, relative to New Harbour Formation slate. These results are not unexpected, however, as Unit A defines the basal part of the GHT in LL81-5A which hosts trace element- and metal enrichment (described below in detail).

When Unit A metawackes are compared to average sandstone, similar concentration variations as those noted above, such as Mn, which is enriched 15-fold in metawackes and S, which is enriched 8-fold. Additionally, most trace elements and metals are present in greater concentration in these metawackes over average sandstone. Unit A silty slates contain greater levels of MnO (enriched 5-fold) than average slate, while most trace elements and metals are present in levels within 1.25-1.5-fold those found in average slate.

	New Harbour Formation metawackes mean	New Harbour Formation slates mean
SiO_2	74.40	62.02
Al_2O_3	13.02	19.66
*Fe_2O_3	4.91	7.38
MgO	1.36	2.32
CaO	0.44	0.40
Na_2O	3.04	2.38
K_2O	2.06	4.57
TiO_2	0.61	0.94
MnO	0.06	0.09
P_2O_5	0.10	0.23
Total	100	100
S	0.01	0.01
CO_2	0.21	0.05
C	0.02	0.01
Ba	507	1241
Rb	74	154
Sr	198	181
Y	21	33
Zr	211	223
Nb	12	18
Pb	14	18
Ga	17	28
Zn	61	94
Cu	16	27
Ni	21	43
V	82	147
Cr	69	120
Sc	—	—
Co	—	—
As	13.7	23.4
Mo	1.0	—
Cs	—	—
La	30	34
Ce	—	—
W	—	—
Au	2.0	1.0
Th	7.3	11.8
U	1.3	2.6

Table 6.3. Selected whole-rock major element, trace element and trace metal averages for New Harbour Formation lithologies from west of the village of Green Bay, Luneneburg County, Nova Scotia. Major elements are in Wt. % recalculated volatile-free. Trace elements are in ppm.Trace metals are in ppm, except gold which is in parts per billion ppb. *Total Fe is expressed as Fe_2O_3 (data after Graves and Zentilli, 1988b). Analytical techniques are the same as those reported in Appendix E for drillcore LL81-5A. — = not detected.

	Average Crust	Average Slate	Average Sandstone
SiO_2	60.28	84.23	63.34
Al_2O_3	15.61	5.05	16.39
Fe_2O_3	7.27	1.50	7.32
MgO	3.52	1.24	3.75
CaO	5.16	5.85	3.35
Na_2O	3.87	0.47	1.40
K_2O	3.17	1.38	3.47
TiO_2	0.74	0.27	0.84
MnO	0.12	0.01	0.12
P_2O_5	0.24	0	0.02
Total	100	100	100
S	0.03	0.02	0.24
Ba	425	50	580
Rb	90	60	140
Sr	375	20	300
Y	33	15	26
Zr	165	220	160
Nb	20	1	11
Pb	13	7	20
Ga	15	12	19
Zn	70	16	95
Cu	55	5	45
Ni	75	2	68
V	135	20	130
Sc	22.0	1.0	13.0
Co	25	1	19
As	2.0	1.0	13.0
Mo	1.5	0.2	2.6
Sb	0.2	0.1	1.5
Cs	3.0	0.5	5.0
La	30	16	24
Ce	60	30	50
Sm	6.0	3.7	5.8
Ta	2.0	0.1	0.8
W	1.5	1.6	1.8
Th	7.2	1.7	12.0
U	1.8	0.5	3.7

Table 6.4. Major element, trace element and trace metal composition of average crust, slate and sandstone. Major elements are in Wt. % recalculated volatile-free. Trace elements and metals are in ppm (data after Mason and Moore, 1982). Average crust is included for comparison.

6.1.3.2 Units B and C

As has been mentioned previously in this study, lithologies in Unit B are extensively recrystallized and most primary sedimentary features are absent. In order to correctly contrast this lithology with others, it is necessary to understand the present nature of this unit as well as the nature of its protolith. Waldron (1992) suggested that the protolith of Unit B was a clay-rich sediment. Graves and Zentilli (1988b) suggested that it had a protolith characteristic of deep-sea, organic-rich, terrigenous sediments (at least the silty slates in this unit). Most meta-argillites in this unit may thus be interpreted as originally organic-rich, fine-grained sediments. Thus, Unit B meta-argillites can be considered to have had a protolith similar to Unit C black slates.

With this in mind, it is possible to compare the geochemistry of both of these lithologies to that of standard black shales to assess enrichment and depletion patterns. However, any comparisons must be done carefully, as there are several, often divergent, definitions of black shale and metalliferous black shale in use (Huyck, 1990). Huyck (1990) proposes that a black shale be defined as a dark colored (grey or black), fine-grained (silt-sized or finer), laminated sedimentary rock that generally is argillaceous and contains appreciable organic carbon (> 0.5 Wt. %) while a metalliferous black shale be defined as a black shale that is enriched in any given element by a factor of 2-fold (with the exception of Be, Co, Mo and U, for which a concentration of 1-fold is sufficient) relative to the proposed United States Geological Survey Standard SDO-1 (U.S.G.S. Devonian Ohio Shale, from Kentucky).

The purpose of the present discussion, therefore, is to compare the geochemical trends noted for Unit B meta-argillites and Unit C black slates, with standard black shale data, in an attempt to

assess similarities and determine relative enrichments and depletions of metals and other elements. Table 6.5 presents geochemical data from the proposed U.S.G.S. black shale standard SDO-01, along with data from Graves and Zentilli (1988a).

	Proposed U.S.G.S. black shale standard SDO-01 (Huyck, 1990)			Drillcore LL81-5A (Graves and Zentilli, 1988a)	
	Recommended[1]	Average[2]	Range[3]	Unit B meta-argillites	Unit C slates
SiO_2	49.28 ± 0.63			56.02	60.56
Al_2O_3	12.27 ± 0.23			19.12	24.47
*Fe_3O_3	9.34 ± 0.21			9.95	5.74
MgO	1.54 ± 0.038			2.63	1.74
CaO	1.05 ± 0.047			1.81	0.13
Na_2O	0.38 ± 0.026			0.47	1.71
K_2O	3.35 ± 0.061			3.74	4.52
TiO_2	0.710 ± 0.031			1.05	0.89
MnO	0.0419 ± 0.005			5.07	0.17
P_2O_5	0.110 ± 0.007			0.15	0.07
S	5.35 ± 0.44			0.48	1.39
CO_2	1.01 ± 0.21			3.52	0.02
C (total)	9.95 ± 0.44				
C (organic measured)			8.98-10.4		
C (organic	9.678 ± 0.452			0.25	1.88
Ba	397 ± 38			1242	1205
Rb		126 ± 3.9		128	160
Sr	75.1 ± 11.0			113	385
Y	40.6 ± 6.5			35	46
Zr	165 ± 24			148	186
Nb	11.4 ± 1.2			14	16
Pb	27.9 ± 5.2			33	12
Ga	16.8 ± 1.8			26	27
Zn	64.1 ± 6.9			121	96
Cu	60.2 ± 9.6			53	23
Ni	99.5 ± 9.9			68	24
V	160 ± 21			154	174
Cr	66.4 ± 7.6			115	160
Sc	13.2 ± 1.5			18.2	24.6
Co	46.8 ± 6.3			39.2	24.5
As	68.5 ± 8.5			87.2	5.3
Mo	134 ± 21			27.8	10.0

	Proposed U.S.G.S. black shale standard SDO-01 (Huyck, 1990)			Drillcore LL81-5A (Graves and Zentilli, 1988a)	
	Recommended[1]	Average[2]	Range[3]	Unit B meta-argillites	Unit C slates
Sb			4.1-4.8	1.4	1.9
Cs		6.9 ± 1.2		6.4	11.6
La	38.5 ± 4.4			49	70
Ce	79.3 ± 7.8			103	129
Tb	1.2 ± 0.31			1.5	2.0
Yb	3.4 ± 0.46			3.3	5.5
Lu	0.52 ± 0.099			0.6	0.9
Hf		4.7 ± 0.75		4.7	6.0
Ta		1.1 ± 0.13		1.0	1.6
W			3.3	5.0	3.3
Au			0.002-0.0035	0.0068	0.0048
Th	10.5 ± 0.55			10.0	14.4
U	48.8 ± 6.5			2.8	6.0

Table 6.5. Geochemical composition of the proposed Unites States Geological Survey (U.S.G.S.) black shale standard SDO-01 (Devonian Ohio Shale, from Kentucky) (data after Huyck, 1990), compared to whole-rock data from Graves and Zentilli (1988a). [1-3] confidence limits in descending order, reflecting decreasing confidence in reported values. Major elements are in Wt. %, trace elements and metals are in ppm. *Total Fe is expressed as Fe_2O_3.

Comparing the geochemical composition of SDO-01 to meta-argillites from LL81-5A, it can be seen that overall, these lithologies are quite similar. Using the definition of enrichment proposed by Hyuck (1990), several metals can be classified as enriched in Unit B meta-argillites, including MnO (up to 137-fold), Ba (up to ~3.5-fold) and Au (up to ~3-fold). Although Hyuck (1990) does not propose an accompanying definition for depletion, many metals in these meta-argillites are present in concentrations significantly less than their respective concentrations in SDO-01. These include Mo (up to ~6-fold less), Sb (up to ~3-fold less) and U (up to ~20-fold less). Additionally, it is also notable that S and C are present in concentrations up to ~10-fold and ~40-fold less, respectively, relative to SDO-01.

According to the definition of a metalliferous black shale proposed by Huyck (1990), Unit B

meta-argillites are classified as metalliferous in Mn, Ba and Au. However, this lithology contains a mean organic carbon concentration of only 0.25 Wt. %. According to the definition of a black shale proposed by Hyuck (1990), shale must contain > 0.5 Wt. % organic carbon in order to be classified as black shale. Therefore, this lithology cannot be classified as the metamorphosed equivalent of metalliferous black shale, but as previously discussed, the protolith of this lithology was likely an organic carbon-rich shale. Oxidation of organic carbon during early diagenesis resulted in manganese carbonate production (Graves and Zentilli, 1988b), but enough organic carbon remained to buffer the trace element and metal content of this lithology (Milton Graves, pers. comm., 1997). Therefore, this lithology, while not presently considered black slate, is metalliferous black slate, according to the definitions of Hyuck (1990).

On the other hand, Unit C black slates are equivalent to metalliferous black slates as defined by Hyuck (1990). Enriched metals include MnO (up to 4-fold), Ba (up to ~3-fold) and Sr (up to ~4.5-fold). Marginally enriched metals include Cr, Sc, La, Cs, La, Tb, Lu and Au. Many metals are present in significantly lesser concentrations relative to SDO-01, including Pb (up to ~3-fold less), Cu (up to 3-fold less), Ni (up to ~5-fold less), As (up to 14.5-fold less), Mo (up to 15.5-fold less) and U (up to 9-fold less). Non-metallic elements present in substantially lesser quantities relative to SDO-01 include S (up to ~4-fold less), CO_2 (up to 61-fold less) and C (organic) (~5-fold less). However, although depleted relative to SDO-01, organic carbon is present at 1.88 Wt. % in Unit C slates. Therefore, using the definitions of black shale and metalliferous black shale proposed by Hyuck (1990), Unit C slates can be classified as the metamorphosed equivalents of metalliferous black shale.

Chapter 7
Conclusions and Recommendations

7.1 Conclusions

1. Drillcore LL81-5A, recovered from Caribou gold district, northeastern Halifax County, Nova Scotia, represents 500 stratigraphic metres of metamorphosed and deformed siliciclastic rocks of the Late Cambrian or older to Early Ordovician Meguma Supergroup, specifically, rocks of the upper Goldenville Group-Halifax Group transition (GHT).

2. Three conformable stratigraphic units are noted in this drillcore. In order of decreasing age, these include: Unit A (36 stratigraphic metres)- composed of fining upward sequences of light-grey, carbonate-rich metawackes and silty slates; Unit B (112 stratigraphic metres)- composed of green, interbedded, manganiferous, pyrrhotitic meta-argillites and very fine- to fine-grained, locally carbonate-rich metawackes and Unit C (351 stratigraphic metres)- composed of fining upward sequences of light-grey, pyrrhotitic, locally carbonate-rich, parallel- and ripple cross-laminated metasiltstone and carbonaceous slate, generally corresponding to base-cut-out Bouma sequences. Soft sediment deformation structures are locally abundant in this unit.

3. These units are equivalent to undivided Goldenville Group lithologies and Moshers Island and Cunard formations of the lower Halifax Group, respectively.

4. Fining-upward, generally sharply-bounded sedimentary sequences, many with a succession of sedimentary structures indicative of upwardly decreasing water energy, suggests deposition of the sedimentary protoliths of these units from gravity flows, likely turbidity currents.

5. Early-formed ilmenite is present throughout units A and B, whereas ilmenite is absent in Unit C and rutile is the dominant oxide present. Early-formed oxides and sulphides are overgrown by pre- and/or syn-deformational spessartine garnet in Unit B. Late-formed, possibly post-deformational, Mn-poor ilmenite is present throughout units A and B, as is late-formed rutile in Unit C. Spessartine garnet in Unit B is found disseminated, in aggregates and in quartz- and carbonate-rich coticules and nodules, which formed during early diagenesis at the expense of manganese carbonate.

6. Unit B meta-argillites host a trace element and trace metal assemblage that includes Ba, Pb, Zn, Ni, As and Mo, and are significantly enriched in MnO relative to other lithologies studied in LL81-5A. Unit C slates contain a trace element and metal assemblage of Ba, Rb, Sr, V, Cr, Sc, Cs, La, Ce and U and are interpreted as metalliferous black slates. Unit A metawackes are depleted in most trace elements and metals relative to the other main lithologies studied, whereas Unit C metasiltstones contain average relative concentrations of most trace elements and metals.

7. Decreasing grain size, an increasing carbonaceous material and trace element and trace metal influence through the GHT in LL81-5A, implies deposition of these sediments within a progressively anoxic, coarse sediment-starved basin.

7.2 Recommendations

- Sedimentological cycles throughout LL81-5A need to be better understood (thinning and thickening of intervals, coarse to fine ratios etc.). These may help further local and regional understanding of the sedimentological development of the GHT.

- More drillcore from Caribou gold district needs to be studied to see if more Meguma stratigraphy is present outside of what is present in LL81-5A. A thicker and more representative section of Goldenville Group lithologies would be valuable for further stratigraphic studies.

- A magnetic susceptibility profile of drillcore LL81-5A might be a useful tool for stratigraphic correlation with other Meguma Supergroup localities.

- Cone-in-cone-type structures present in Unit C are an interesting phenomenon (not restricted to this drillcore) that deserve more attention.

- The weathering zone present at the top of drillcore LL81-5A presents an opportunity to gather acid rock weathering-related information.

- More microprobe work is required to better understand the mineralogies of oxides, sulphides and carbonates.

- Only one whole-rock analysis has been conducted on slates from Unit A. More samples need to be studied in order to properly understand the geochemical properties of this lithology. Location of more Goldenville Group stratigraphy in the district would be helpful in in this regard.

- Studies could be conducted to try to further knowledge on the origin and enrichment of trace elements and metals in LL81-5A.

- A large amount of sulphur isotope data have been gathered on this drillcore that need to be closely studied. This should help further understanding of the genesis of sulphide minerals in this drillcore and in the Meguma Supergroup as a whole.

References Cited

Bell, L.V. 1948. Caribou Mine. *In* Structural geology of Canadian ore deposits. Canadian Institute of Mining and Metallurgy, Jubilee Volume, pp. 927-936.

Bennett, M.A. 1989. Quartz-spessartine metasediments (coticules) and their protoliths in North Wales. Geology Magazine, **126**: 435-442.

Binney, W.P., Jenner, K.A., Sangster, A.L. and Zentilli, M. 1986. A stratabound zinc-lead deposit in Meguma Group metasediments at Eastville, Nova Scotia. Maritime Sediments and Atlantic Geology, **22**: 65-88.

Bouma, A.H. 1962. Sedimentology of some flysch deposits. Elsevier Publishing Company, Amsterdam, 168 p.

Brewer, P.G. and Spencer, D.W. 1974. Distribution of some trace elements in Black Sea and their flux between dissolved and particulate phases. *In* The Black Sea- geology, chemistry, and biology. *Edited by* E.T. Degens and D.A. Ross. American Association of Petroleum Geologists, Memoir 20, pp. 137-143.

Clarke, D.B. and Halliday, A.N. 1980. Strontium isotope geology of the South Mountain Batholith. Geochimica et Cosmochimica Acta, **44**: 1045-1058.

Clarke, D.B., Muecke, G.K. and Chatterjee, A.K. 1985. The South Mountain Batholith: geology, petrology and geochemistry. *In* Guide to the granites and mineral deposits of southwestern Nova Scotia. *Edited by* A.K. Chatterjee and D.B. Clarke. Nova Scotia Department of Mines and Energy, Paper 85-3, preprint, pp. 1-14.

Clarke, D.B., Barr, S.M. and Donohoe, H.V. 1980. Granitoid and other plutonic rocks of Nova Scotia. *In* Proceedings: The Caledonides in the U.S.A. *Edited by* D.R. Wones. I.G.C.P. Project 27: The Caledonide Orogen, Department of Geological Science, Virginia Polytechnic Institute and State University, Memoir 2, pp. 107-116.

Crosby, D.G. 1962. Wolfville map-area, Nova Scotia. Geological Survey of Canada, Memoir 325, 67 p.

Dzulynski, S. and Walton, E.K. 1965. Sedimentary features of flysch and greywackes. Elsevier Publishing Company, Amsterdam, 274 p.

Eberz, G.W., Clarke, D.B., Chatterjee, A.K. and Giles, P.S. 1991. Chemical and isotopic composition of the lower crust beneath the Meguma lithotectonic zone, Nova Scotia: evidence from granulite facies xenoliths. Contributions to Mineralogy and Petrology, **109**: 69-88.

Faribault, E.R. 1899. The gold measures of Nova Scotia and deep mining. Journal of the Canadian Mining Institute, **2**: 119-129.

Faribault, E.R. 1914. Greenfield and Liverpool Town map-areas, Nova Scotia. Geological Survey of Canada, Summary Report 1912, pp. 372-382.

Fransolet, A.M. and Kramm, U. 1983. Mineralogie und petrologie Mn-reiche metapelite. Fortschr. Miner. Bd. **61**: 31-69.

Graves, M.C. and Zentilli, M. 1982. A review of the geology of gold in Nova Scotia. *In* Geology of Canadian gold deposits. *Edited by* R.W. Hodder and W. Petruk. Canadian Institute of Mining and Metallurgy, Special Volume 24, pp. 233-242.

Graves, M.C. and Zentilli, M. 1988a. Geochemical characterization of the Goldenville-Halifax formation transition zone of the Meguma Group, Nova Scotia. Geological Survey of Canada Open File Report 1829, 110 p.

Graves, M.C. and Zentilli, M. 1988b. The lithochemistry of metal enriched coticules in the Goldenville-Halifax transition zone of the Meguma Group, Nova Scotia. *In* Current Research, Part B, Geological Survey of Canada, Paper 88-1B, pp. 251-261.

Harris, I.M. and Schenk, P.E. 1975. The Meguma Group. *In* Ancient sediments of Nova Scotia. *Edited by* I.M. Harris. Eastern Section Society of Economic Paleontologists and Mineralogists, Guidebook, pp. 17-38.

Haynes, S.J. 1986. Geology and chemistry of turbidite-hosted gold deposits, greenschist facies, eastern Nova Scotia, Canada. *In* Turbidite-hosted gold deposits. *Edited by* J.D. Keppie, R.W. Boyle and S.J. Haynes. Geological Association of Canada Special Paper 32, pp. 161-177.

Haysom, S.J. 1994. The opaque mineralogy, petrology, and geochemistry of the Meguma Group metasediments, Rawdon area, Nova Scotia. Unpublished BSc. thesis, Dalhousie University, Halifax, Nova Scotia, 45 p.

Hicks, R.J. 1996. Low-grade metamorphism in the Meguma Group, southern Nova Scotia. Unpublished MSc. thesis, Dalhousie University, Halifax, Nova Scotia, 294 p.

Hingston, R.W. 1985. The manganiferous slates of the Cambro-Ordovician Meguma Group at Lake Charlotte, Halifax County, Nova Scotia. Unpublished BSc. thesis, Dalhousie University, Halifax, Nova Scotia, 67 p.

Huyck, H.L.O. 1990. Metalliferous black shales and related ore deposits: proceedings 1989 United States working group meeting International Geological Correlation Program, Project 254. United States Department of the Interior, United States Geological Survey, Circular 1058, pp. 42-56.

Jackson, C.T. and Alger, F. 1828. Mineralogy and geology of a part of Nova Scotia. American Journal of Science, **XIV**: 305-330.

Jenner, K.A. 1982. A study of sulfide mineralization in the Meguma Group sediments Gold Brook, Colchester County Nova Scotia. Unpublished BSc. thesis, Dalhousie University, Halifax, Nova Scotia, 60 p.

James E. Tilsley and Associates Ltd. 1983. Report on geology, development history and exploration potential. Lake Mine Resources Incorporated, John Logan Enterprises Limited, Nova Scotia Department of Mines and Energy Assessment Report 11E/02B 21-H-07(24), 44 p., 5 maps.

Kennan, P.S. and Kennedy, M.J. 1983. Coticules- a key to correlation along the Appalachian-Caledonian Orogen? *In* Regional Trends in the Geology of the Appalachian-Caledonian-Hercynian-Mauritanide Orogen. *Edited by* P.E. Schenk. NATO ASI Series C, v. 116, pp. 355-362.

Keppie, J.D. 1985. Geology and tectonics of Nova Scotia. *In* Excursion 1- Appalachian geotraverse. *Edited by* J.D. Keppie, K.L. Currie, J.B. Murphy, R.K. Pickerell, L.R. Fyffe and P. St.-Julien. Geological Association of Canada/Mineralogical Association of Canada, Fredericton 85, 181 p.

Keppie, J.D.1979. Geological map of the province of Nova Scotia. Nova Scotia Department of Mines and Energy, 1:500 000.

Klein, C. and Hurlbut, C.S., Jr. 1993. Manual of mineralogy. John Wiley and Sons Inc., United States of America, 681 p.

Krogh, T.E and Keppie, J.D. 1986. Detrital zircon ages indicating a North African provenance for the Goldenville Formation of Nova Scotia. Geological Association of Canada, Program with Abstracts, **11**: 9.

Lamens, J., Geukens, F. and Viaene, W. 1986. Geological setting and genesis of coticules (spessartine metapelites) in the Lower Ordovician of the Stavelot Massif, Belgium. Journal of the Geological Society, **143**: 253-258.

Lane, T.E. 1981. The stratigraphy and sedimentology of the White Rock Formation (Silurian), Nova Scotia, Canada. Unpublished MSc. thesis, Dalhousie University, Halifax, Nova Scotia, 270 p.

Lefort, J.P. and Haworth, R. 1981. Geophysical correlations between basement features in North Africa and eastern New England: and their control over North Atlantic structural evolution. Société géologique et minéralogique de Bretagne, **13**: 103-116.

MacInnis, I.N. 1986. Lithogeochemistry of the Goldenville-Halifax transition (GHT) in the manganiferous zinc-lead deposit at Eastville, Nova Scotia. Unpublished BSc. thesis, Dalhousie University, Halifax, Nova Scotia, 137 p.

Malcolm, W. 1929. Gold fields of Nova Scotia. Geological Survey of Canada, Memoir 156, 253 p.

Malcolm, W. 1976. Gold fields of Nova Scotia. Geological Survey of Canada, Memoir 385 (reprint of Memoir 156 without plates or maps), 253 p.

Mwenifumbo, C.J., Killeen, P.G. and Graves M.C. 1990. Borehole geophysical logging at the Lake Charlotte manganese prospect, Meguma Group, Nova Scotia. *In* Mineral deposit studies in Nova Scotia, Volume 1. *Edited by* A.L. Sangster. Geological Survey of Canada, Paper 90-8, pp. 195-202.

Milodowski, A.E. and Zalasiewicz, J.A. 1991. The origin and sedimentary, diagenetic and metamorphic evolution of chlorite-mica stacks in Llandovery sediments of central Wales, U.K. Geology Magazine, **128**: 263-278.

Miyashiro, A. 1973. Metamorphism and metamorphic belts. George Allen and Unwin, London, 492 p.

Muecke, G.K., Elias, P. and Reynolds, P.H. 1988. Hercynian-Alleghanian overprinting of an Acadian terrane: $^{40}Ar/^{39}Ar$ studies in the Meguma Zone, Nova Scotia, Canada. Chemical Geology (Isotope Geoscience Section), **73**: 153-167.

O' Brien, B.H. 1986. Preliminary report on the geology of the Mahone Bay area, Nova Scotia. *In* Current Research, Part A. Geological Survey of Canada, Paper 86-1A, pp. 439-444.

Pe-Piper, G. and Loncarevic, B.D. 1989. Offshore continuation of Meguma Terrane, southwestern Nova Scotia. Canadian Journal of Earth Sciences, **26**: 176-191.

Pickerill, R.K. and Keppie, J.D. 1981. Observations on the ichnology of the Meguma Group (?Cambro-Ordovician) of Nova Scotia. Maritime Sediments and Atlantic Geology, **17**: 130-138.

Piper, D.J.W. 1978. Turbidite muds and silts on deep-sea fans and abyssal plains. *In* Sedimentation in submarine canyons, fans and trenches. *Edited by* D.J. Stanley and G. Kelling. Dowden, Hutchinson and Ross, Stroudsburg, Pennsylvania, pp. 163-176.

Poole, W.H. 1971. Graptolites, copper and potassium-argon in Goldenville Formation, Nova Scotia. Geological Survey of Canada, Paper 71-1A, pp. 9-11.

Pratt, B.R. and Waldron, J.W.F. 1991. A Middle Cambrian trilobite faunule from the Meguma Group of Nova Scotia. Canadian Journal of Earth Sciences, **28**: 1843-1853.

Renard, A. 1878. Sur la structure et la composition minéralogique du coticule et sur sesrapports avec le phyllade oligistifère. Mémoires Courrronés de l'Académie Royale Belge 41, pp. 42.

Reynolds, P.H., Zentilli, M. and Muecke, G.K. 1981. K-Ar and $^{40}Ar/^{39}Ar$ geochronology of granitoid rocks from southern Nova Scotia: its bearing on the geological evolution of the Meguma Zone of the Appalachians. Canadian Journal of Earth Sciences, **18**: 386-394.

Roy, S. 1981. Manganese deposits. Academic Press, London, 451 p.

Ryan, R.J., Fox, D., Horne, R.J., Corey, M.C. and Smith, P.K. 1995. Preliminary stratigraphy of the Meguma Group in central Nova Scotia. *In* Nova Scotia Department of Natural Resources Report of Activities 1995. Nova Scotia Department of Natural Resources, pp. 27-34.

Sangster, A.L. 1987. Sulphur isotope studies, Meguma Terrane, Nova Scotia, a preliminary report. *In* Nova Scotia Department of Mines and Energy, Report of Activities 1987, Part A. Nova Scotia Department of Mines and Energy, Report, 87-5, pp.207-208.

Sangster, A.L. 1990. Metallogeny of the Meguma Terrane, Nova Scotia. *In* Mineral deposit studies in Nova Scotia, Volume 1. *Edited by* A.L. Sangster. Geological Survey of Canada, Paper 90-8, pp.115-162.

Sangster, A.L. 1992. Light stable isotope evidence for a metamorphogenic origin for bedding-parallel, gold-bearing veins in Cambrian flysch, Meguma Group, Nova Scotia. Exploration Mining Geologist, **1**: 69-79.

Schiller, E.A. and Taylor, F.C. 1965. Spessartite-quartz rocks (coticules) from Nova Scotia. The American Mineralogist, **50**: 1477-1481.

Schenk, P.E. Sequence stratigraphy and Gondwanan provenace of the Meguma Zone (Cambrian to Devonian) of Nova Scotia, Canada. In preparation, 26 p.

Schenk, P.E. 1970. Regional variation of the flysch-like Meguma Group (lower Paleozoic) of Nova Scotia compared to recent sedimentation off the Scotian Shelf. *In* Flysch sedimentology in North America. *Edited by* J. Lajoie. Geological Association of Canada, Special Paper 7, pp. 127-153.

Schenk, P.E. 1981. The Meguma Zone of Nova Scotia- a remnant of Western Europe, South America, or Africa? *In* Geology of North Atlantic borderlands. *Edited by* J.M. Kerr, A.J. Ferguson and L.C. Machan. Canadian Society of Petroleum Geologists Memoir 7, pp.119-148.

Schenk, P.E. 1991. Events and sea-level changes on Gondwana's margin: the Meguma Zone (Cambrian to Devonian) of Nova Scotia, Canada. Geological Society of America Bulletin, 103, pp. 512-521.

Schenk, P.E. 1995a. Annapolis Belt. *In* Geology of the Appalachian-Caledonian Orogen in Canada and Greenland. *Edited by* H. Williams. Geological Survey of Canada, Geology of Canada, no. 6, pp. 367-383 (Also The Geological Society of America, The Geology of North America, v. F-1).

Schenk, P.E. 1995b. Meguma Zone. *In* Geology of the Appalachian-Caledonian Orogen in Canada and Greenland. *Edited by* H. Williams. Geological Survey of Canada, Geology of Canada, no. 6, pp. 261-277 (Also The Geological Society of America, The Geology of North America, v. F-1).

Schenk, P.E. and Adams, P.J. 1986. Sedimentology of the Risser's Beach Member of the Meguma Group (lower Paleozoic) of Nova Scotia: a highly efficient deep-sea fan system. Geological Society of America, Northeastern Section, Abstracts with Programs, **18**: 64.

Seabright Explorations Inc. 1988. Report on exploration and mining histories, prospecting and geological mapping, soil and till geochemical surveys, magnetic, VLF-EM and IP surveys, drilling and drill core assays. M.P. Cullen, P.C. Webster, and R. MacInnis, Eastern Geophysics Limited, Assessment Report 88-275, 1 000 p., 78 maps.

Sherritt Gordon Mines Ltd. 1981. Report on an EM survey and drilling. B. Atkinson, John Logan Enterprises Limited, Burrows, K.C., Assessment Report 11E/02B 21-H-07(15), 198 p., 14 maps.

Smith, P.K. 1984. Summary of the Caribou gold district. Nova Scotia Department of Mines and Energy, Open File Report 585, 55 p., 5 maps.

Stevenson, I.M. 1959. Shubenacadie and Kennetcook map-areas, Colchester, Hants and Halifax counties, Nova Scotia. Geological Survey of Canada, Memoir 302, 88 p.

Stow, D.A.V, Alam, M. and Piper, D.J.W. 1984. Sedimentology of the Halifax Formation, Nova Scotia: lower Paleozoic fine-grained turbidites. *In* Fine-grained sediments: deep water processes and facies. *Edited by* D.A.V. Stow and D.J.W. Piper. Geological Society of London, Special Publication 15, pp. 127-144.

Taylor, F.C. and Schiller, E.A. 1966. Metamorphism of the Meguma Group of Nova Scotia. Canadian Journal of Earth Sciences, **3**: 959-974.

Terry, R.D. and Chilingar, George, V. 1955. Journal of Sedimentary Petrology, **25**: 229-234.

Vine, J.D. and Tourtelot, E.B. 1970. Geochemistry of black shale deposits- a summary report. Economic Geology, **65**: 253-272.

Waldron, J.W.F. 1987. Sedimentology of the Goldenville-Halifax transition in the Tancook Island area, South Shore, Nova Scotia. Geological Survey of Canada, Open File Report 1535, 49 p.

Waldron, J.W.F. 1992. The Goldenville-Halifax transition, Mahone Bay, Nova Scotia: relative sea-level rise in the Meguma source terrane. Canadian Journal of Earth Sciences, **29**: 1091-1105.

Waldron, J.W.F. and Graves, M.C. 1987. Preliminary report on sedimentology of sandstones and bioclastic material in the Meguma Group, Mahone Bay, Nova Scotia. *In* Current Research, Part A, Geological Survey of Canada, Paper 87-1A, pp. 409-414.

Williams, H. 1995c. Summary and Overview. *In* Geology of the Appalachian-Caledonian Orogen in Canada and Greenland. *Edited by* H. Williams. Geological Survey of Canada, Geology of Canada, no. 6, pp. 845-890 (Also The Geological Society of America, The Geology of North America, v. F-1).

Woodman, J.E. 1904. The sediments of the Meguma Series of Nova Scotia. American Geologist, **34**: 13-34.

Yardley, B.W.D. 1989. An introduction to metamorphic petrology. Longman Group UK Limited, England, 248 p.

Appendix A
Samples

Introduction

Sixty-five samples, averaging ~15 cm in length, were collected during logging of drillcore LL81-5A, between July and September, 1996. Sampling was conducted in an effort to obtain samples most representative of lithologies, sedimentary structures, mineralization, deformation structures etc. present. Unique, non-representative features were sampled as well. Samples were collected by cutting the core lengthwise into two equal-sized pieces using a rock saw and archiving one piece of this core and returning the other to the appropriate core box. Nineteen polished thin sections were prepared from 19 of these samples. Of the samples collected, only those that have actually been used in this study are documented in the table below.

Appendix A- Samples

Sample	Depth (m)	Description	Thin Section Produced	Microprobed	Unit
LL81-5A-005-01	029.10-028.96	carbonaceous slate with a large quantity of cleavage-parallel pyrrhotite blebs	Yes	Yes	C
LL81-5A-013-01	075.75-075.50	highly folded, laminated, pyrrhotitic, medium-grained metasiltstone	Yes	No	C
LL81-5A-017-01	095.42-095.27	thin-bedded, fining upward sequences, consisting of convoluted parallel- and ripple cross laminated, pyrrhotitic metasiltstone overlain by muddy, parallel-laminated meta-argillite and capped by carbonaceous slate	No	No	C
LL81-5A-020-01	113.81-113.70	pyrrhotitic, carbonaceous silty slate with an interbed of pyrrhotitic, very fine-grained metasiltstone.	Yes	Yes	C
LL81-5A-034-01	195.56-195.43	folded, silty, carbonaceous slate and very fine-grained metasiltstone, with pyrrhotitic, fine-grained metawacke ball and pillow structures	Yes	No	C
LL81-5A-042-03	237.96-237.84	alternating pyrrhotitic parallel-laminations of carbonate-rich, very fine-grained metawacke and carbonaceous slate, grading into an interval of pyrrhotitic, carbonate-rich metawacke, showing rusty staining in hand sample	Yes	No	C
LL81-5A-042-02	241.01-240.92	parallel-laminated, medium-grained metasiltstone with a crosscutting carbonate-pyrrhotite vein showing normal offset	Yes	No	C
LL81-5A-043-02	242.83-242.68	typical carbonaceous, grey silty slate with pyrrhotitic, fine-grained metasiltstone and fine-grained metasiltstone ball structures	Yes	No	C
LL81-5A-047-01	266.46-266.34	carbonaceous, arsenopyrite- and pyrrhotite-rich slate with minor cone-in-cone-type structures	Yes	Yes	C
LL81-5A-053-02	301.37-301.25	carbonaceous slate interbedded with pyrrhotitic metasiltstone	No	No	C
LL81-5A-053-01	299.72-299.62	convoluted parallel- and ripple cross-laminated, pyrrhotitic, medium-grained metasiltstone	Yes	No	C
LL81-5A-065-01	368.65-368.51	carbonaceous slate with pyrrhotitic, fine-grained metasiltstone interbeds	Yes	No	C
LL81-5A-072-01	410.14-409.95	pyrrhotitic, extremely carbonate-rich, carbonaceous slate with cone-in-cone-type structures	Yes	Yes	C
LL81-5A-081-02	461.88-461.72	carbonaceous slate with pyrrhotitic medium-grained metasiltstone interbed	Yes	Yes	C
LL81-5A-082-02	467.76-467.60	chloritic silty slate with coticules	Yes	Yes	B
LL81-5A-082-01	471.73-471.58	coticule- and nodule-rich, chloritic silty slate,	No	No	B
LL81-5A-084-01	475.10-474.96	chloritic silty slate with coticules and nodules	Yes	No	B
LL81-5A-086-02	485.61-485.42	contorted coticule within chloritic silty slate	No	No	B

Sample	Depth (m)	Description	Thin Section Produced	Microprobed	Unit
LL81-5A-091-01	513.20-513.07	parallel-laminated, chloritic, pyrrhotitic, fine-grained metasiltstone overlain by chloritic, pyrrhotitic, medium-grained metasiltstone	Yes	No	B
LL81-5A-093-01	528.64-528.57	chloritic silty slate overlain by convoluted ripple cross- and parallel-laminated metasiltstone	No	No	B
LL81-5A-095-01	536.48-536.34	chloritic silty slate with poorly-developed coticules	Yes	Yes	B
LL81-5A-101-01	571.95-571.82	chloritic, pyrrhotitic silty slate	Yes	No	B
LL81-5A-105-01	598.71-598.55	carbonate-rich, medium-grained metawacke overlain by silty slate	No	No	A
LL81-5A-107-01	607.04-606.91	carbonate-rich, fine-grained metawacke with a silty slate interbed	Yes	Yes	A
LL81-5A-110-02	627.80-627.70	chloritic silty slate with carbonate- and muscovite- filled fractures throughout, similar to chloritic silty slate seen in Unit B	Yes	No	A

Table E.1. All samples obtained from LL81-5A and used in this study. Depths are drilling depths, not stratigraphic depths. Lithologies are generally based on dominant lithology observed in hand sample and thin section. See Appendix B for thin section information corresponding to samples from which thin sections have been produced. Microprobe data for probed samples is presented in Appendix D. Units corresponding to individual samples are discussed in Chapter 4.

Appendix B
Petrography

Introduction

Nineteen polished thin sections were made from 19 samples collected from LL81-5A, to: identify mineral phases present; determine lithologies present and conduct microprobe analyses. In this appendix, petrographic and lithological information is presented. Discussions of this can be found in chapters 4-6. Appendix E presents microprobe data. Thin section information was acquired using both transmitted and reflected light microscopy, between December, 1996 and January, 1997. Most of the sections analysed are too fine-grained to permit full visual mineralogical study. When mineral percentages have not been assigned, it is because of this fine-grained nature precluding determination. In these cases, minerals are listed in approximate order of relative percentages. Sample depths correspond to the depths of the core samples from which the thin sections have been produced and are not corrected for stratigraphic depth. Mineral percent estimates have been determined using the percent abundance chart of Terry *et al.* (1955). Table B-1 presents a summary of average relative mineralogical compositions of the main lithologies present in LL81-5A. Photomicrographs of selected thin sections are present at the end of this appendix.

Lithology	Minerals										
	chlorite	muscovite	chlorite-muscovite porphyroblasts	quartz	spessartine garnet	feldspar	rutile	ilmenite	carbonate	carbonaceous material	pyrrhotite
Unit C metasiltstones	2	1	4	3	–	–	6	–	7	8	5
Unit C slates	3	4	2	–	–	–	5	–	–	1	6
Unit B silty slates	1	2	–	7	3	–	–	5	4	–	6
Unit A metawackes	3	2	–	1	–	5	6	–	4	–	7
Unit A silty slates	2	1	–	3	–	–	4	–	–	–	5

Table B.1. Average scaled relative mineralogical abundances of the main lithologies present in LL81-5A, as reproduced and discussed in Chapter 5. Number 1 corresponds to the most abundant phase present and increasing numbers denote decreasing average abundance Note that these lithologies are mineralogically quite similar to one another and seem to contrast mainly in the relative abundance of individual phases. Only the most common minerals are noted. – = not detected.

Unit C

Sample: LL81-5A-005-01

Depth: 029.10-028.96 m

Lithology: black, carbonaceous, pyrrhotitic slate

Mineralogy:	very difficult to discern.	
	carbonaceous material, chlorite, muscovite, small pyrrhotite blebs and rutile	
	large pyrrhotite blebs	15 %

Notes:

Chlorite and muscovite are present mainly within chlorite and chlorite-muscovite porphyroblasts, which are common. These are strongly oriented parallel to cleavage planes. Large pyrrhotite blebs (averaging ~0.9 mm in length and ~0.15 mm in width) are oriented parallel to cleavage and both these and small disseminated pyrrhotite blebs (generally < 0.05 mm in diameter) host overgrowths of rutile and an unknown phase, likely an hydroxide. These grains appear to be highly altered. Most large pyrrhotite blebs host muscovite and chlorite pressure shadows. Rutile is present as cleavage-parallel blebs and disseminated blebs. Grains are generally strongly aligned.

Sample: LL81-5A-013-01

Depth: 075.75-075.50 m

Lithology: folded, light-grey, parallel-laminated, pyrrhotitic, medium-grained metasiltstone

Mineralogy: light laminations-

fine-grained groundmass: muscovite, quartz, carbonaceous material, chlorite, rutile and small pyrrhotite blebs

dark laminations-

fine-grained groundmass: carbonaceous material, dark irresolvable phases, chlorite, muscovite, quartz, rutile and small pyrrhotite blebs

large pyrrhotite blebs (overall) 2 %

Notes:

Chlorite and muscovite are present as individual groundmass phases as well as within chlorite and chlorite-muscovite porphyroblasts, which are strongly oriented parallel to cleavage planes. Large pyrrhotite blebs are oriented parallel to cleavage planes as well. Small pyrrhotite blebs are disseminated. Many pyrrhotite blebs have rutile intergrowths and rims. Rutile is present as blebs oriented parallel to cleavage and disseminated blebs, many of which are poikiloblastic (these average ~0.05 mm in length and diameter, respectively). Many groundmass pyrrhotite blebs have rutile intergrowths. Most grains are strongly aligned.

Sample: LL81-5A-020-01

Depth: 113.81-113.70 m

Lithology: black, carbonaceous silty slate with a parallel-laminated, medium-grey, very fine-grained metasiltstone interbed

Mineralogy:	carbonaceous silty slate-	
	fine-grained groundmass: carbonaceous material, muscovite, chlorite, small pyrrhotite blebs and rutile (the latter two total ~1 %)	
	large pyrrhotite blebs	1 %
	metasiltstone interbed-	
	fine-grained groundmass: muscovite, chlorite, carbonaceous material, irresolvable opaques, quartz, rutile and small pyrrhotite blebs (the latter two total ~1 %)	
	large pyrrhotite blebs	2 %

Notes:

Rutile is present as blebs oriented parallel to cleavage planes and as disseminated blebs (averaging ~0.01 mm in length and diameter, respectively). Small pyrrhotite blebs average ~0.01 mm in length and many have rutile intergrowths. Many disseminated rutile blebs are poikiloblastic.

Slate: chlorite and chlorite-muscovite porphyroblasts are oriented parallel to cleavage planes. Pyrrhotite is present in the bottom slate bed, but not in the top bed. Large pyrrhotite blebs are smaller than the those in the metasiltstone bed and many have coarse-grained muscovite pressure shadows (coarse-grained relative to the groundmass). Large pyrrhotite blebs are oriented parallel to cleavage planes and are highly altered, with rims of an unknown phase, possibly an hydroxide. Most of these blebs have rims of rutile as well. The base of the bottom slate bed contains more rutile than the upper slate bed. The upper bed contains rutile, mainly as cleavage-parallel blebs.

Metasiltstone: this is parallel-laminated. hlorite and muscovite are present as individual groundmass phases as well as within chlorite and chlorite-muscovite porphyroblasts. Large pyrrhotite blebs are oriented parallel to cleavage and are much longer and thicker in this lithology. Most are rimmed by rutile and are highly altered, with rims of possibly an hydroxide phase, similar to that observed in the slate.

Sample: LL81-5A-034-01

Depth: 195.56-195.43 m

Description: folded, silty, carbonaceous slate and interbedded very fine-grained metasiltstone

Mineralogy:

slate-	
fine-grained groundmass: carbonaceous material, chlorite, muscovite, rutile and small pyrrhotite blebs (latter two total ~1.5 %)	
large pyrrhotite blebs	< 1 %
metasiltstone-	
fine-grained groundmass: chlorite, muscovite, carbonaceous material, rutile, small pyrrhotite blebs (the latter two total ~1.5 %) and irresolvable phases	
large pyrrhotite blebs	20 %

Notes:

Chlorite and muscovite are present as individual groundmass phases as well as within chlorite and chlorite-muscovite porphyroblasts. Rutile is present as strongly aligned blebs and disseminated blebs of a variety of sizes (generally between < ~0.005 and 0.06 mm in length and diameter, respectively). Groundmass pyrrhotite is present as strongly aligned tiny blebs throughout both lithologies. Some of these have rutile rims. Large pyrrhotite blebs are < 1 mm in length. Large pyrrhotite blebs in the metasiltstone are strongly oriented parallel to cleavage planes and range in size from 0.5 to 5 mm in length. Pyrrhotite blebs are oriented along a cleavage fan within the metasiltstone interbed on the fold.

Sample: LL81-5A-042-03

Depth: 237.96-237.84 m

Lithology: massive, light-grey, very fine-grained metawacke

Mineralogy:		
	calcite	44 %
	muscovite	30 %
	quartz	20 %
	rutile	3 %
	large pyrrhotite blebs	2 %
	small pyrrhotite blebs	1 %

Notes:

Rutile blebs are small (typically ~0.02 mm in diameter) and most are disseminated, while only a few are oriented parallel to cleavage planes. Many of the disseminated blebs are highly poikiloblastic. Many of these blebs have pyrrhotite intergrowths and rims. Many small pyrrhotite blebs have rutile rims. Large pyrrhotite blebs average ~3 mm in length and ~1 mm in width and are oriented parallel to cleavage planes. Many of these have rutile rims. Most grains show moderate to strong alignment. The hand specimen is rusty on its weathered surface.

Sample: LL81-5A-42-02

Depth: 241.01-240.92 m

Lithology: parallel-laminated, medium-grey, medium-grained metasiltstone with a thin vein

Mineralogy:

light laminations-

fine-grained groundmass: muscovite, quartz, chlorite, carbonaceous material, rutile and small pyrrhotite blebs (the latter two total < ~1 %)

dark laminations-

fine-grained groundmass: carbonaceous material, chlorite, muscovite, quartz, rutile and small pyrrhotite blebs (the latter two total < ~1 %)

large pyrrhotite blebs (overall) 2 %

Notes:

Chlorite and muscovite are present as individual groundmass phases as well as within chlorite and chlorite-muscovite porphyroblasts. These porphyroblasts are strongly oriented parallel to cleavage planes, as are most grains. Many large pyrrhotite grains have coarse-grained muscovite and quartz along their contacts with host rock. Rutile grains are present as grains oriented parallel to cleavage planes and as disseminated grains, some of which are poikiloblastic. These grains are generally < 0.02 mm in length and diameter, respectively. Small pyrrhotite grains are generally < 0.02 mm in length and are present as blebs oriented parallel to cleavage planes and as disseminated blebs. Many of these are rimmed by rutile. A vein averaging ~0.85 mm in thickness and showing normal offset of approximately 0.5 mm, cuts through the sample. It contains pyrrhotite in its top part and muscovite, quartz and calcite below this. The vein is lined by coarse-grained muscovite and quartz. See Figure B.1 for a photomicrograph of this thin section.

Sample: LL81-5A-043-02

Depth: 242.83-242.68 m

Lithology: carbonaceous, grey silty slate with parallel-laminated, light-grey, fine-grained metasiltstone and fine-grained metasiltstone ball structures

Mineralogy:	slate-	
	fine-grained groundmass: carbonaceous material, chlorite, muscovite, (an) irresolvable phase(s), small pyrrhotite blebs and rutile (the latter two total ~1 %)	
	large pyrrhotite blebs	~2 %
	metasiltstone-	
	fine-grained groundmass: muscovite, quartz, chlorite, (an) irresolvable phase(s), small pyrrhotite blebs and rutile (the latter two total < 1 %)	
	large pyrrhotite blebs	5 %

Notes:

Grey slate: chlorite and muscovite are present as individual groundmass phases as well as within chlorite and chlorite-muscovite porphyroblasts. Small pyrrhotite blebs are both oriented parallel to cleavage planes and disseminated and range from < 1 mm-1 cm in length and diameter, respectively, but most are ~1 mm. Two cleavage-parallel blebs have minor rutile overgrowths. Rutile is present as both cleavage-parallel blebs and as disseminated blebs. Some blebs have pyrrhotite overgrowths. Large pyrrhotite blebs are oriented parallel to cleavage. Porphyroblasts and most elongate grains are strongly aligned.

Metasiltstone: chlorite and muscovite are present as individual groundmass phases and as well as within chlorite and chlorite-muscovite porphyroblasts. Dark laminations contain abundant chlorite and chlorite-muscovite porphyroblasts. Groundmass pyrrhotite blebs are disseminated and are generally < 0.01 mm in diameter. Rutile is present as cleavage-parallel blebs and as disseminated blebs, generally < 0.01 mm in length and diameter, respectively. Cleavage-parallel rutile blebs are not strongly aligned, while elongate grains of other phases are strongly aligned. Large pyrrhotite blebs are cleavage-parallel.

Sample: LL81-5A-047-01

Depth: 266.46-266.34 m

Lithology: black, carbonaceous slate with poorly-developed cone-in-cone-type structures

Mineralogy:	fine-grained groundmass: carbonaceous material, chlorite, muscovite, carbonate, small pyrrhotite blebs and rutile (the latter two total 1.5 %)	
	large pyrrhotite blebs	2 %
	arsenopyrite	1 %
	pyrite	< 1 %

Notes:

Cone structures are well-developed at the base of the thin section, but above this, development is poor. They are crude, dark, cone-like structures, sometimes nestled together and within one another, surrounded by (an) unknown light colored carbonate phase(s). These structures are similar to those seen in LL81-5A-053-01, described below. Chlorite and muscovite are present as groundmass phases and are also present within chlorite and chlorite-muscovite porphyroblasts oriented parallel to cleavage planes. Large pyrrhotite blebs average ~1 mm in length and ~0.15 mm in width and are oriented parallel to cleavage. Some of these have rutile intergrowths and rims. Some large pyrrhotite blebs have coarse-grained muscovite-chlorite pressure shadows (coarse relative to groundmass). Small pyrrhotite blebs are disseminated. Rutile is present as small cleavage-parallel blebs and as poikiloblastic blebs, averaging ~0.02 mm in length and diameter, respectively. Arsenopyrite and pyrite grains are idioblastic. Rutile and groundmass pyrrhotite grains are not consistently strongly aligned, while large pyrrhotite blebs show strong alignment.

Sample: LL81-053-01

Depth: 299.72-299.62 m

Lithology: medium grey, alternating convoluted parallel- and ripple cross-laminated, medium-grained metasiltstone

Mineralogy: light laminations-

fine-grained groundmass: muscovite, quartz, chlorite, irresolvable dark phases (carbonaceous material may be present), small pyrrhotite blebs and rutile

dark laminations-

fine grained groundmass: irresolvable dark phases and lesser chlorite, muscovite, quartz, small pyrrhotite blebs and rutile

large pyrrhotite blebs (overall) 3 %

Notes:.

Dark laminations are defined mainly by irresolvable dark phases. Chlorite and muscovite are present as individual groundmass phases and as chlorite and chlorite-muscovite porphyroblasts, which are abundant throughout, but more highly concentrated in dark laminations. Large pyrrhotite blebs average ~4 mm in length, are oriented parallel to cleavage and many have coarse-grained muscovite and quartz along their contacts with host rock. Both pyrrhotite and rutile are present as blebs oriented parallel to cleavage planes and as disseminated blebs, generally ~0.02 mm in length and diameter, respectively. Many of the rutile blebs are poikiloblastic. Grains are strongly aligned, throughout.

Sample: LL81-5A-065-01

Depth: 368.65-368.51 m

Lithology: black, carbonaceous slate with medium grey, parallel-laminated, very fine-grained metasiltstone

Mineralogy: slate-

fine-grained groundmass: carbonaceous material, muscovite, chlorite, small pyrrhotite blebs and rutile (the latter two total ~1.5 %)

metasiltstone-

fine-grained groundmass: muscovite, chlorite, small pyrrhotite and rutile blebs (the latter two total ~1.5 %)

large pyrrhotite blebs (overall) 3 %

Notes:

Carbonaceous material in the slate makes characterization difficult. Many large pyrrhotite blebs have rutile intergrowths and many have coarse-grained pressure shadows (coarse relative to groundmass) of muscovite and quartz. Rutile is present as blebs oriented parallel to cleavage and as disseminated, strongly poikiloblastic blebs, generally < ~0.02 mm in length and diameter, respectively. Small pyrrhotite blebs are both cleavage-parallel and disseminated and many have pressure shadows of muscovite and chlorite. There is strong alignment of minerals throughout.

Sample: LL81-5A-072-01

Depth: 410.14-409.95 m

Lithology: massive, black meta-argillite with well-developed cone-in-cone-type structures

Mineralogy: fine-grained groundmass: irresolvable phases and small pyrrhotite blebs

large pyrrhotite blebs 1%

Notes:

The groundmass is too fine-grained and irresolvable to note any phases, except for pyrrhotite blebs. There is a spectrum of pyrrhotite sizes from < ~0.02 mm up to several millimetres in diameter. Some large pyrrhotite blebs host minor chalcopyrite. Cone structures decrease in size downwards from the top of the thin section, which is the top of the bed in hand sample. Cones are rimmed by (an) unknown fine-grained carbonate phase(s). Some large pyrrhotite blebs show preferred orientation.

Sample: LL81-5A-081-02

Depth: 461.88-461.72 m

Lithology: carbonaceous silty slate with a light-grey, parallel-laminated, medium-grained metasiltstone interbed

Mineralogy:		
	metasiltstone-	
	fine-grained groundmass: chlorite, muscovite, quartz and rutile	85 %
	large pyrrhotite blebs	15%
	slate-	
	fine-grained groundmass: carbonaceous material, chlorite, muscovite, rutile and small pyrrhotite blebs	99 %
	large pyrrhotite blebs	< 1 %

Notes:

Silty slate: chlorite and muscovite are present as groundmass phases and as chlorite and chlorite-muscovite porphyroblasts oriented parallel to cleavage planes. Rutile is present as blebs oriented parallel to cleavage planes and as disseminated blebs, generally ~0.02 mm in length and diameter, respectively. Many disseminated blebs are poikiloblastic. The topmost slate layer has much less rutile than the bottom slate layer. Pyrrhotite in the groundmass is present as disseminated blebs and as blebs oriented parallel to cleavage planes. Larger pyrrhotite blebs average < 2 mm in length, but are only present in the bottom slate layer. Grains are strongly aligned throughout this lithology. See Figure B.2 for a photomicrograph of slate from this thin section..

Metasiltstone: chlorite and muscovite are present as groundmass phases as well as chlorite and chlorite-muscovite porphyroblasts oriented parallel to cleavage. There is much more groundmass chlorite and muscovite present within the groundmass outside of porphyroblast in the metasiltstone, than in the slate. Rutile is present as disseminated blebs and as blebs oriented parallel to cleavage, generally ~0.02 mm in length and diameter, respectively. Large pyrrhotite blebs are oriented parallel to cleavage and are generally ~3 mm length and ~1 mm in width. Some larger pyrrhotite grains have minor chalcopyrite mineralization. Minerals are strongly aligned throughout this lithology.

Unit B

Sample: LL81-5A-082-02

Depth: 467.76-467.60 m

Lithology: folded coticule in chloritic silty slate

Notes:

Very similar to LL81-5A-084-01, described below. Host rock is a green, fine-grained and banded silty slate. Light bands are composed of carbonate, quartz, chlorite, muscovite and spessartine garnet. Dark bands are composed of chlorite, garnet (~35 %), muscovite and possibly other phases, but the lithology is too fine-grained to confirm this. Chlorite definesa foliation that wraps around garnet in the dark bands. Ilmenite blebs strongly oriented parallel to cleavage planes and averaging ~0.02 mm in length are present throughout the host rock, as are disseminated pyrrhotite blebs averaging ~0.02 mm in diameter. A few large cleavage-oriented pyrrhotite blebs are present. Some of these blebs contain intergrown chalcopyrite. A single large, folded coticule is present, composed of idioblastic spessartine garnet, quartz and minor carbonate. Garnet and carbonate are present in granoblastic aggregates, which are fractured and infilled with quartz. The folding represents ~2 cm of shortening.

Sample: LL81-5A-084-01

Depth: 475.10-474.96 m

Lithology: coticule and nodules in chloritic silty slate

Notes:

Very similar to LL81-5A-082-02, described above. Host rock is green, fine-grained and banded. Light bands are composed of muscovite, quartz, calcite, spessartine garnet, chlorite, ilmenite and pyrrhotite. Dark bands are composed of spessartine garnet (~35%), chlorite and possibly other phases, but the lithology is too fine-grained to confirm this. Ilmenite is present as blebs ~0.02 mm in length, oriented parallel to cleavage planes, throughout. Pyrrhotite is present as disseminated blebs averaging ~0.02 mm in diameter, throughout. Ovoid nodules ~1-2 mm in diameter, composed of spessartine garnet and calcite, are present, almost exclusively in the light bands. Bands wrap around these nodules. A single undistorted coticule is present. This is composed mainly of quartz, ranging in size from >0.01 mm to ~0.3 mm in diameter, calcite and idioblastic spessartine garnet. Garnet is present mainly in aggregates. Very fine-grained quartz is found along the contact between the coticule and host rock. On the left-hand side of the coticule, quartz grains are elongate and strongly preferentially oriented.

Sample: LL81-5A-091-01

Depth: 513.20-513.07 m

Lithology: greenish-grey, parallel-laminated, fine-grained metasiltstone, overlain by massive, greenish-grey, medium-grained metasiltstone

Mineralogy:	bottom half (fine-grained metasiltstone)-	
	fine-grained groundmass: chlorite, muscovite and ilmenite (5 %)	
	large pyrrhotite blebs	< 1%
	top half (medium-grained metasiltstone)-	
	fine-grained groundmass: chlorite, muscovite and ilmenite (5 %)	
	large pyrrhotite blebs	2%

Notes:

Ilmenite is present as disseminated, strongly poikiloblastic, ovoid-shaped blebs, averaging ~0.1 mm in diameter,. Most of these blebs have pressure shadows of coarse-grained chlorite and muscovite (coarse-grained relative to the groundmass) in the bottom half of the thin section, but not in the top half. Large pyrrhotite blebs, averaging ~1-2 mm in length and ~0.25 mm in width, many with minor local chalcopyrite mineralization, are present in both layers. Most of these have pressure shadows and rims of coarse-grained chlorite and muscovite (coarse-grained relative to the groundmass) and are oriented parallel to cleavage planes. Grains and pressure shadows throughout the thin section show strong preferential orientation, but orientation between the top and bottom halves differ by approximately 30°.

Sample: LL81-5A-095-01

Depth: 536.48-536.34 m

Lithology: green, fine-grained silty slate, with coarser-grained, light colored lenses

Mineralogy:	fine grained groundmass: chlorite, muscovite, ilmenite and other irresolvable phases	89%
	spessartine garnet	10%
	large pyrrhotite and chalcopyrite blebs	< 1%

Notes:

Very similar to LL81-5A-101-01, described below. Garnets are idioblastic, average ~0.08 mm in diameter and are found either individually or in aggregates that locally envelope pyrrhotite and/or chalcopyrite blebs, to some extent. Many garnet grains and aggregates have pressure shadows of fine-grained muscovite (coarse grained relative to the groundmass) and chlorite. Ilmenite is present as small (generally << ~0.1 mm long and << ~0.1 mm wide) blebs oriented parallel to cleavage. Light colored lenses contain fine-grained (coarse-grained relative to the groundmass) muscovite, chlorite, irresolvable carbonate minerals, spessartine garnet and pyrrhotite and chalcopyrite. Some sulphide blebs consist of pyrrhotite and chalcopyrite intergrowths. Pressure shadows and groundmass grains are strongly preferentially oriented, except within the lenses. See Figure B.3 for a photomicrograph of this thin section.

Sample: LL81-5A-101-01

Depth: 571.95-571.82 m

Lithology: green, fine-grained silty slate with coarser-grained lenses

Mineralogy:	fine grained groundmass: chlorite, muscovite, ilmenite and (an)other irresolvable phase(s)	89 %
	spessartine garnet	10 %
	large pyrrhotite and chalcopyrite blebs	< 1%

Notes:

Garnet is idioblastic, grains average ~0.08 mm in diameter and are found either individually or in aggregates along with blebs of pyrrhotite and/or chalcopyrite, generally with pressure shadows of fine-grained muscovite and chlorite. Larger sulphide blebs are oriented parallel to cleavage planes and have coarse-grained muscovite along their borders. Ilmenite is present as small (generally < ~0.01 mm in length) blebs oriented parallel to cleavage. Lenses contain fine-grained muscovite, chlorite, irresolvable carbonate minerals, spessartine garnet and large, unoriented blebs of pyrrhotite and chalcopyrite and some blebs consist of intergrowths of both of these. This thin section is very similar to LL81-5A-095-01, described above. See Figure B.4 for a photomicrograph of this thin section.

Unit A

Sample: LL81-5A-107-01

Depth: 607.04-606.91 m

Lithology: light grey, fine-grained metawacke with a light green silty slate interbed.

Mineralogy: metawacke-

quartz	40 %
muscovite	18 %
chlorite	15 %
carbonate (mainly calcite, but most is very fine-grained and difficult to identify)	15 %
feldspar (mainly orthoclase)	5 %
ilmenite	4 %
small pyrrhotite blebs	2 %
large pyrrhotite blebs	< 1 %
silty slate-	
fine-grained groundmass: muscovite, with lesser chlorite, quartz andilmenite (5 %).	~99 %
large pyrrhotite blebs	< 1 %

Notes:

Metawacke: quartz is present as tiny groundmass grains and larger grains averaging ~0.15 mm in diameter. Both types are typically anhedral. Muscovite and chlorite grains are present as groundmass grains, while muscovite is also present as larger laths, several tenths of a millimeter long, that locally define a minor cleavage. Ilmenite is present as strongly poikiloblastic, disseminated blebs averaging ~0.1 mm in diameter, many of which have minor pyrrhotite rims and intergrowths. Pyrrhotite is present also as large blebs oriented parallel to cleavage planes, smaller cleavage-parallel blebs averaging ~1 mm in length and small disseminated blebs averaging ~0.1 mm in diameter. Many large pyrrhotite blebs host minor chalcopyrite and one hosts a cluster of idioblastic arsenopyrite crystals averaging ~0.02 mm in diameter. Many disseminated pyrrhotite blebs in the groundmass host rutile intergrowths. Carbonate is present mainly as calcite in the form of groundmass-sized grains and larger grains, up to ~0.15 mm in diameter. Overall, grains in this thin section are generally not recrystallized and the occurrence of metamorphism is suggested mainly only by the presence of chlorite and secondary muscovite (laths). See Figure B.5 for a photomicrograph of metawacke from this thin section.

Slate: muscovite is present as laths several tenths of a millimetre long, crudely aligned in two directions at ~40° to each other, defining two slaty cleavages. Rutile is present as disseminated blebs averaging ~0.1 mm in diameter. Many of these are highly poikiloblastic and some are intergrown with pyrrhotite. Large pyrrhotite blebs average ~0.35 mm in length and are oriented parallel to cleavage planes.

Sample: LL81-5A-110-01

Depth: 627.80-627.70 m

Lithology: massive, greenish-dark grey, chloritic silty slate, with thin mineralized fractures

Mineralogy:	fine-grained groundmass: chlorite, muscovite, ilmenite and other irresolvable phases	99%
	large pyrrhotite blebs	1%

Notes:

Fractures average < 0.1 mm in width and contain fine-grained (irresolvable) carbonate minerals and muscovite. Rutile is present as ~0.04 mm long, blebs oriented parallel to cleavage. Some of these have fine-grained muscovite and chlorite pressure shadows. Large pyrrhotite blebs average ~1-2 mm in length and ~0.5 mm in width, are oriented parallel to cleavage planes and often contain minor chalcopyrite intergrowths. Several large pyrrhotite blebs contain minor coarse-grained muscovite along their contacts with host rock. Visible minerals and pressure shadows are strongly preferentially oriented. This lithology is the same as that encountered in chloritic silty slates in Unit B.

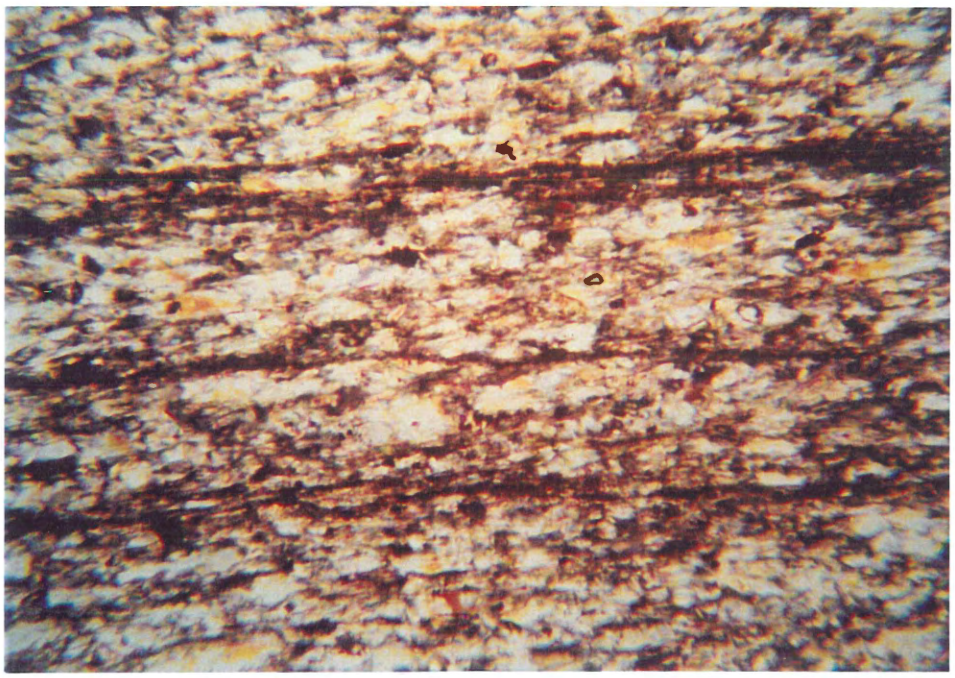

Figure B.1. Photomicrograph of metasiltstone from LL81-5A-042-02. Photograph taken in transmitted light under crossed polars. Field of view is 1.8 mm.

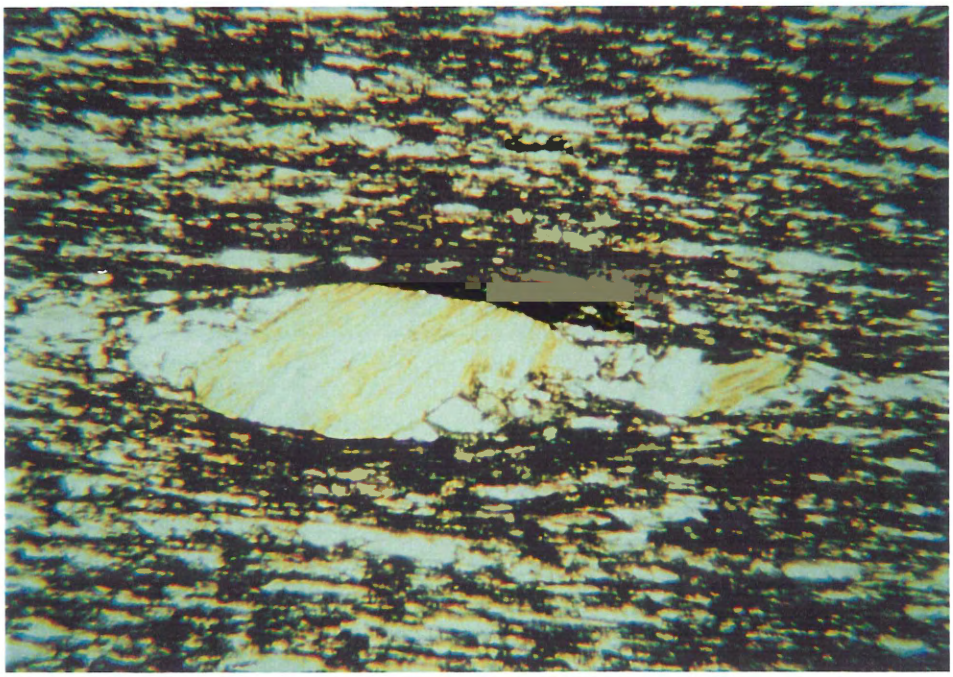

Figure B.2. Photomicrograph of carbonaceous slate from LL81-5A-081-02. Note strongly-oriented, ovoid-shaped chlorite-muscovite porphyroblasts. Photograph taken in transmitted light under uncrossed polars. Field of view is 1.8 mm.

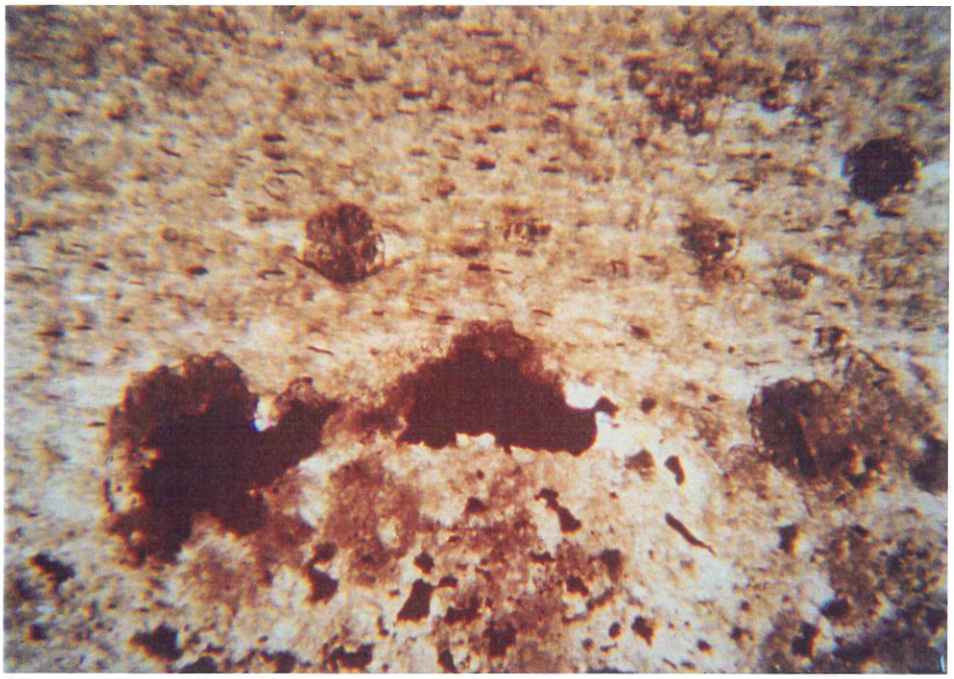

Figure B.3. Photomicrograph of a poorly-developed carbonate lens and typical chloritic silty slate from LL81-5A-095-01. Note pressure shadows on idioblastic spessartine garnets in the top half of the photo. Small, dark, strongly-oriented grains are ilmentite. Photo taken in transmitted light under crossed polars. Field of view is 1.8 mm.

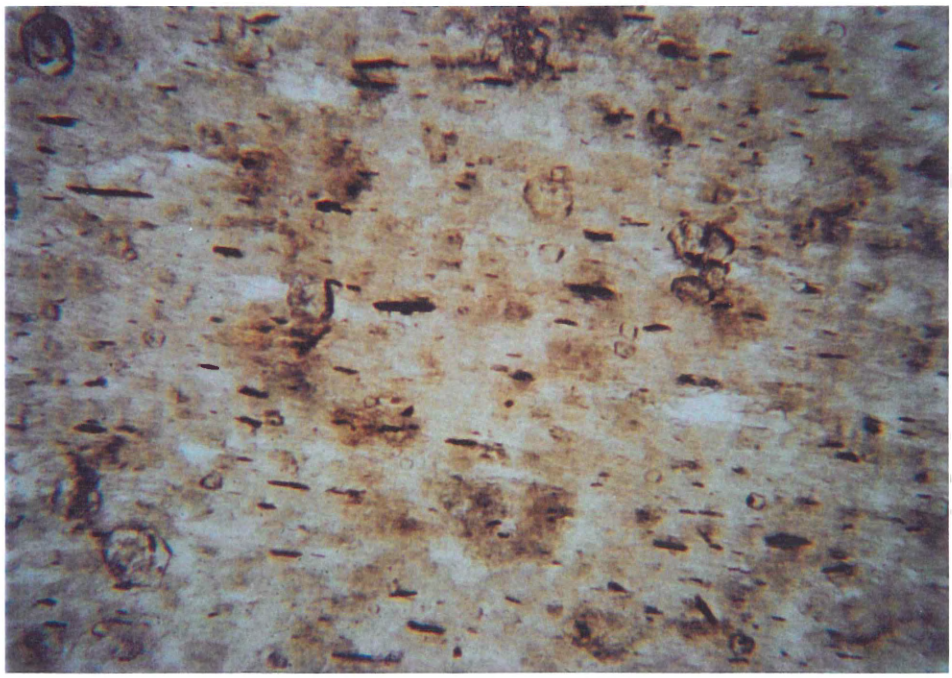

Figure B.4. Photomicrograph of chloritic silty slate from LL81-5A-101-01. Idioblastic grains are spessartine garnet. Small, dark, strongly-oriented grains are ilmenite. Photo taken in transmitted light under crossed polars. Field of view is 1.8 mm.

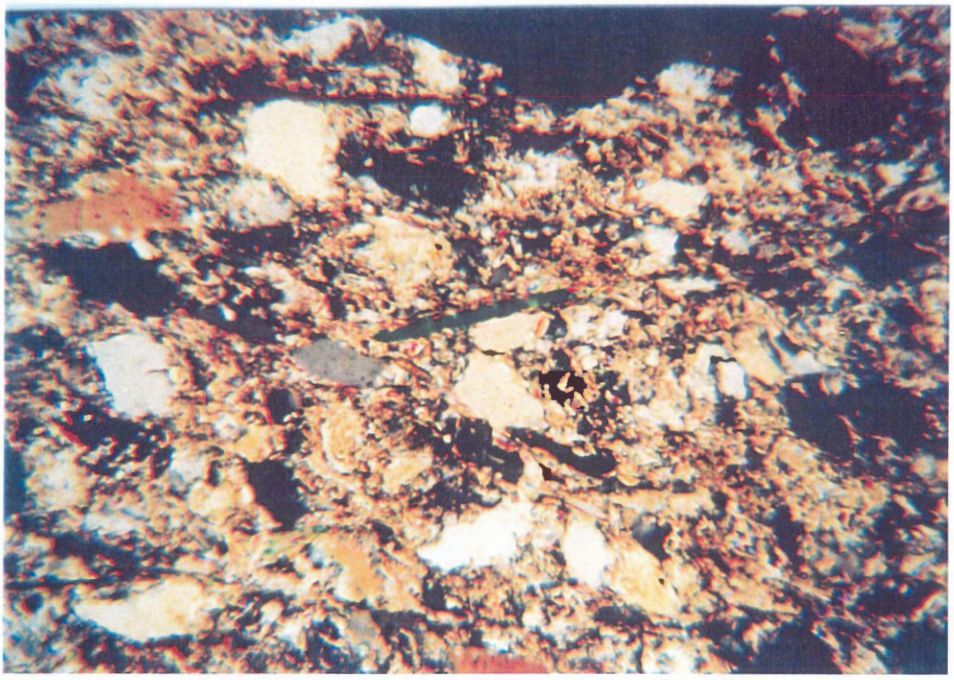

Figure B.5. Photomicrograph of metawacke from LL81-5A-107-01. Large grains are mainly quartz. Photo taken in transmitted light under crossed polars. Field of view is 1.8 mm.

Appendix C
Stratigraphic Log

Introduction

In 1980, Sherritt Gordon Mines Ltd. conducted an extensive exploration program in Caribou gold district, including the Lake Mine property, in an effort to follow the down-plunge extension of the Lake Lode auriferous vein. This program included the drilling of 16 diamond drillholes, resulting in 2680 m of core. Drillcore LL81-5A was recovered from the south side of the Caribou dome, on the northeastern edge of Burkner Lake, directly south of the abandoned Lake Mine development, at this time. .

LL81-5A was visually analysed, logged and sampled by the author between July and September, 1996, at the Nova Scotia Department of Natural Resources Drill Core Library in Stellarton, Pictou County, where the core has been stored since 1984. Using lithological, sedimentological and mineralogical information, the rocks present in this core were divided into three conformable stratigraphic units, as shown below. Representative sections of these units were drafted and many of these profiles are displayed below. Units were corrected for stratigraphic thicknesses using stratal dip measurements obtained at regular intervals throughout the drillcore. Full descriptions of these units are present in Chapter 4. Appendix A provides a list of samples acquired from this core and used in this study, while Appendix B presents petrographic information for these samples.

Drillhole Details for LL81-5A

Property: Lake Mine	Latitude: 8+00 S	Angle: -75°
Claim: 57-B	Longitude: 6+00 W	Core Diameter: NQ
Reference Map: 11E/2B	Bearing: 350° from magnetic north	Total Depth: 628.80 m

Units Present in LL81-5A

Unit	Drilling Depth (m)	Stratigraphic Thickness (m)		Description
overburden	0.00-3.40			
C	3.40-465.50 (top absent)	351		fining upward sequences of pyrrhotitic, in-part carbonate-rich metasiltstones and carbonaceous slate
B	465.50-589.18	113	32	coticule- and nodule-rich lithologies, similar to those noted directly below
			56	interbedded chloritic, pyrrhotitic meta-argillites and very fine- to fine-grained metawacke
			25	monotonously interbedded chloritic, pyrrhotitic silty slates
A	589.18-628.80 (bottom absent)	36		fining upward sequences of metawackes and silty slates

Key

Sedimentary Structures	
O	ball and pillow structures/load casts
~	convoluted laminations
⟋	ripple cross-laminations
≡	parallel laminations
Structures	
≈≈≈	poorly-developed coticule
Bedding Plane Contacts	
——	sharp and flat
- - - -	gradational over < 0.5 cm
—•—	gradational over > 0.5 cm
—M—	missing

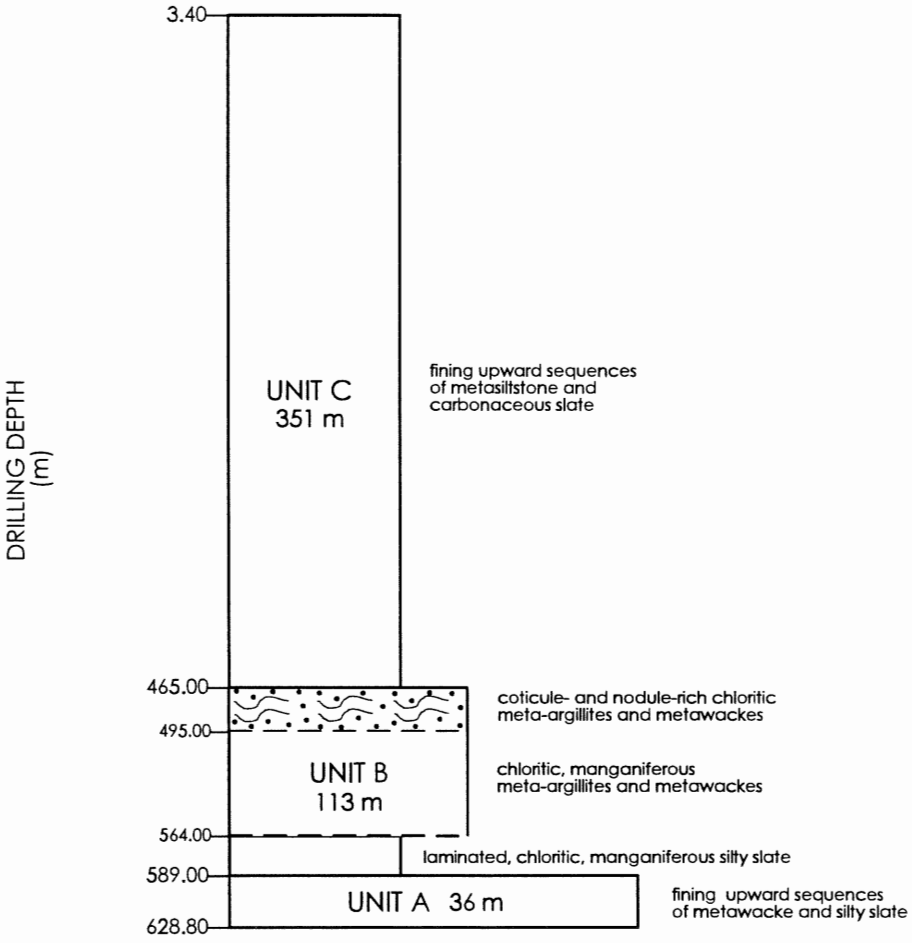
DRILLING DEPTH (m)
3.40
UNIT C
351 m
fining upward sequences
of metasiltstone and
carbonaceous slate
465.00
495.00
coticule- and nodule-rich chloritic
meta-argillites and metawackes
UNIT B
113 m
chloritic, manganiferous
meta-argillites and metawackes
564.00
laminated, chloritic, manganiferous silty slate
589.00
UNIT A 36 m
fining upward sequences
of metawacke and silty slate
628.80

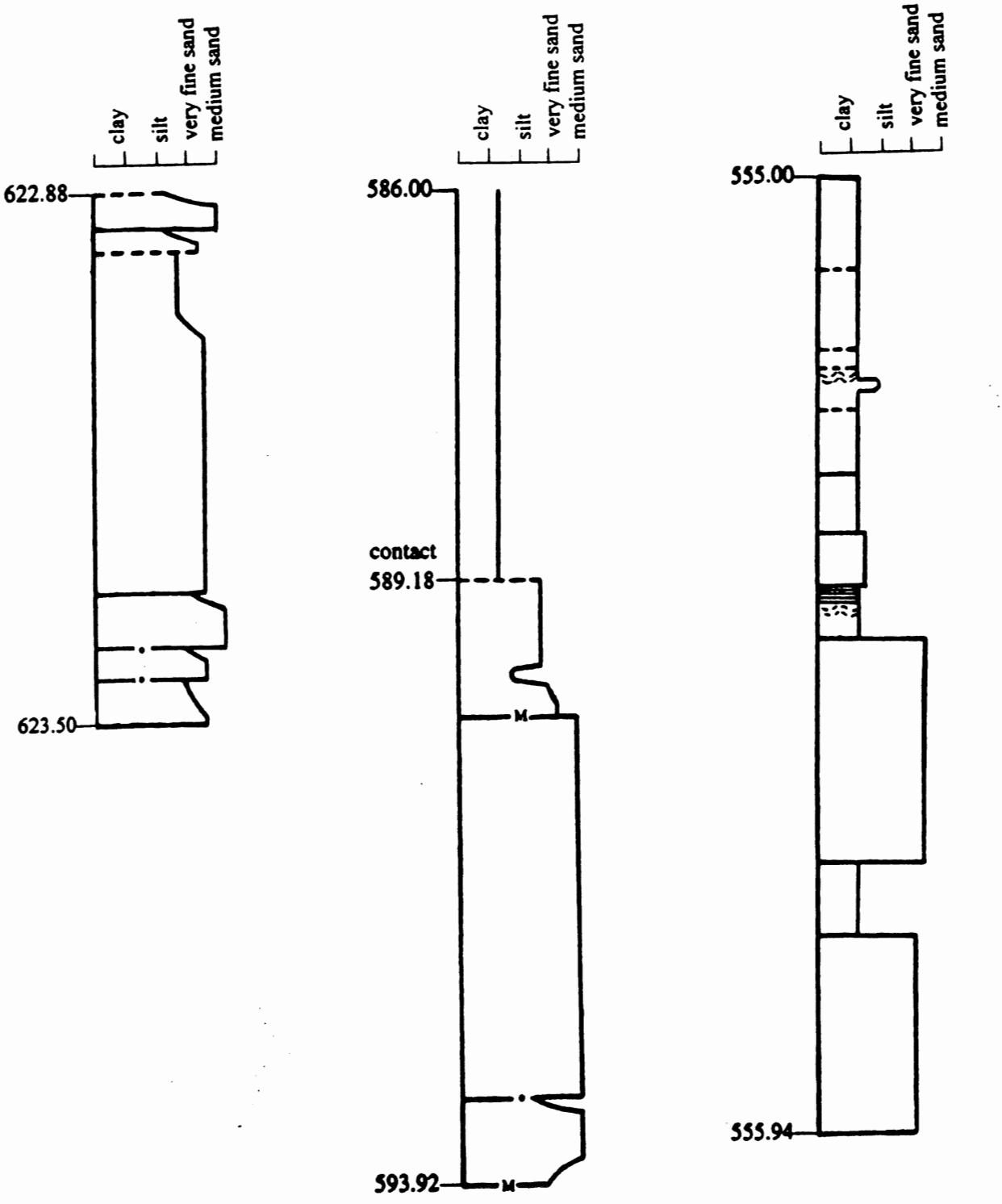

Depths are drilling depths and are in metres.

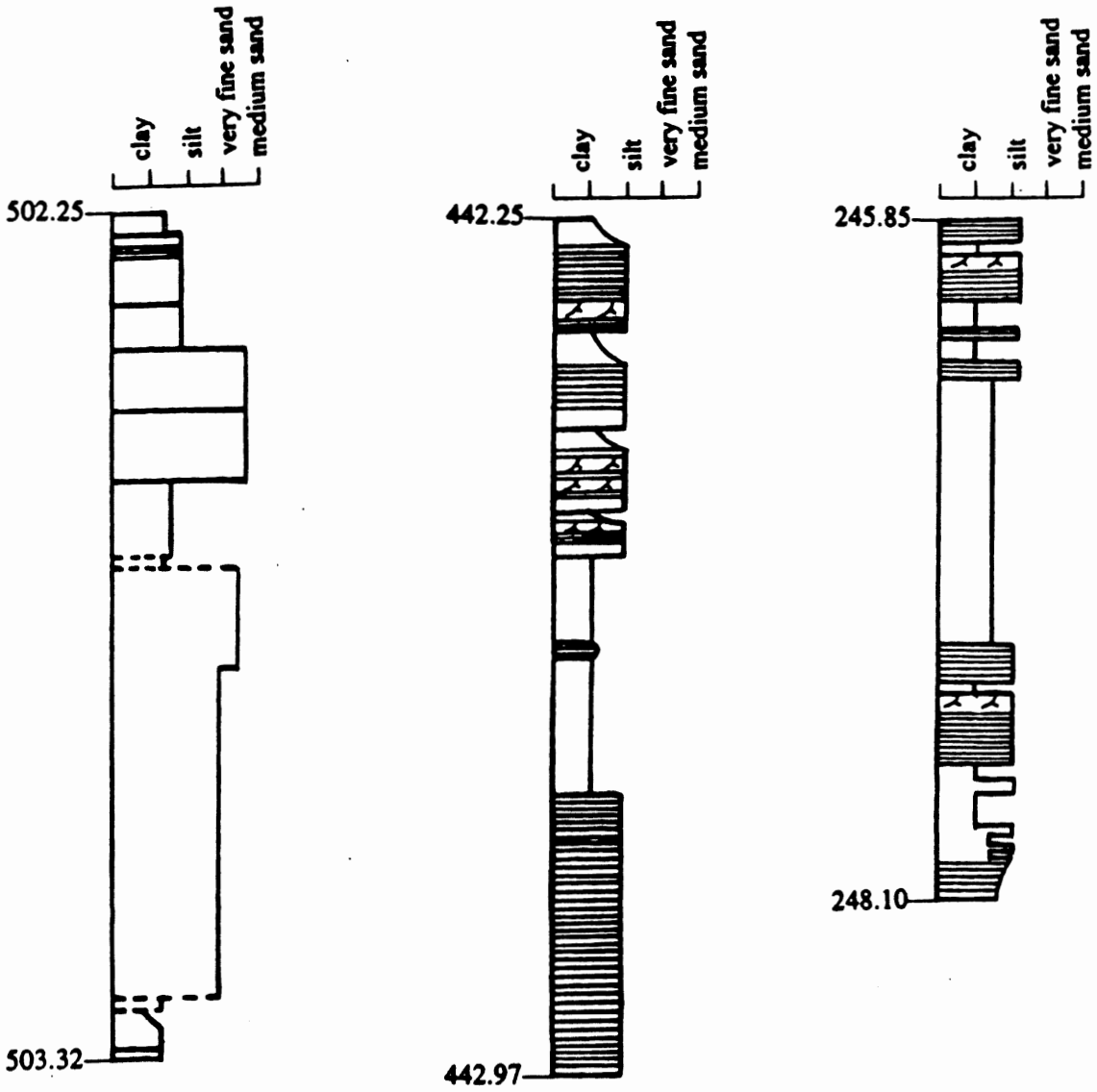
clay
silt
very fine sand
medium sand
502.25
503.32
442.25
442.97
245.85
248.10

Appendix C- Stratigraphic Log

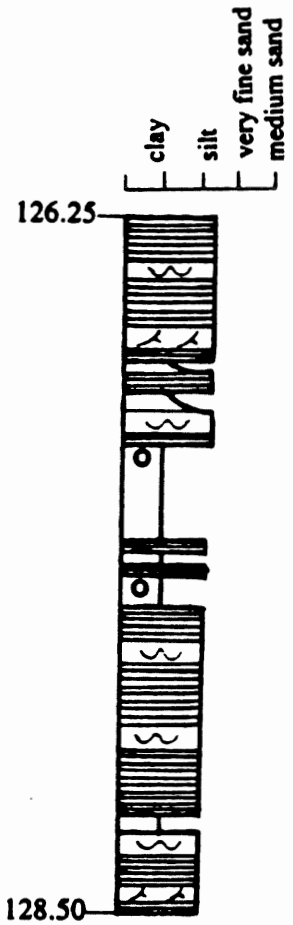

Appendix D
Mineral Chemistry Data

Introduction

Mineral chemistry data were obtained using the JEOL 733 electron beam microprobe at Dalhousie University in February, 1997. This system is equipped with four wavelength dispersive spectrometers and an Oxford Link eXL energy dispersive system. Sixty microprobe analyses were conducted on six samples from LL81-5A, with the following breakdown: 27 sulphide, 18 garnet, 13 oxide and 2 arsenide analyses. A probe spot of approximately 1 μm was used and the microprobe was calibrated using mineralogical standards (garnet, jadeite and kaersutite for silicates and oxides and pyrrhotite and chalcopyrite for sulphides). An energy dispersive spectra, which provided a resolution of 137 eV at 5.9 keV was employed and analysis of this spectra was conducted with an accelerating voltage of 15 kV and a beam current of 15.47 nA for a period of 40 seconds. Efforts were made to analyse the most common and geochemically significant phases and to acquire results which accurately represent variations in composition both within individual grains, within individual samples and between samples obtained from LL81-5A. Many of the grains analysed are extremely small and were thus difficult to probe. Tables D.1-3 profile garnet, oxide and sulphide/arsenide microprobe data, respectively.

Sample	Grain	Analysis	SiO_2	Al_2O_3	FeO (t)	MnO	MgO	CaO	P_2O_5	Total	Formula	Mineral	Notes
082-02	1	1	36.2	20.56	9.23	31.83	—	2.09	—	99.9	$(Mn, Fe, Ca)_3(Al, Fe)_2(SiO_4)_3$	spessartine garnet	core of grain outside coticule
082-02	1	2	36.31	20.24	15.04	26.03	0.29	2.18	—	100.09	$(Mn, Fe, Ca)_3(Al, Fe)_2(SiO_4)_3$	spessartine garnet	rim of grain outside coticule
082-02	2	3	37.34	20.63	8.84	32.59	—	2.12	—	101.52	$(Mn, Fe, Ca)_3(Al, Fe)_2(SiO_4)_3$	spessartine garnet	core of grain outside coticule
082-02	2	4	36.53	20.64	14.28	26.3	0.25	2.4	—	100.4	$(Mn, Fe, Ca)_3(Al, Fe)_2(SiO_4)_3$	spessartine garnet	rim of grain outside coticule
082-02	3	5	36.7	20.52	14.37	26.91	—	2.3	—	100.79	$(Mn, Fe, Ca)_3(Al, Fe)_2(SiO_4)_3$	spessartine garnet	core of grain outside coticule
082-02	3	7	36.42	20.38	14.79	25.75	—	2.36	—	99.7	$(Mn, Fe, Ca)_3(Al, Fe)_2(SiO_4)_3$	spessartine garnet	rim of grain outside coticule
082-02	4	8	35.95	20.07	10.5	30.43	—	2.37	—	99.31	$(Mn, Fe, Ca)_3(Al, Fe)_2(SiO_4)_3$	spessartine garnet	core of grain within coticule
082-02	4	9	36.62	20.53	13.08	27.81	0.22	2.25	—	100.51	$(Mn, Fe, Ca)_3(Al, Fe)_2(SiO_4)_3$	spessartine garnet	rim of grain within coticule
082-02	5	10	36.38	20.48	9.6	30.85	—	2.56	—	99.86	$(Mn, Fe, Ca)_3(Al, Fe)_2(SiO_4)_3$	spessartine garnet	core of grain within coticule
082-02	5	11	35.99	20.62	12.41	27.47	—	2.26	0.32	99.06	$(Mn, Fe, Ca)_3(Al, Fe)_2(SiO_4)_3$	spessartine garnet	rim of grain within coticule
082-02	6	12	36.36	20.74	11.27	29.98	0.26	2.39	—	101.01	$(Mn, Fe, Ca)_3(Al, Fe)_2(SiO_4)_3$	spessartine garnet	core of grain within coticule
082-02	6	13	36.83	20.82	14.26	27.5	0.29	1.73	—	101.42	$(Mn, Fe, Ca)_3(Al, Fe)_2(SiO_4)_3$	spessartine garnet	rim of grain within coticule
082-02	7	14	36.57	20.51	12.28	28.95	—	2.63	—	100.94	$(Mn, Fe, Ca)_3(Al, Fe)_2(SiO_4)_3$	spessartine garnet	core of grain outside coticule
082-02	7	15	36.58	20.81	15.01	26.61	0.25	1.96	—	101.24	$(Mn, Fe, Ca)_3(Al, Fe)_2(SiO_4)_3$	spessartine garnet	rim of grain outside coticule
095-01	8	16	36.53	20.47	9.02	29.05	0.23	3.8	0.6	99.71	$(Mn, Fe, Ca)_3(Al, Fe)_2(SiO_4)_3$	spessartine garnet	core of grain in silty slate
095-01	8	17	36.71	20.66	13.78	25.6	0.32	3.42	—	100.48	$(Mn, Fe, Ca)_3(Al, Fe)_2(SiO_4)_3$	spessartine garnet	rim of grain in silty slate
095-01	9	18	36.71	20.32	9.59	28.44	—	4.81		99.87	$(Mn, Fe, Ca)_3(Al, Fe)_2(SiO_4)_3$	spessartine garnet	core of grain in silty slate
095-01	9	19	36.56	20.62	14.17	25.13	0.28	3.48	—	100.23	$(Mn, Fe, Ca)_3(Al, Fe)_2(SiO_4)_3$	spessartine garnet	rim of grain in silty slate
													— = not detected

Table D.1. Microprobe data for garnets from LL81-5A.

Sample	Grain	Analysis	SiO_2	TiO_2	Al_2O_3	FeO (t)	MnO	CaO	NaO	K_2O	Total	Formula	Mineral	Notes
020-01	19	29	0.21	99.21	—	0.69	—	—	—	—	100.11	TiO_2	rutile	rim on large pyrrhotite bleb in black slate
020-01	20	30	0.2	99.59	—	0.43	—	—	—	—	100.22	TiO_2	rutile	inward rim on large pyrrhotite bleb in black slate
020-01	20	31	2.15	94.76	1.41	0.36	—	—	—	0.3	98.99	TiO_2	rutile	outward rim on large pyrrhotite bleb in black slate
020-01	22	32	2.18	91.94	0.96	0.48	—	—	—	0.35	95.92	TiO_2	rutile	cleavage-parallel bleb in black slate
047-01	17	27	2.4	92.77	1.34	0.36	—	0.53	—	0.29	99.07	TiO_2	rutile	cleavage-parallel bleb in black slate
047-01	18	28	2.96	96.76	0.37	—	—	0.35	—	0.2	100.63	TiO_2	rutile	cleavage-parallel bleb in black slate
082-02	13	23	0.19	52.17	—	32.28	14.44	—	—	—	99.03	$(Fe, Mn)TiO_3$	ilmenite	cleavage-parallel bleb in silty slate outside coticule
082-02	14	24	0.21	52.3	—	32.89	14.44	—	—	—	99.85	$(Fe, Mn)TiO_3$	ilmenite	cleavage-parallel bleb in silty slate outside coticule
095-01	10	20	0.2	52.53	—	36.02	10.78	—	—	—	99.54	$(Fe, Mn)TiO_3$	ilmenite	cleavage-parallel bleb in silty slate
095-01	11	21	0.2	51.84	—	35.29	11.26	—	0.28	0.15	99.03	$(Fe, Mn)TiO_3$	ilmenite	cleavage-parallel bleb in silty slate
095-01	12	22	4.64	48.08	2	31.36	12.12	—	0.4	0.6	99.19	$(Fe, Mn)TiO_3$	ilmenite	cleavage-parallel bleb in silty slate
107-01	15	25	—	52.87	—	43.19	3.26	—	—	—	98.68	$(Fe, Mn)TiO_3$	ilmenite	disseminated bleb in silty slate
107-01	16	26	0.2	53.32	—	42.99	3.24	—	0.3	—	100.04	$(Fe, Mn)TiO_3$	ilmenite	disseminated bleb in silty slate
														— = not detected

Table D.2. Microprobe data for oxides from LL81-5A.

Sample	Grain	Analysis	Cu	Zn	Fe	As	S	Mn	Pb	Ni	Co	W	Total	Formula	Mineral	Notes
005-01	38	55	—	—	60.94	—	39.15	—	—	—	—	—	100.09	FeS	pyrrhotite	core of large bleb in black slate
005-01	38	56	—	—	60.93	—	38.96	—	—	—	—	—	99.88	FeS	pyrrhotite	rim of large bleb in black slate
005-01	39	57	—	—	61.33	—	39.02	—	—	—	—	—	100.35	FeS	pyrrhotite	core of large bleb in black slate
005-01	39	58	—	—	57.09	—	37.31	—	—	—	—	0.36	99.75	FeS	pyrrhotite	rim of large bleb in black slate
020-01	33	45	—	—	59.46	—	38.53	—	—	—	—	—	97.99	FeS	pyrrhotite	core of large bleb in silty slate
020-01	33	46	—	—	61.06	—	39.13	—	—	—	—	—	100.19	FeS	pyrrhotite	rim of large bleb in silty slate
020-01	34	47	—	—	61.47	—	39.25	—	—	—	—	—	100.72	FeS	pyrrhotite	core of large bleb in silty slate
047-01	40	59	—	—	61.17	—	38.75	—	—	—	—	—	99.92	FeS	pyrrhotite	core of large bleb
047-01	41	60	—	—	61.17	—	39.01	—	—	—	—	—	100.18	FeS	pyrrhotite	core of small bleb
047-01	42	61	—	—	48.09	1.2	52.68	—	—	—	—	—	101.97	FeS_2	pyrite	core of large grain
047-01	43	62	—	—	48.27	—	53.79	—	—	—	—	—	102.06	FeS_2	pyrite	rim of large grain
047-01	43	63	—	—	61.74	—	38.99	—	—	—	—	—	100.92	FeS	pyrrhotite	core of small bleb
047-01	44	64	—	—	35.7	45.26	20.32	—	—	—	—	—	101.28	FeAsS	arsenopyrite	core of large grain
047-01	44	65	—	—	35.46	45.64	20.17	—	—	—	0.63	—	101.89	FeAsS	arsenopyrite	rim of large grain
081-02	35	48	—	—	61.3	—	39.34	—	—	—	—	—	100.64	FeS	pyrrhotite	core of large bleb in metasiltstone
081-02	35	49	—	—	60.53	0.26	38.26	—	—	—	—	—	99.04	FeS	pyrrhotite	rim of large bleb in metasiltstone
082-02	36	50	—	—	61.38	—	39.48	—	—	—	—	—	100.85	FeS	pyrrhotite	core of large bleb outside coticule
082-02	36	51	—	—	60.64	—	39.21	—	—	0.52	—	—	100.36	FeS	pyrrhotite	rim of large bleb outside coticule
082-02	36	52	—	—	32.02	—	33.25	—	—	34.12	0.56	—	99.95	$(Fe, Ni)_9S_8$	pentlandite	vein on side of large pyrrhotite bleb
082-02	36	53	—	—	31.11	—	32.79	—	—	32.23	1.87	—	98.99	$(Fe, Ni)_9S_8$	pentlandite	vein on side of large pyrrhotite bleb
082-02	37	54	—	—	61.25	—	39.43	—	—	—	—	—	100.68	FeS	pyrrhotite	bleb outside coticule
095-01	29	40	—	—	62.56	—	38.4	—	—	0.39	—	—	101.35	FeS	pyrrhotite	core of large bleb in primitive coticule
095-01	29	41	—	—	62.68	—	37.82	—	—	0.39	—	—	100.9	FeS	pyrrhotite	rim of large bleb in primitive coticule
095-01	30	42	32.99	—	30.75	—	34.17	0.3	—	—	—	—	98.2	$CuFeS_2$	chalcopyrite	rim of grain in primitive coticule
095-01	31	43	—	—	61.76	—	38.53	—	—	—	—	0.34	100.63	FeS	pyrrhotite	rim of bleb in primitive coticule
095-01	32	44	—	—	—	—	12.67	—	85.73	—	—	—	98.4	PbS	galena	small grain in primitive coticule
107-01	27	37	—	59.48	8.1	—	32.36	—	—	—	—	—	99.94	ZnS	sphalerite	side of large pyrrhotite bleb in silty slate
107-01	28	38	—	—	61.54	0.31	38.6	—	—	0.44	—	0.35	101.24	FeS	pyrrhotite	core of large bleb in silty slate
107-01	28	39	—	—	61.86	—	38.57	—	—	—	—	0.39	100.82	FeS	pyrrhotite	rim of large bleb in silty slate

— = not detected

Table D.3. Microprobe data for sulphides and arsenides from LL81-5A.

Appendix E
Geochemical Data

Introduction

This appendix presents whole-rock geochemical data acquired from samples obtained from drillcore LL81-5A by Graves and Zentilli (1988a). This information is presented in tables E.1 and E.2. Analytical methods utilized in the acquisition of this data, as well as other relevant information, are presented below. Sulphur isotope studies were conducted on samples obtained from this core by Sangster (1987), but the data have not been published and are unavailable. Data presented in this appendix are discussed in Chapter 6.

Graves and Zentilli (1988a)

Major Elements:	in weight percent volatile-free recalculated to 100 % all analyses were conducted at Dalhousie University using standard atomic absorption analysis, except P_2O_5, which was evaluated using colorimetric technique and FeO, S, CO_2 and C, which were analysed using wet chemical titration due to time limitations, some of the analyses were conducted using fused glasses on the electron beam microprobe at Dalhousie University
Trace Elements:	in parts per million (ppm) all analyses by X-ray fluorescence undertaken at Regional XRF Facility, St. Mary's University, Halifax, Nova Scotia
Trace Metals:	in ppm except gold, which is in parts per billion all analyses by non-destructive instrumental neutron activation (INAA), Bondar Clegg and Company Ltd., Ottawa, Ontario

Sample	Depth	Unit	Lithology	Description	SiO_2	Al_2O_3	Fe_2O	FeO	MgO	CaO	Na_2O	K_2O	TiO_2	MnO	P_2O_5	S	CO_2	C
86351	52.67	C	1	black and green-black slate with pyrrhotite and pyrite	66.29	22.72	0.54	2.18	1.27	0.1	2.24	4.21	0.36	0.02	0.07	0.09	—	2.29
86350	53.05	C	2	cross-bedded and parallel-laminated metasiltstone	66.64	20.34	1.67	3.18	1.5	0.21	2.19	3.68	0.49	0.03	0.06	0.98	—	1.12
86353	100.7	C	1	black slate	55.67	26.65	2.54	4.87	1.91	0.27	2.14	5.47	0.31	0.05	0.11	2.82	0.01	3.94
86352	101.42	C	2	white and grey laminated metasiltstone	67.23	19.79	1.53	3.63	1.57	0.26	2.15	3.45	0.26	0.03	0.09	1.49	0.26	1.58
86356	148.14	C	1	cross-bedded metasiltstone	74.5	14.3	2.09	3.45	1.57	0.06	1.5	2.22	0.22	0.04	0.05	1.49	—	0.49
86355	148.38	C	2	black slate	61.8	25.14	0.93	2.75	1.5	0.12	2.19	5.03	0.44	0.03	0.07	0.54	0.01	3.04
86354	148.67	C	1	black slate	58.98	25.92	1.82	3.66	1.53	0.17	2.38	5.07	0.35	0.03	0.07	2.29	—	2.83
86343	195.07	C	1	deformed slate and metasiltstone ball	63.79	21.42	1.58	4.5	2.07	0.22	1.98	3.78	0.52	0.05	0.08	2.17	—	2.28
86342	195.16	C	1	typical black slate	58.56	27.24	1.18	3.22	1.71	0.01	1.7	4.93	1.37	0.04	0.06	0.47	—	1.19
86341	195.33	C	2	cross-bedded metasiltstone	72.72	14.15	3.3	3.71	1.48	0.19	1.29	2.31	0.75	0.05	0.05	2.01	—	0.21
86344	244.01	C	1	black slate with metasiltstone laminations	56.05	26.96	2.94	4.01	1.95	0.19	2.44	4.79	0.51	0.05	0.11	2.07	—	2.57
86348	294.55	C	2	metasiltstone	67.63	15.33	3.32	4.34	1.89	3.17	0.79	2.31	0.85	0.29	0.1	2.39	3.4	0.32
86347	294.69	C	1	slate	67.77	22.26	0.65	1.89	1.16	0.04	1.86	3.04	1.19	0.06	0.07	0.18	—	1
86346	294.8	C	2	cross-bedded metasiltstone	64.91	18.52	5.46	4.14	1.52	0.79	1.15	2.96	0.32	0.12	0.1	3.56	0.35	0.6
86332	352.93	C	2	cross-bedded white metasiltstone	81.3	8.12	2.23	2.82	1.18	1.97	0.32	1.35	0.39	0.21	0.1	1.59	1.78	0.18
86331	353.13	C	1	grey slate	70.59	17.91	1.23	3.42	1.59	0.08	0.88	3.12	1	0.11	0.07	1.12	0.04	0.44
86335	397.37	C	2	cross-bedded white meta-siltstone	72.97	11.77	1.78	3.93	2.91	2.64	0.41	2.04	0.69	0.8	0.05	1.2	4.51	0.45
86333	397.66	C	1	blue-grey slate	58.12	25.73	2.52	4.38	1.65	0.06	1.43	4.5	1.14	0.39	0.06	1.46	—	1.31
86134	444.3	C	1	black slate with silt laminations	61.59	23.5	1.68	4.46	1.79	0.06	1.43	3.89	1.3	0.21	0.05	1.15	—	0.92
86135	444.5	C	2	grey metasiltstone with slate partings	70.86	15.48	2.84	4.37	1.79	0.23	0.83	2.44	0.86	0.27	0.04	1.84	0.17	0.21
86103	454.36	C	2	calcic light-grey metasiltstone	59.9	11.94	1.46	2.46	1.07	16.44	1.21	2.18	0.47	2.79	0.08	1.05	12.25	2.24
86131	459.37	C	2	light-grey metasiltstone with minor slate partings	72.12	13.92	3.51	3.85	1.47	0.17	1.55	2.21	0.78	0.35	0.07	2.19	0.08	2.19
86130	459.56	C	1	black slate	54.89	24.52	3.25	6.6	2.66	0.16	0.99	4.82	1.39	0.63	0.08	2.39	0.23	1.27
86126	460.71	C	2	grey metasiltstone with sulphides	72.4	13.51	4.44	3.11	1.56	0.24	1.54	2.1	0.7	0.35	0.05	2.17	0.18	0.14
86125	460.87	C	1	black slate with sulphides	56.34	25.11	3.46	4.62	2.2	0.24	0.86	5.4	1.29	0.43	0.05	2.09	—	1.71
86102	464.57	B	4	grey meta-argillite with sulphides	52.41	18.25	1.83	11.15	3.56	1.82	0.17	2.08	1.24	7.29	0.19	1.17	2.42	0.56
86129	465.7	B	4	calcic white speckled bed	49.49	15.78	0.4	11.27	2.7	5.11	0.16	2.15	1.26	11.42	0.26	0.16	10.43	0.58
86128	467.24	B	4	nodular green-grey banded meta-argillite	46.53	16.96	0.28	12.98	2.77	4.28	0.18	2.37	1.34	12.09	0.23	0.51	9.36	0.7
86127	469.74	B	4	nodular green-grey banded meta-argillite	51.51	18.16	0.73	10.54	2.05	2.7	0.51	2.96	1.27	9.32	0.23	0.46	8.3	0.12
86090	491.18	B	4	green-grey parallel-laminated banded meta-argillite	65.36	18.12	0.62	5.67	2.07	0.59	0.78	3.66	1.12	1.94	0.08	0.02	0.39	0.06
86327	510.65	B	3	grey metawacke	71.55	14.35	0.65	4.69	2.08	0.74	2.9	2.02	0.67	0.26	0.09	0.67	0.46	0.07
86328	510.92	B	1	grey slate	65.43	18.07	0.45	6.51	2.55	0.28	2.14	3.44	0.73	0.28	0.12	1.12	0.08	0.06
86075	549.54	B	4	black slaty meta-argillite with sulphides	63.53	20.62	0.68	5.49	2.4	0.11	0.54	5.61	0.66	0.28	0.07	0.95	0.09	0.04
86326	527.81	B	4	green slaty meta-argillite with sulphides	55.65	22.07	0.62	10.65	3.3	0.35	0.44	4.63	0.92	1.29	0.09	0.11	0.22	0.05
86325	554.88	B	4	parallel-laminated meta-argillite	61.8	20.31	0.78	7.06	2.63	0.39	0.93	4.93	0.7	0.36	0.1	0.87	0.08	0.12
86074	560.17	B	2	cross-bedded metasiltstone	72.78	15.44	0.43	3.22	1.32	0.74	1.37	3.51	0.63	0.48	0.07	0.01	0.71	0.11
86073	564.7	B	4	dark green slaty meta-argillite with silt wisps	57.85	21.79	0.96	7.86	2.21	0.93	0.55	5.26	0.89	1.63	0.07	0.03	0.36	0.06
86324	599.21	A	3	graded bed from metasiltstone to slate with sulphides	70.11	15.95	1.16	4.12	1.56	0.59	1.74	3.76	0.71	0.21	0.09	0.54	0.35	0.07
86323	601.93	A	3	metawacke	86.53	7.08	0.31	1.2	0.5	1.1	1.3	1.44	0.4	0.1	0.03	0.03	0.9	0.22
86322	607.6	A	3	calcic metawacke, possibly bioturbated	87.5	6.48	0.1	0.85	0.34	1.62	1.18	1.41	0.37	0.07	0.07	0.06	0.7	0.45
86321	624.99	A	3	calcic metawacke	80.98	10.69	0.4	2.03	0.82	0.82	1.36	2.11	0.52	0.21	0.06	0.01	0.32	—
86320	628.33	A	1	slate	56.98	21.49	0.6	9.82	2.95	0.84	0.09	5.68	0.89	0.59	0.06	0.15	0.44	0.08

— = not detected

Table E.1. Major element whole-rock geochemical data for samples from LL81-5A (data after Graves and Zentilli, 1988a).

Sample	Ba	Rb	Sr	Y	Zr	Nb	Pb	Ga	Zn	Cu	Ni	V	Cr	Na%	Sc	Fe	Co	As	Br	Mo	Sb	Te	Cs	La	Ce
86351	—	—	—	—	—	—	—	—	—	—	—	—	—	—	—	—	—	—	—	—	—	—	—	—	—
86350	—	—	—	—	—	—	—	—	—	—	—	—	—	—	—	—	—	—	—	—	—	—	—	—	—
86353	—	—	—	—	—	—	—	—	—	—	—	—	—	—	—	—	—	—	—	—	—	—	—	—	—
86352	—	—	—	—	—	—	—	—	—	—	—	—	—	—	—	—	—	—	—	—	—	—	—	—	—
86356	—	—	—	—	—	—	—	—	—	—	—	—	—	—	—	—	—	—	—	—	—	—	—	—	—
86355	—	—	—	—	—	—	—	—	—	—	—	—	—	—	—	—	—	—	—	—	—	—	—	—	—
86354	—	—	—	—	—	—	—	—	—	—	—	—	—	—	—	—	—	—	—	—	—	—	—	—	—
86343	—	—	—	—	—	—	—	—	—	—	—	—	—	1.5	28.9	1.6	—	—	—	20	0.3	—	12	85	147
86342	1349	189	353	60	164	19	12	27	87	10	18	201	170	1.2	24.4	3.4	—	8.6	—	18	0.7	—	12	82	135
86341	690	93	103	14	220	14	11	20	87	41	25	79	72	1	10	5.9	—	24	—	4	0.4	—	5	20	37
86344	—	—	—	—	—	—	—	—	—	—	—	—	—	1.4	28.5	5.9	32	—	—	16	1.2	11	11	71	122
86348	610	90	189	12	254	14	9	19	105	42	34	124	81	0.62	14	6.3	—	3.3	—	5	1.1	—	6.9	10	19
86347	733	122	487	52	151	15	11	23	60	4	4	168	162	1.5	22.2	1	—	—	—	5	0.6	—	11	88	159
86346	—	—	—	—	—	—	—	—	—	—	—	—	—	0.75	18	11	58	30	—	4	1.8	—	8	14	22
86332	275	49	90	15	205	8	11	12	63	21	20	44	40	0.27	6.3	4.4	11	271	—	3	0.4	—	4	12	25
86331	679	122	226	26	286	15	13	21	69	14	18	140	121	0.65	17	4.3	13	—	—	4	0.9	—	9	33	72
86335	481	76	116	29	278	12	5	18	86	21	15	54	49	0.3	7.8	4.7	—	5	5	2	0.7	—	5	25	52
86333	1114	181	506	44	166	16	17	33	95	28	31	175	151	1.1	23.7	4.8	20	—	—	12	2.3	—	13	72	135
86134	963	148	574	50	187	18	10	26	95	24	30	157	160	1.1	23.7	4.9	—	11	—	6	2.4	—	10	60	115
86135	648	99	267	23	233	7	13	18	97	34	25	91	91	0.39	8.4	5.9	12	130	—	2	0.9	—	4	29	69
86103	623	70	329	42	115	9	24	15	41	18	13	53	47	0.86	9.1	3.1	—	0.7	—	2	1.2	—	4.7	33	74
86131	766	82	143	45	167	13	12	16	92	40	18	91	79	1.2	12	5.7	—	4.8	—	2	0.9	—	5.5	27	61
86130	1700	169	272	46	170	16	13	26	152	46	39	198	168	0.66	27.9	6.1	33	1	—	10	3.8	—	14	77	148
86126	734	78	134	24	138	11	15	15	90	38	21	96	87	1.3	12	5.9	—	1.4	—	3	0.8	—	4.8	28	61
86125	1895	192	276	41	178	16	10	33	112	32	31	179	185	0.73	29.4	7.2	—	0.5	—	9	3.3	—	13	79	146
86102	1068	72	79	39	148	15	1	27	162	51	95	205	132	0.18	19	10	—	131	—	10	1.8	—	4	49	113
86129	1257	74	132	34	144	15	32	21	99	37	93	171	102	0.18	18	9.2	—	171	2	—	0.9	—	4	40	95
86128	1265	81	133	36	145	13	48	27	118	106	121	195	106	0.18	19	11	—	217	2.4	5	1.3	—	4.3	40	101
86127	1988	101	144	37	163	14	7	31	122	24	85	92	121	0.38	17	8.8	56	94	—	—	0.9	—	5	42	95
86090	1184	130	97	32	178	17	5	22	77	24	49	149	107	0.63	16	5.4	31	53	—	—	0.9	—	4	40	90
86327	462	70	128	29	172	10	13	17	95	18	12	109	101	2.11	13	4.4	13	5	—	8	1.5	—	4	29	55
86328	821	125	118	28	180	11	17	22	111	32	26	181	132	2.1	16	6	18	2	—	3	2.1	—	5	42	80
86075	1066	193	111	35	141	14	8	24	119	24	20	105	80	0.49	15	5.3	—	3.6	—	2	1.6	11	10	32	65
86326	1141	157	77	33	121	13	—	28	149	67	60	130	132	0.42	21.4	11	49	52	—	—	1.4	—	9	56	109
86325	966	171	122	37	172	11	5	30	130	31	27	178	137	0.73	20.1	6.3	23	6	—	94	1.8	—	8	48	90
86074	687	120	139	28	156	12	18	15	59	9	30	82	73	0.61	10	3.9	17	26	—	—	0.9	—	4	52	87
86073	1242	176	119	31	120	14	154	25	112	113	64	161	115	0.42	18	8.7	—	57	—	—	1.6	—	9	91	172
86324	702	134	238	26	215	14	8	17	88	33	25	95	97	1.4	13	4	13	9	—	—	1.5	—	7	46	94
86323	224	49	202	13	201	8	12	10	23	3	9	34	41	1.1	4.6	1.2	—	9	—	—	0.7	—	3	26	47
86322	—	—	—	—	—	—	—	—	—	—	—	—	—	0.84	7.1	1	7	15	—	4	1.2	—	4.6	40	74
86321	—	—	—	—	—	—	—	—	—	—	—	—	—	0.91	4.8	2.1	6	10	—	1	0.7	—	3.1	25	44
86320	1212	194	98	39	142	15	54	26	130	46	48	122	125	0.16	22	11	33	29	—	—	1	—	10	37	65

— = not detected

Table E.1. Trace element and trace metal whole-rock geochemical data for samples from LL81-5A (data after Graves and Zentilli, 1988a).

Sample	Se	Tb	Yb	Lu	Hf	Ta	W	Au	Th	U
86351	—	—	—	—	—	—	—	—	—	—
86350	—	—	—	—	—	—	—	—	—	—
86353	—	—	—	—	—	—	—	—	—	—
86352	—	—	—	—	—	—	—	—	—	—
86356	—	—	—	—	—	—	—	—	—	—
86355	—	—	—	—	—	—	—	—	—	—
86354	—	—	—	—	—	—	—	—	—	—
86343	10	2.2	7	1.1	7	1.5	3	—	18	9.1
86342	11	2.8	7	1	5	—	—	—	16	8.8
86341	2.9	0.8	2	0.3	7	—	—	—	10	3
86344	8.4	2.3	6	0.9	6	1.8	1	—	16	7.9
86348	2.1	0.9	2	0.5	9	—	—	—	8.9	2.5
86347	11	2	5	0.9	5	1	—	—	13	5.2
86346	2.4	0.8	3	0.6	13	1.3	2	6	11	3.9
86332	2.5	—	—	—	7	—	—	—	6.1	2.2
86331	4.9	1	5	0.9	10	1	—	—	12	3.9
86335	5.2	1	—	0.6	11	1	—	—	12	3.1
86333	9.1	2	—	0.8	5	2	5	5	14	7.3
86134	7.6	2	5	0.8	5	—	—	4	12	4.3
86135	5.8	1	—	0.6	11	—	3	—	12	2.9
86103	5.9	1.5	3	0.6	4	—	—	4	5.1	1.4
86131	5.4	1.8	4	0.6	6	—	—	—	7.2	1.9
86130	10	2	—	0.8	6	2	4	5	17	5.3
86126	4.8	1.1	2	0.4	5	—	—	—	6.4	1.6
86125	9.5	1.8	5	0.9	6	—	—	5	15	5.1
86102	7.7	2	—	0.6	7	—	—	8	10	2.8
86129	6.5	2	—	0.6	6	—	—	—	7.3	2.5
86128	6	1.5	4	0.7	3	—	—	8	7.9	2.2
86127	6.4	1	—	0.5	4	1	10	—	7.7	1.7
86090	7.1	1	—	0.7	4	1	3	—	9	1.6
86327	4.8	1	—	—	5	—	2	—	6.7	2.6
86328	6.6	1	—	0.5	6	—	3	5	7.2	2.9
86075	6	1.6	3	0.5	5	—	—	5	10	5.1
86326	7.8	2	—	0.6	4	1	4	—	14	1.8
86325	6.6	1	3	0.6	6	1	4	4	10	3.8
86074	7.2	1	—	0.7	8	1	3	—	12	3.2
86073	11	1	—	0.6	3	—	4	9	14	3.4
86324	6.5	1	—	0.6	7	1	3	—	11	2.6
86323	3.5	—	—	—	8	—	7	—	7	1.6
86322	5.4	0.9	2	0.4	15	1	3	—	12	2.8
86321	3.1	0.5	—	0.3	6	0.7	—	—	5.5	1.2
86320	5.2	1.2	3	0.6	4	1.3	3	3	13	2

— = not detected

Table E.1. Trace element and trace metal whole-rock geochemical data for LL81-5A cont...

	SiO_2	Al_2O_3	Fe_2O_3	FeO	MgO	CaO	Na_2O	K_2O	TiO_2	MnO	P_2O_5	S	CO_2	C
Unit C slates														
mean	60.56	24.47	1.9	3.84	1.74	0.13	1.71	4.52	0.89	0.17	0.07	1.39	0.02	1.88
standard deviation	4.95	2.5	0.98	1.24	0.39	0.08	0.56	0.78	0.43	0.19	0.02	0.9	0.06	1
number of samples analysed	12	12	12	12	12	12	12	12	12	12	12	12	12	12
Unit C metasiltstones														
mean	70.26	14.76	2.8	3.58	1.63	2.2	1.24	2.44	0.56	0.45	0.07	1.83	1.92	0.81
standard deviation	5.22	3.36	1.2	0.57	0.44	4.42	0.57	0.61	0.22	0.74	0.02	0.68	3.43	0.75
number of samples analysed	12	12	12	12	12	12	12	12	12	12	12	12	12	12
Unit B meta-argillites														
mean	56.02	19.12	0.77	9.18	2.63	1.81	0.47	3.74	1.05	5.07	0.15	0.48	3.52	0.25
standard deviation	6.2	2.05	0.42	2.56	0.5	1.74	0.26	1.32	0.24	4.64	0.07	0.41	4.22	0.26
number of samples analysed	9	9	9	9	9	9	9	9	9	9	9	9	9	9
Unit A metawackes														
mean	81.28	10.05	0.49	2.05	0.81	1.03	1.4	2.18	0.5	0.15	0.06	0.16	0.57	0.19
standard deviation	6.91	3.77	0.4	1.27	0.47	0.38	0.21	0.96	0.13	0.06	0.02	0.22	0.24	0.17
number of samples analysed	4	4	4	4	4	4	4	4	4	4	4	4	4	4

Table E.2. Major element whole-rock geochemical data for samples from LL81-5A (data after Graves and Zentilli, 1988a).

	Ba	Rb	Sr	Y	Zr	Nb	Pb	Ga	Zn	Cu	Ni	V	Cr	Na%
Unit C slates														
mean	1205	160	385	46	186	16	12	27	96	23	24	174	160	1.04
standard deviation	432	28	126	10	42	1	2	4	28	13	11	20	18	0.31
number of samples analysed	7	7	7	7	7	7	7	7	7	7	7	7	7	8
Unit C metasiltstones														
mean	603	80	171	26	201	11	13	17	83	32	21	79	68	0.74
standard deviation	148	15	80	12	53	3	5	2	19	10	6	25	19	0.36
number of samples analysed	8	8	8	8	8	8	8	8	8	8	8	8	8	9
Unit B meta-argillites														
mean	1242	128	113	35	148	14	33	26	121	53	68	154	115	0.4
standard deviation	281	45	22	2	19	2	48	3	24	33	31	37	17	0.19
number of samples analysed	9	9	9	9	9	9	8	9	9	9	9	9	9	9
Unit A metawackes														
mean	463	92	220	20	208	11	10	14	56	18	17	65	69	1.06
standard deviation	239	43	18	7	7	3	2	4	33	15	8	31	28	0.22
number of samples analysed	2	2	2	2	2	2	2	2	2	2	2	2	2	4

Table E.2. Trace element and trace metal whole-rock geochemical data for samples from LL81-5A (data after Graves and Zentilli, 1988a).

	Sc	Fe	Co	As	Br	Mo	Sb	Te	Cs	La	Ce	Se	Tb	Yb
Unit C slates														
mean	24.6	24.6	24.5	5.3		10	1.9	—	11.6	70	129	8.9	2	5.5
standard deviation	3.8	3.8	8.4	4.6		4.8	1.2	—	1.6	16	25	1.9	0.5	0.8
number of samples analysed	8	8	4	4	0	8	8	1	8	8	8	8	8	6
Unit C metasiltstones														
mean	10.8	10.8	27	52.2	—	3	0.9		5.3	22	47	4.1	1.1	2.7
standard deviation	3.4	3.4	21.9	86.5	—	1.1	0.4		1.2	8	20	1.5	0.3	0.7
number of samples analysed	9	9	3	9	1	9	9	0	9	9	9	9	8	6
Unit B meta-argillites														
mean	18.2	8.4	39.2	87.2	2.2	27.8	1.4	—	6.4	49	103	7.2	1.5	3.3
standard deviation	1.9	2.1	11.9	68.9	0.2	38.4	0.4	—	2.4	16	28	1.5	0.4	0.5
number of samples analysed	9	9	5	9	2	4	9	1	9	9	9	9	9	3
Unit A metawackes														
mean	7.4	2.1	8.7	10.8		2.5	1		4.4	3.4	65	4.6	0.8	—
standard deviation	3.4	1.2	3.1	2.5		1.5	0.3		1.6	9	21	1.4	0.2	—
number of samples analysed	4	4	3	4	0	2	4	0	4	4	4	4	3	1
												— = not detected		

Table E.2. Trace element and trace metal whole-rock geochemical data for samples from LL81-5A cont...

	Lu	Hf	Ta	W	Au	Th	U
Unit C slates							
mean	0.9	6	1.6	3.3	4.8	14.4	6
standard deviation	0.1	1.6	0.5	1.7	0.4	1.8	1.7
number of samples analysed	8	8	5	3	4	8	8
Unit C metasiltstones							
mean	0.5	8.1	1.2	2.5	5	8.7	2.5
standard deviation	0.1	2.9	0.1	0.5	1	2.5	0.8
number of samples analysed	8	9	2	2	2	9	9
Unit B meta-argillites							
mean	0.6	4.7	1	5	6.8	10	2.8
standard deviation	0.1	1.3	0	2.5	1.9	2.4	1.1
number of samples analysed	9	9	4	5	5	9	9
Unit A metawackes							
mean	0.4	9	0.9	4.3		8.9	2.1
standard deviation	0.1	3.5	0.1	1.9		2.7	0.7
number of samples analysed	3	4	3	3	0	4	4

Table E.2. Trace element and trace metal whole-rock geochemical data for samples from LL81-5A cont...